

INFORMATION TO USERS

This manuscript has been reproduced from the microfilm master. UMI films the text directly from the original or copy submitted. Thus, some thesis and dissertation copies are in typewriter face, while others may be from any type of computer printer.

The quality of this reproduction is dependent upon the quality of the copy submitted. Broken or indistinct print, colored or poor quality illustrations and photographs, print bleedthrough, substandard margins, and improper alignment can adversely affect reproduction.

In the unlikely event that the author did not send UMI a complete manuscript and there are missing pages, these will be noted. Also, if unauthorized copyright material had to be removed, a note will indicate the deletion.

Oversize materials (e.g., maps, drawings, charts) are reproduced by sectioning the original, beginning at the upper left-hand corner and continuing from left to right in equal sections with small overlaps. Each original is also photographed in one exposure and is included in reduced form at the back of the book.

Photographs included in the original manuscript have been reproduced xerographically in this copy. Higher quality 6" x 9" black and white photographic prints are available for any photographs or illustrations appearing in this copy for an additional charge. Contact UMI directly to order.

UMI

**A Bell & Howell Information Company
300 North Zeeb Road, Ann Arbor MI 48106-1346 USA
313/761-4700 800/521-0600**

University of Alberta

Energy Use and Emissions of a Range-Extending Hybrid Electric Vehicle

by

Victor Ying Ben Yung



**A thesis submitted to the Faculty of Graduate Studies and Research in partial fulfillment of
the requirements for the degree of Master of Science**

Department of Mechanical Engineering

Edmonton, Alberta

Spring 1997



National Library
of Canada

Acquisitions and
Bibliographic Services

395 Wellington Street
Ottawa ON K1A 0N4
Canada

Bibliothèque nationale
du Canada

Acquisitions et
services bibliographiques

395, rue Wellington
Ottawa ON K1A 0N4
Canada

Your file *Votre référence*

Our file *Notre référence*

The author has granted a non-exclusive licence allowing the National Library of Canada to reproduce, loan, distribute or sell copies of his/her thesis by any means and in any form or format, making this thesis available to interested persons.

The author retains ownership of the copyright in his/her thesis. Neither the thesis nor substantial extracts from it may be printed or otherwise reproduced with the author's permission.

L'auteur a accordé une licence non exclusive permettant à la Bibliothèque nationale du Canada de reproduire, prêter, distribuer ou vendre des copies de sa thèse de quelque manière et sous quelque forme que ce soit pour mettre des exemplaires de cette thèse à la disposition des personnes intéressées.

L'auteur conserve la propriété du droit d'auteur qui protège sa thèse. Ni la thèse ni des extraits substantiels de celle-ci ne doivent être imprimés ou autrement reproduits sans son autorisation.

0-612-21230-0

University of Alberta

Library Release Form

Name of Author: Victor Ying Ben Yung

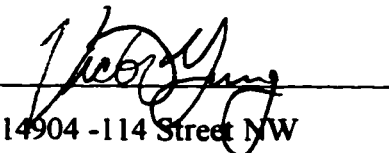
Title of Thesis: Energy Use and Emissions of a Range-Extending Hybrid Electric Vehicle

Degree: Master of Science

Year this Degree Granted: 1997

Permission is hereby granted to the University of Alberta Library to reproduce single copies of this thesis and to lend or sell such copies for private, scholarly, or scientific research purposes only.

The author reserves all other publication and other rights in association with the copyright in the thesis, and except as hereinbefore provided, neither the thesis nor any substantial portion thereof may be printed or otherwise reproduced in any material form whatever without the author's prior written permission.


14904 -114 Street NW
Edmonton, Alberta,
Canada
T5X 1G8

14 APRIL , 1997

"I do not believe that we are to be flung back into the abysmal darkness by those fiercesome discoveries which human genius has made. Let us make sure that they are our servants, not our masters," Winston Churchill

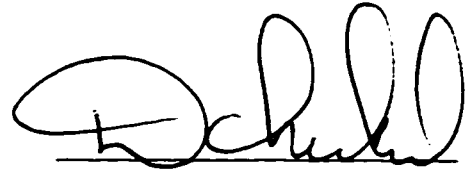
"Everything should be as simple as possible — but not simpler," Albert Einstein

"You never know how long these things will take," Victor Yung, 9 May, 1996

University of Alberta

Faculty of Graduate Studies and Research

The undersigned certify that they have read, and recommended to the Faculty of Graduate Studies and Research for acceptance, a thesis entitled Energy Use and Emissions of Hybrid Electric Vehicles submitted by Victor Ying Ben Yung in partial fulfillment of the requirements for the degree of Master of Science.



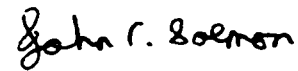
Dr. M.D. Checkel



Dr. J.D. Dale



Dr. T.W. Forest



Dr. J.C. Salmon

9 April, 1997

Abstract

The desire to reduce urban air pollution and petroleum consumption has renewed interest in the development of electric vehicles. A hybrid electric vehicle (HEV) may be a practical way to introduce electric vehicles in the near term. An HEV can have the ability of a *pure* electric vehicle to produce zero local emissions for short driving trips, while retaining the long range capability of a conventional combustion-powered vehicle.

Experiments were performed with the University of Alberta's range-extending hybrid research vehicle (HRV) in on-road driving conditions and in simulated conditions on a chassis dynamometer. The objective was to quantify the effects of introducing hybrid electric vehicles as replacements for current gasoline fueled automobiles. It is anticipated that widespread use of HEVs could significantly reduce petroleum consumption by shifting transportation energy use to electricity generated from other sources, and improve urban air quality by moving the production of pollutants to rural areas. However, it was found that with coal as a source of energy, the HRV requires about 5.0 MJ of coal energy per kilometre traveled. A similar conventional vehicle needs only 3.45 MJ of crude oil energy per kilometre. Also, operating the HRV from coal-generated electricity would increase emissions of CO₂, NO_x and SO₂, although reductions in CO and HC emissions would be expected. Careful analysis of vehicle component efficiency is needed to properly predict the effects of HEV use.

Acknowledgements

I wish to thank some of the many people who helped me complete my research:

My family for their support and patience throughout my life

**Dr. M.D. Checkel and Dr. J.D. Dale for their guidance and advice during my years
of undergraduate and graduate studies**

**My friends and fellow members of the HEV Project for their dedication and the
many hours of work towards building vehicles that actually work and
towards fixing them when they did not work**

The sponsors of the HEV Project for supporting our efforts

**The Government of Canada and Edmonton Power for their contribution to the
Hybrid Vehicle Evaluation Project**

**Al Muir, Max Schubert, Albert Yuen, Bernie Faulkner, Don Fuhr, Tony
van Straten, and Terry Nord for sharing their skills, knowledge, and
experience**

**Oleg Zastavniouk, Robert Hatchard, and Matt Johnson for the games of Snapple™
hockey and other diversions**

**Stephen Fitzpatrick and Jeffrey Kinakin for the challenging (and occasionally not
so challenging) games of chess**

**Edward Savage for games of Bookminton and lively discussions during the
Combustion Lab Philosophy Hour**

Table Of Contents

1. Introduction.....	1
1.1. Vehicle emissions and their effects	1
1.2. Urban air quality	3
1.3. Vehicle emission regulations	6
1.4. Hybrid electric vehicles	8
1.5. Overview of research	10
2. HEV design and components	12
2.1. Hybrid vehicle classification	12
2.2. Energy storage.....	16
2.3. Powertrain components.....	20
2.4. Battery charging system	23
2.5. Summary of chapter	23
3. Experimental research.....	25
3.1. Design of hybrid electric research vehicle	25
3.2. Data acquisition system.....	36
3.3. Operation.....	41
3.4. Chapter summary	44
4. Energy consumption analysis	45
4.1. Driving cycles and results of standard tests.....	45
4.2. Tractive energy requirements of the HRV	49
4.3. Powertrain performance analysis	60
4.4. Vehicle accessory load	64
4.5. Battery performance analysis.....	67
4.6. Battery charger energy and efficiency	77
4.7. Vehicle energy and efficiency	82
4.8. Resource energy	84
5. Air pollution emissions.....	87

5.1. Gasoline energy cycle emissions	87
5.2. Electricity cycle emissions	89
6. Summary and recommendations	94
6.1. Energy consumption	94
6.2. Pollutant emissions	97
6.3. Future work	97
References	99
Appendix A. Sample data file from the data acquisition system.....	104
Appendix B. Uncertainty in calculated electrical energy and distance traveled	106
Appendix C. Calibration of data acquisition system	109
Appendix D. Uncertainty in linear curve fits and means	116
Appendix E. Emissions from the production of gasoline	119

List of Tables

Table 1-1. Canadian emissions of common pollutants in 1990	3
Table 1-2. National Ambient Air Quality Objectives	4
Table 2-1. Classification of hybrid electric vehicles.....	13
Table 2-2. Component specifications for theoretical HEVs.....	13
Table 2-3. Typical specifications of current battery types	17
Table 2-4. Typical specifications of fuels.....	19
Table 3-1. Measured vehicle parameters for determining energy consumption	38
Table 3-2. Information recorded in logbook	39
Table 4-1. Dynamometer test results.....	47
Table 4-2. Specifications of the Hybrid Electric Research Vehicle	51
Table 4-3. Estimated tractive energy for the HRV in the FTP-78 test cycle	53
Table 4-4. Estimated specific positive tractive energy for three different drivers	57
Table 4-5. Electrical power requirements	67
Table 5-1. Combustion engine exhaust emissions	88
Table 5-2 Estimated gasoline energy cycle air emissions for a conventional vehicle.....	89
Table 5-3. Emissions from typical fossil fueled peak power generating plants in Alberta, Canada.....	90
Table 5-4. Emissions from producing electricity for the HRV	91
Table 5-5. Emission comparison of different vehicle energy cycles	92

List of Figures

Figure 1-1. Average annual level of NAAQO pollutants	5
Figure 1-2. Number of hours that ground level ozone exceeded MAC objective	5
Figure 1-3. Number of days that TSP exceeded MAC objective	6
Figure 1-4. Passenger vehicle tailpipe exhaust emission regulations	7
Figure 2-1. Energy flow in a parallel hybrid electric vehicle	14
Figure 2-2. Energy flow in a series hybrid electric vehicle.....	15
Figure 3-1. The Hybrid Electric Research Vehicle	25
Figure 3-2. Physical arrangement of hybrid powertrain in the HRV	26
Figure 3-3. Simplified drawing of coupling mechanism.....	28
Figure 3-4. Side section of battery box in the vehicle.....	30
Figure 3-5. Arrangement of 12 VDC lead-acid modules in the battery box.	31
Figure 3-6. Schematic of the HRV high voltage system.....	32
Figure 3-7. Simplified schematic of the HRV battery charger power electronics	33
Figure 3-8. Sample charge routine	35
Figure 4-1. Energy flow in the Hybrid Electric Research Vehicle.....	46
Figure 4-2. 1978 Federal Test Procedure driving schedule	47
Figure 4-3. Kinetics of a vehicle in motion	49
Figure 4-4. Positive tractive energy during U of A tests	54
Figure 4-5. Specific positive tractive energy during U of A tests.....	55
Figure 4-6. Positive tractive energy during Edmonton Power tests	56
Figure 4-7. Specific positive tractive energy during Edmonton Power tests	56
Figure 4-8. Negative tractive energy during U of A tests.....	58
Figure 4-9. Specific negative tractive energy during U of A tests.....	58
Figure 4-10. Negative tractive energy during Edmonton Power tests.....	59
Figure 4-11. Specific negative tractive energy during Edmonton Power tests	59
Figure 4-12. Positive drive energy, $E_{\text{pos,drive}}$, used by electric drive system during U of A tests	61

Figure 4-13. Negative drive energy, $E_{neg,drive}$, produced by regenerative braking during U of A tests.....	62
Figure 4-14. Powertrain drive efficiency, η_{drive} , during U of A tests	63
Figure 4-15. Regenerative braking efficiency, η_{regen} , during U of A tests	64
Figure 4-16. Average accessory power and ambient temperature during fleet service with Edmonton Power	65
Figure 4-17. Accessory energy during U of A tests	66
Figure 4-18. Average accessory power during U of A tests	66
Figure 4-19. Effect of regenerative braking on observed battery capacity	69
Figure 4-20. Observed battery capacity during U of A tests ($E_{batt,disch}$, as a function of input energy, $E_{charge} + E_{batt,regen}$).....	70
Figure 4-21. Observed battery capacity during U of A tests ($E_{batt,disch}$, as a function of charge energy, $E_{charge} + E_{batt,regen}$).....	70
Figure 4-22. Vehicle range for varying levels of charge energy, E_{charge}	71
Figure 4-23. Effect of regenerative braking on observed battery performance.....	72
Figure 4-24. Actual battery efficiency, η_{batt} , during U of A tests	74
Figure 4-25. Observed battery efficiency, $\eta_{obs,batt}$, during U of A tests	74
Figure 4-26. Observed battery efficiency, $\eta_{obs,batt}$, for various vehicle ranges during U of A tests	75
Figure 4-27. Battery pack and ambient temperature during in-service tests with Edmonton Power	76
Figure 4-28. Typical battery charger performance over a 12 h charge.....	78
Figure 4-29. Instantaneous battery charger efficiency, $\eta_{i,charger}$, as a function of output power, P_{charge}	79
Figure 4-30. Battery charger energy efficiency, $\eta_{charger}$, as a function of charge energy, E_{charge}	80
Figure 4-31. Charge energy, E_{charge} , produced from utility grid energy, $E_{utility}$	80
Figure 4-32. Charge energy, E_{charge} , delivered over a range of charge times.....	81
Figure 4-33. Utility grid energy, $E_{utility}$, required to achieve vehicle range	82

Figure 4-34. Variation in overall electrical energy efficiency, η_{elec} , with vehicle range.....	83
Figure 4-35. Equivalent gasoline energy consumption	84
Figure 4-36. Efficiency of producing and distributing two forms of energy	85
Figure 4-37. Specific resource energy consumption for electricity produced from coal ...	86
Figure 5-1. Estimated electric energy requirement of the HRV for FTP-78 cycle.....	91

List of Symbols, Nomenclature, and Abbreviations

ρ	density (kg/m ³)
θ	angle (°)
η_{batt}	actual energy storage efficiency of the battery pack (%)
η_{charger}	energy efficiency of the battery charger over a charge cycle (%)
η_{drive}	powertrain drive efficiency (%)
η_{elec}	overall electrical energy efficiency of the vehicle (%)
$\eta_{\text{i,charger}}$	instantaneous efficiency of the battery charger at a specific time and charge rate (%)
$\eta_{\text{net,batt}}$	net energy storage efficiency of the battery pack (%)
$\eta_{\text{obs,batt}}$	observed energy storage efficiency of the battery pack (%)
η_{regen}	regenerative braking efficiency (%)
a	acceleration (m/s ²)
A	area (m ²)
C_D	aerodynamic drag coefficient
CO	carbon monoxide
CO ₂	carbon dioxide
C_R	rolling resistance coefficient
DAS	data acquisition system
E	energy (J or kW-h)
$E_{\text{batt,disch}}$	energy flowing out of the battery pack (kW-h)
$E_{\text{batt,regen}}$	energy returned to the battery pack from regenerative braking (kW-h)
E_{charge}	energy supplied to the battery pack from the battery charger (kW-h)
$E_{\text{neg,drive}}$	electrical energy produced by regenerative braking (kW-h)
$E_{\text{neg,trac}}$ or NTE	negative tractive energy (kW-h)
energy density	energy per unit volume (W-h/m ³)

engine	a combustion engine — a device which converts chemical energy stored in a fuel to mechanical energy through combustion
$E_{\text{pos.drive}}$	electrical energy supplied to the drive system (kW-h)
$E_{\text{pos.trac}}$ or PTE	positive tractive energy (kW-h)
E_{utility}	energy used by the charger from the electric utility grid (kW-h)
EV	<i>pure</i> electric vehicle, or the operating mode of the hybrid research vehicle where tractive energy is solely derived from the battery pack
F_A	aerodynamic drag force (N)
F_G	grade resistive force (N)
F_R	rolling resistance force (N)
F_T	tractive force (N)
g	gravitational constant (9.81 m/s^2)
HC	hydrocarbons — organic compounds
HEV	a hybrid electric vehicle, or the operating mode of the hybrid research vehicle where tractive energy is derived from both the battery pack and the fuel
HRV	hybrid electric research vehicle
$h\nu$	light energy
HVE Project	Hybrid Vehicle Evaluation Project
I_{access}	electrical current used by the vehicle accessories (A)
$I_{\text{batt.disch}}$	electrical current flowing out of the battery pack (A)
$I_{\text{batt.regen}}$	electrical current flowing to the battery pack from regenerative braking (A)
ICE	internal combustion engine, or the operating mode of the hybrid research vehicle where tractive energy is solely derived from the fuel
$I_{\text{neg.drive}}$	electrical current produced by regenerative braking (A)
$I_{\text{pos.drive}}$	electrical current flowing to the electric drive system (A)
m	mass (kg)
motor	an electric motor — a device which converts electrical energy to mechanical energy

NAAQO	National Ambient Air Quality Objectives
NMHC	non-methane hydrocarbons
NO_x	oxides of nitrogen — nitrous oxide, NO; and nitrogen dioxide, NO₂
P	power (W)
P_{charge}	output power from the battery charger (W)
P_{utility}	input power required by the battery charger (W)
SNTE	specific negative tractive energy (kW-h/km)
specific energy	energy per unit mass (W-h/kg)
specific power	power per unit mass (W/kg)
SPTE	specific positive tractive energy (kW-h/km)
t	time (s)
TSP	total suspended particulates
U of A	University of Alberta
v	speed (m/s)
VOC	volatile organic compounds

1. Introduction

Transportation plays a vital role in both industrialized and developing societies. An extensive, reliable, and efficient transportation system is needed for the movement of people and products, given the importance of trade in most economies. Railways were the primary means of land based travel and trade for many years during and following the industrialization of the western world. However, the invention of the automobile, powered by a fossil fuel-burning internal combustion engine (ICE), began a fundamental shift in the transportation system. The integration of mass production techniques in the motor vehicle industry and a plentiful supply of inexpensive petroleum derived-fuel made the purchase and operation of private vehicles affordable for the general population. Motor vehicles became and remain the dominant form of transportation in developed countries. However, the use of large numbers of vehicles has also created serious air quality problems.

Air pollution caused by automobiles was noticed many years ago in densely populated areas, such as the Los Angeles basin during the 1940s [1]^{*}. Besides possible long term and large scale effects on the planet, vehicle exhaust has known detrimental effects on human health. Vehicle emissions are more serious than some other sources of pollution because vehicles generally emit pollutants in areas of high population density. The problem is less severe in Canadian cities because of lower population and vehicle densities. However, Canada's urban centres face air quality problems and these problems will become more serious if air pollution is not controlled.

1.1. Vehicle emissions and their effects

Gasoline is the most popular fuel for motor vehicles. Canadian consumption of gasoline by on-road motor vehicles totaled 31.49 billion litres in 1990 [2]. Gasoline is convenient to use and inexpensive due to its high energy density and the abundance of petroleum on the global market. However, besides the primary combustion products of water and carbon dioxide, exhaust from gasoline powered vehicles contains pollutants that

^{*} Numbers in brackets denote references listed following Chapter 6

are known to adversely affect the health of human beings and other living organisms. The primary regulated pollutants emitted by gasoline powered motor vehicles are carbon monoxide (CO), oxides of nitrogen (NO_x — the combination of nitric oxide, NO, and nitrogen dioxide, NO₂), and unburned hydrocarbons (HC). In the human body, CO inhibits the ability of hemoglobin to carry oxygen. Exposure to CO in concentrations of 100 ppm can cause headaches and concentrations over 600 ppm can lead to death [3]. As early as 1951, NO_x and HC were found to participate in the reactions that produce photochemical smog [4].

In the presence of sunlight, nitrogen dioxide in the atmosphere will cause the formation of ground level ozone (O₃) through the equilibrium of the three reactions [5, 6]:



where $h\nu$ is energy from sunlight

M is a molecule that absorbs excess vibrational energy

Ozone can cause respiratory problems, damage vegetation, and degrade materials like rubber. Ground level ozone also creates photochemical smog by initiating a complex series of chemical reactions involving water vapour and hydrocarbons. In this series of reactions, NO is converted to NO₂ which propagates the overall process of photochemical smog formation. NO₂ also reacts with water to form nitric acid (HNO₃), a component of acid rain [7].

Typical gasoline engine pollutant emissions per kilogram of fuel burned are in the range of 200 g of CO, 20 g of NO_x, and 25 g of HC [8]. The significance of these values becomes apparent when we consider the large amount of fuel consumed. Table 1-1 gives the mass of common pollutants produced in Canada and indicates the contribution of motor vehicles to human sources of pollution. Gasoline fueled motor vehicles accounted for 55% of human produced CO, 23% of HC*, and 19% of NO_x. Small contributions are

* Measurements of unburned hydrocarbons (HC) and volatile organic compounds (VOC) assumed to be equivalent.

also made to the national generation of particulate material (particulates) at 0.5% and sulfur dioxide (SO₂) at 0.4%.

Diesel is the second most widely used fuel for motor vehicles. Emissions from diesel engines are significant given that consumption of diesel by on-road vehicles in Canada during 1990 (8.37 billion litres) was about 26% of the consumption of gasoline [2]. Table 1-1 shows that diesel vehicles produced 4 times more SO₂ and 8 times more particulate matter than gasoline vehicles. SO₂ can be oxidized to sulphur trioxide (SO₃) which then contributes to acid rain by combining with water to form sulphuric acid [7]. Particulates from diesel engines, in the form of soot and smoke, contain carcinogenic compounds. Diesel vehicles also produced 16% of total national NO_x emissions. Emissions of CO and HC are much less than from gasoline engines because of the lean fuel/air mixtures that are used in diesel engines.

Table 1-1. Canadian emissions of common pollutants in 1990†

Source of pollutant	CO (Mg)	HC (Mg)	NO _x (Mg)	SO ₂ (Mg)	Particulates (Mg)
All sources	10 012 612	2 617 336	2 057 239	3 236 133	1 271 312
On-road gasoline fueled vehicles‡	5 493 824	601 348	402 357	13 367	6 980
On-road diesel fueled vehicles§	151 147	38 210	327 939	36 886	32 171
Tire wear	0	815	0	0	36 650

† Values from the Pollution Data Branch of Environment Canada [9]

‡ Includes automobiles, light-duty trucks, heavy-duty trucks, motorcycles. Excludes off-road use of gasoline.

§ Includes light-duty diesel vehicle, light-duty diesel trucks, heavy-duty diesel trucks. Excludes other diesel vehicles.

Tire wear is listed in Table 1-1 to indicate that there is pollution produced by vehicle use that is not related to the energy used for propulsion.

1.2. Urban air quality

Countries around the world have recognized the negative effects of air pollution on human health and on the health of plants and animals in the environment. In 1969, the government of Canada introduced the Clean Air Act, and the National Air Pollution Surveillance (NAPS) Network was established to monitor air pollution. National Ambient Air Quality Objectives (NAAQOs), listed in Table 1-2, were established under the Canadian Environmental Protection Act for five common air pollutants: carbon monoxide,

nitrogen dioxide, ground level ozone, sulphur dioxide (SO₂), and total suspended particulates (TSP). The maximum desirable concentration (MDC) is a long term goal for air quality. The maximum acceptable concentration (MAC) is designed to protect people and the environment from adverse effects of air pollution. The maximum tolerable concentration (MTC) is a level where action is required to protect the health of the general population.

Table 1-2. National Ambient Air Quality Objectives†

Pollutant	Averaging time	Maximum desirable concentration	Maximum acceptable concentration	Maximum tolerable concentration
Carbon monoxide	1-hour	13 ppm	31 ppm	–
	8-hour	5 ppm	13 ppm	17 ppm
Nitrogen dioxide	1-hour	–	213 ppb	532 ppb
	24-hour	–	106 ppb	160 ppb
	annual	32 ppb	53 ppb	–
Ozone	1-hour	50 ppb	82 ppb	153 ppb
Sulphur dioxide	1-hour	172 ppb	344 ppb	–
	24-hour	57 ppb	115 ppb	306 ppb
	Annual	11 ppb	23 ppb	–
Total suspended particulates	24-hour	–	120 µg/m ³	400 µg/m ³
	annual	60 µg/m ³	70 µg/m ³	–

† Values from Environment Canada [10]

Data from the NAPS Network, given in Figure 1-1, shows a general improvement in urban air quality. The average annual concentration of CO, NO_x, SO₂, and TSP decreased during the period from 1979 to 1993. Peak concentrations of pollutants, which are significantly higher than the average levels, still cause unacceptable air quality but the amount of time that the MAC objective is exceeded has decreased as well. TSP and ground level ozone are normally the determining pollutants in air quality as CO, NO_x, and SO₂ levels rarely exceed maximum acceptable concentrations [11].

Figure 1-2 shows the average number of hours during a year that ground level ozone exceeded 82 ppm at NAPS monitoring stations. Figure 1-3 shows the average number of days during a year that TSP exceeded 120 µg/m³. Ozone formation is strongly dependent on weather. The summers of 1983 and 1988 produced conditions that favoured ozone formation. Except for these two years, a general decrease occurred in the

number of hours that ground level ozone exceeded acceptable levels. The number of days that TSP exceeded acceptable levels decreased as well from 1979 to 1993.

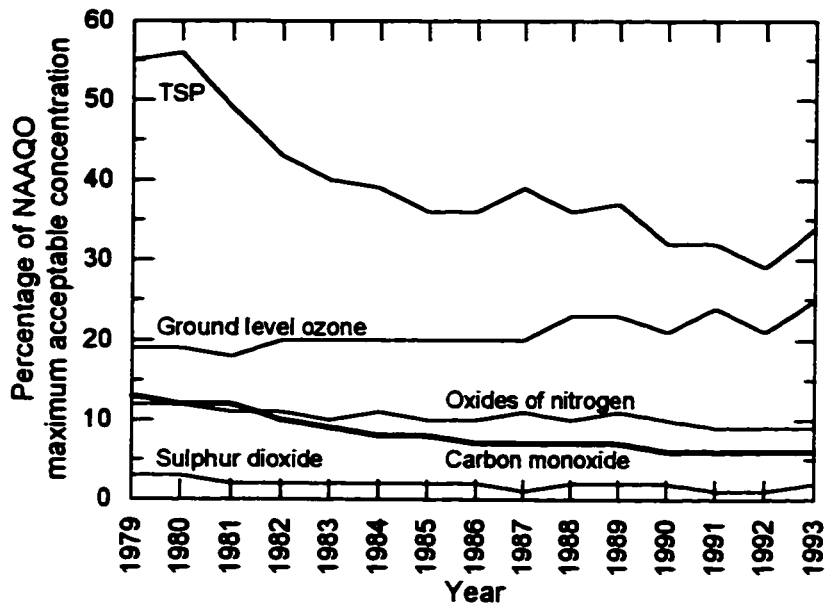


Figure 1-1. Average annual level of NAAQO pollutants [10]

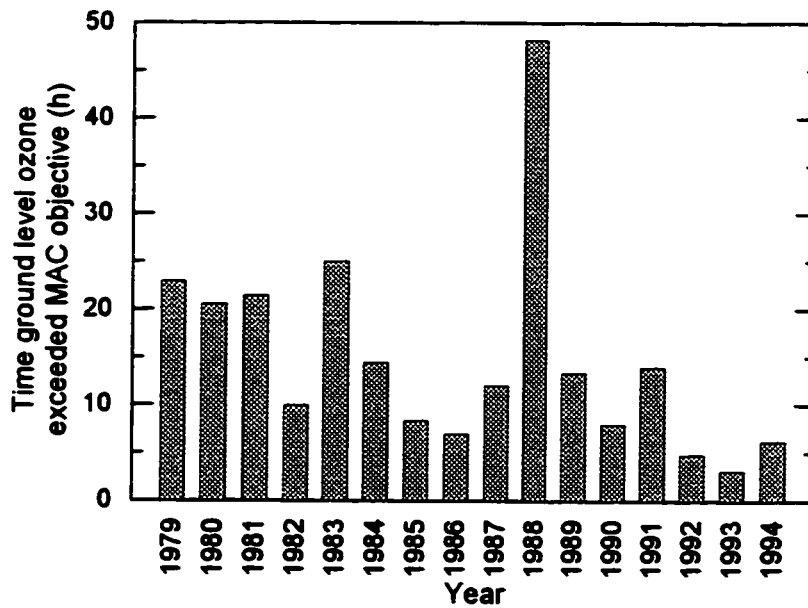


Figure 1-2. Number of hours that ground level ozone exceeded MAC objective [10]

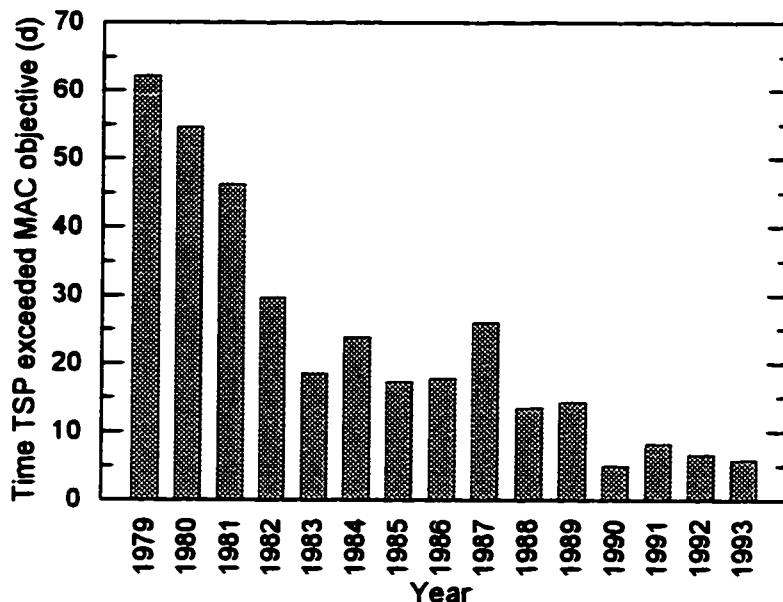


Figure 1-3. Number of days that TSP exceeded MAC objective [10]

The overall improvement in air quality is due in part to a reduction in motor vehicle emissions resulting from emission standards set by government legislation in Canada and the United States. Air pollution is carried by air currents and can cause problems in areas far from where the pollution is generated. It has been estimated that during the summer half the ozone in eastern Canada comes from the United States [12]. Further improvements in air quality will require reductions of emissions from all sources, including motor vehicles.

1.3. Vehicle emission regulations

Emission control regulations were first implemented in California in the late 1950s to govern engine blow-by gases. Regulations for vehicle tailpipe exhaust were set by California and Japan beginning with model year (MY) 1966. Other jurisdictions soon recognized the need to control vehicle emissions. National regulations in the United States (US) were established for MY 1968 and emission regulations were adopted by the European Economic Community for MY 1970. Canada adopted emission control regulations for MY 1972 that mirrored US Federal emission standards. Most developed countries today have emission regulations governing vehicle exhaust [13].

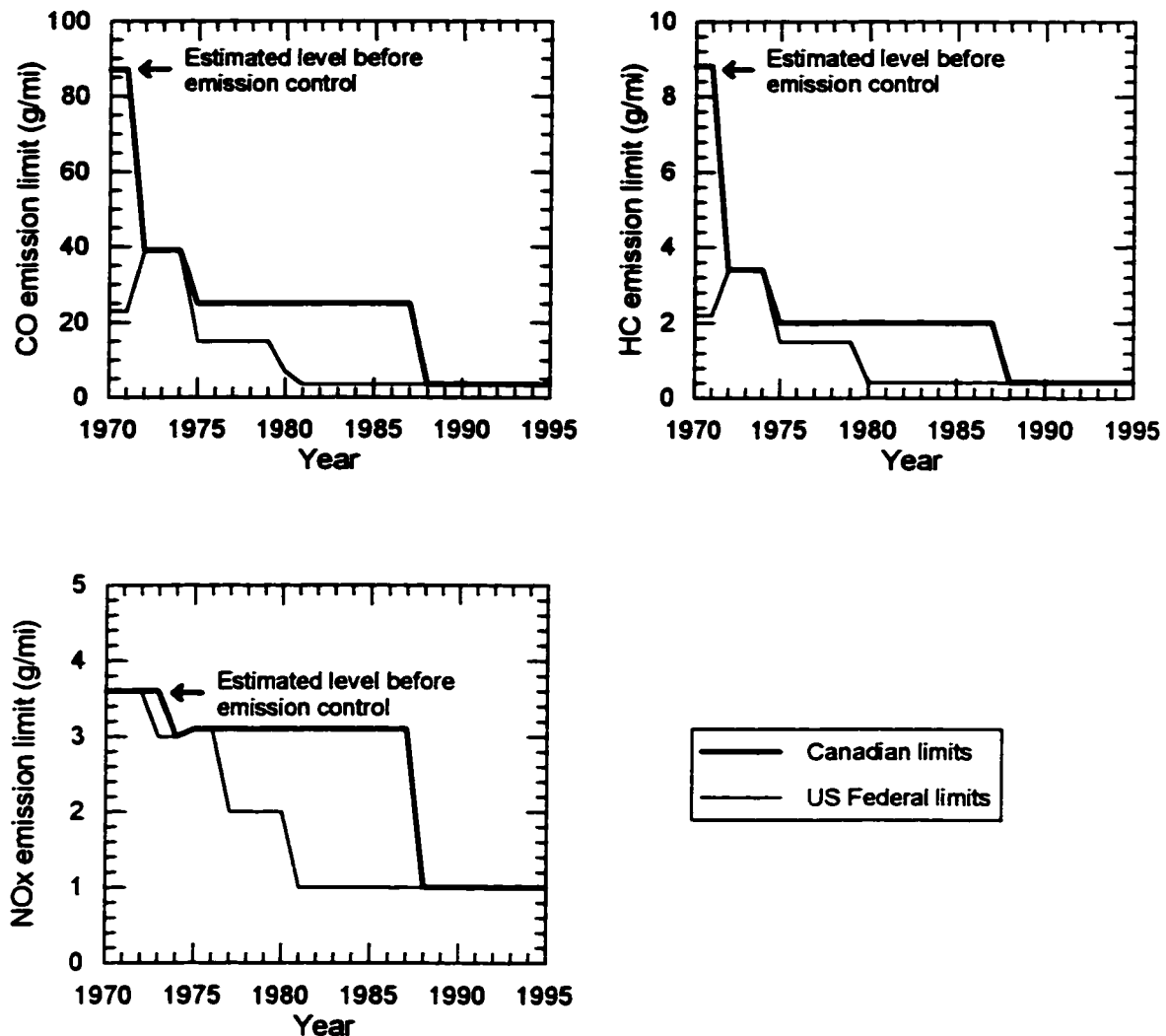


Figure 1-4. Passenger vehicle tailpipe exhaust emission regulations [13]

Government regulations have resulted in major reductions in motor vehicle emissions and subsequent improvements in air quality. For example, while motor vehicles are major sources of CO and NO_x, urban levels of CO and NO_x decreased by 56% and 26%, respectively, between 1979 and 1993. This reduction occurred despite the fact that the estimated distance traveled by passenger vehicles increased by 13% [12]. Figure 1-4 shows the maximum emission of CO, HC, and NO_x from passenger vehicles allowed by Canadian and US Federal standards from 1970 to 1995. During the period from 1975 to 1987, Canadian standards allowed higher emission levels than US Federal standards. It was believed that since air quality in Canada was significantly better than in the US,

stringent regulations would unnecessarily increase fuel consumption and the price of vehicles. In time, it became apparent that vehicles with new technology for controlling emissions (i.e., electronic fuel injection) had better fuel economy and were being sold at the same price as vehicles with older technology (i.e., carburetors) [14]. Therefore, Canadian standards were harmonized with US Federal standards in 1988. Current regulations for CO, HC, and NO_x limit vehicles to 4.7%, 3.9%, and 28%, respectively, of the estimated emissions from vehicles sold before the introduction of emission controls.

Since 1981, emission regulations in the US have remained constant in terms of the maximum allowed emissions in new passenger vehicle certification tests. Changes were made which improve the long term effectiveness of emission control systems as vehicles age, and regulations were introduced which limit non-methane hydrocarbons (NMHC). Despite the continuing renewal of the motor vehicle fleet with cleaner vehicles, there is growing concern about air quality due to population and urban traffic growth. Stricter emission standards have been proposed for the next decade to counteract the increase in urban traffic. Some jurisdictions, such as California and British Columbia, have also included mandates for the introduction of electric vehicles.

1.4. Hybrid electric vehicles

Electric vehicles have been proposed as an alternative to conventional combustion powered automobiles, with the desired goals of reducing urban air pollution and petroleum consumption. However, the introduction of a *pure* electric vehicle (EV) for the mass market is severely hindered by low energy storage density of current battery technology and the high cost of advanced battery technology. An EV generally has a short driving range and is expensive to manufacture. A hybrid electric vehicle (HEV) may be a practical way to introduce electric vehicles in the near term. Such a vehicle can have the ability of an EV to produce zero local emissions for short driving trips, and have the long range capability of a combustion-powered vehicle.

1.4.1. The HEV concept

A hybrid electric vehicle can be defined as a vehicle that carries its tractive energy in a rechargeable electrical storage system and a consumable fuel. In most cases, the

rechargeable electrical storage system consists of an electrochemical battery pack. Other potential storage systems include a flywheel with integrated electric drives, or high energy electrical capacitors (ultra-capacitors). Possible fuels for hybrid vehicles include conventional gasoline, diesel, or “alternative fuels” such as propane, ethanol, methanol, natural gas, and hydrogen. The electrical energy stored in the vehicle is converted to mechanical energy for propulsion by an electric motor. The chemical energy stored in the fuel can be converted directly to mechanical energy for propulsion by a combustion engine. Alternatively, the fuel energy can be first converted to electrical energy with a generator set or a fuel cell and then converted to mechanical energy by the electric motor.

The general definition of an HEV encompasses a range of possible hybrid designs. Chapter 2 will discuss different types of hybrid electric vehicles and a variety of vehicle components that can be used in these vehicles.

1.4.2. Emission reduction

The main reason for using electric vehicles is to reduce urban air pollution. The rechargeable energy storage system allows an HEV to use electricity that is generated remotely from the vehicle. Hydroelectric and nuclear generating stations, although they are not completely without environmental concerns, produce little direct air pollution with the generation of electricity. With fossil fuel generation, electricity is generally produced in rural areas away from population centres. This minimizes the number of people directly exposed to pollutants and allows for greater dispersion of pollutants. Also, pollution produced at a small number of generating stations is easier to control than pollution produced by many motor vehicles. Improvements in electrical generating plant emission control systems can be implemented to give an immediate benefit; whereas, improvement in vehicle emission standards requires some time for new vehicles to become a significant part of the total vehicle fleet.

1.4.3. Energy use

Transportation is almost completely dependent on petroleum-based fossil fuels. Of the 2 073 petajoules of energy used for transportation in Canada in 1995, 86% was derived from petroleum [15]. One benefit of electric vehicles is that the electricity

consumed by these vehicles can be generated from many different fuels. This will allow countries with insufficient domestic petroleum production to reduce their dependency on imported petroleum. Alternative fuels have been promoted to replace traditional gasoline and diesel fueled vehicles; however, they face a major problem: the lack of a comprehensive fuel distribution system. The existing infrastructure for distributing electricity allows electric vehicles to avoid this problem. Widespread use of electric vehicles will require infrastructure improvements; however, this can occur on a gradual basis as the number of electric vehicles in operation grows.

1.5. Overview of research

To predict the impact of hybrid electric vehicle use, knowledge regarding the energy consumption and emissions associated with these vehicles is needed. Such information would also be valuable in the design of future HEVs and in predicting the changes in demand for electricity. The overall objective of the research performed for this dissertation is to quantify the effects of introducing hybrid electric vehicles as replacements for current gasoline and diesel fueled automobiles in terms of changes to energy consumption and to emission of air pollutants. Experimental research was done with a hybrid electric vehicle to determine its performance during actual in-use conditions.

Initial experiments were done as a part of the Hybrid Vehicle Evaluation (HVE) Project, a joint undertaking by Natural Resources Canada, the University of Alberta (U of A), and Edmonton Power. The Hybrid Electric Research Vehicle (HRV) was assigned to the Edmonton Power vehicle fleet where it was used for the duration of the year 1995. The in-use study gives several measures of how HEVs are likely to be used and of what their energy demands will be.

Following the conclusion of the HVE Project, further tests were performed at the U of A. The performance of the HRV and its components were measured while systematically varying the amount of energy supplied to the battery pack during charging. These experiments were carried out under more controlled conditions. The HRV was still driven in actual urban traffic to ensure that the data collected would reflect on-road

conditions. However, a single driver performed all the tests and limited driving routes were used.

2. HEV design and components

A wide variety of vehicles are manufactured to meet the many demands of consumers. These vehicles must also be designed within the framework of government regulations. As consumer demands and government regulations change, hybrid electric vehicles may find applications for which they are better suited than conventional combustion vehicles. The potential applications for any vehicle will depend on the performance characteristics of the vehicle. The success of a hybrid vehicle will therefore depend on the capabilities of the components used in the vehicle and how well those capabilities are utilized by the design of the vehicle.

This chapter will introduce many of the design choices that are available when building a hybrid electric vehicle. A description of different hybrid vehicle classes will be presented and some of the common components being considered for use in HEVs will then be discussed. In many cases, components may have substantially different performance characteristics that make them more suitable for a particular type of hybrid vehicle. Energy consumption is affected by the efficiency at which components perform their functions. The masses of components also affect energy consumption since the energy required to propel a vehicle is dependent on vehicle mass.

2.1. Hybrid vehicle classification

The design of an HEV is challenging. Employing two sources of tractive energy in a hybrid vehicle allows greater range of vehicle designs as compared to a conventional combustion vehicle or a pure electric vehicle. To understand the diversity of possible hybrid electric vehicles, it is useful to develop a general system of classification. An HEV can be classified based on the relationship between the two drive systems in the powertrain (the powertrain configuration) and the relationship between the two sources of energy. Table 2-1 shows how hybrids can be classified based on these relationships. Four combinations are possible under this classification scheme: series power-assist hybrid, parallel power-assist hybrid, series range-extending hybrid, and parallel range-extending hybrid. This dissertation will discuss hybrid electric vehicles in terms of these four classes, although other vehicle classifications have been proposed [16].

Table 2-1. Classification of hybrid electric vehicles

Powertrain configuration	Relationship
Series	Fuel energy is first converted to electrical energy which is then converted by the electric motor to mechanical energy to propel the vehicle.
Parallel	Fuel energy is converted directly to mechanical energy to propel the vehicle.
Hybrid type	Relationship
Power-assist	Fuel energy is the primary source of tractive energy. Electrical storage system is used to smooth fluctuations in the tractive energy demand.
Range-extending	Electrical energy is the primary source of tractive energy. Fuel energy is used to extend the range of the vehicle when the electrical energy storage is depleted.

To illustrate the differences between the classes of HEVs, a theoretical hybrid electric vehicle that is the size of a typical compact automobile will be used as an example. A conventional combustion powered vehicle of this size would have a mass of about 1100 kg. In the theoretical hybrid electric vehicle, an electrochemical battery pack is used to store electrical energy and a spark ignition internal combustion engine is used to harness the energy stored in gasoline fuel. Other devices can be used in a hybrid and will be discussed later in this chapter; a battery and a combustion engine are used in the following discussion because they are familiar to most people. Approximate ratings required for the major vehicle components are given in Table 2-2. Due to the additional components required in an HEV, it generally has a greater mass than a conventional vehicle of a similar size.

Table 2-2. Component specifications for theoretical HEVs

Specification	Power-assist	Range-extending
Vehicle mass	1200 kg	1500 kg
Battery capacity	3 kW-h	12 kW-h
Maximum power for parallel configuration		
Electric motor (continuous/intermittent output)	15/25 kW	45/75 kW
Combustion engine	35 kW	40 kW
Maximum power for series configuration		
Electric motor (continuous/intermittent output)	36/60 kW	45/75 kW
Combustion engine	20 kW	23 kW

In general, a power-assist HEV is a fuel powered vehicle like a conventional automobile, but it employs a hybrid powertrain that is designed to use the energy in the

fuel more efficiently. The additional components in a power-assist HEV will increase the mass of the vehicle by about 100 kg. The energy capacity of the battery in a power-assist HEV can be quite small, about 3 kW-h. The combustion engine supplies the average power demand so the vehicle does not normally need to recharge from the utility grid. The battery pack acts as a load-leveling device for the engine to smooth the fluctuations in the tractive power demand. It supplies power to the electric motor to assist acceleration and absorbs available power from regenerative braking and from the engine, if necessary, when vehicle loads are low. Peak tractive power required for reasonable acceleration is about 60 kW. Since the engine in an HEV is not required to supply all peak power, it can be much smaller than in a conventional vehicle. The engine can also be optimized to run more efficiently. The sizes of the engine and electric motor will be dependent on the powertrain configuration.

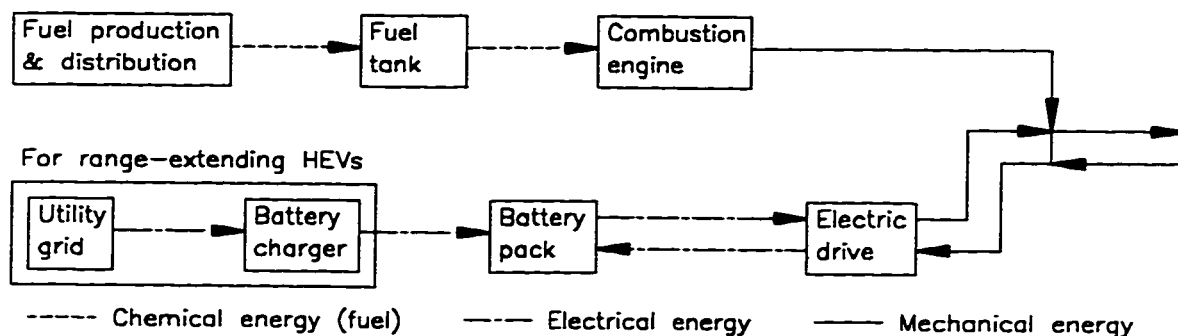


Figure 2-1. Energy flow in a parallel hybrid electric vehicle

If the powertrain in the theoretical hybrid is arranged in a parallel configuration, the flow of energy occurs as shown in Figure 2-1. Mechanical power to propel the vehicle is obtained from the electric motor and from the combustion engine. In a power-assist parallel hybrid, each power system can be sized for high efficiency while still providing adequate peak power. The mechanical output of the electric motor is combined with the output of the engine to accelerate the vehicle. An engine with a maximum output power of 35 kW and an electric motor with an intermittent maximum output of 25 kW would be adequate. The continuous maximum output of an electric motor is only a fraction of the intermittent value, typically around 60%; however, the intermittent power rating is a more

applicable for typical operating conditions in a vehicle. Regenerative braking with the electric motor can be used to recover energy to recharge the battery.

A series powertrain configuration, shown in Figure 2-2, is similar to that found in many locomotives and large mine trucks. In these series vehicles, a combustion engine and generator produce electrical power for an electric motor that propels the vehicle. A series HEV has an additional component, the battery pack. Since the vehicle is mechanically propelled only by the electric motor, the electric drive system must be sized to give adequate peak power, 60 kW. The main advantage of the series configuration is its mechanical simplicity. The transfer of power between the engine and the electric drive is independent of each unit. The engine in a parallel HEV must supply power at varying speeds. The engine in a series HEV can be sized and tuned to run at its optimum operating conditions while supplying the average required power. It can also be shut off when not needed to avoid idling losses. Therefore, it can be more efficient, smaller, and lighter with a maximum output power of about 20 kW. However, the added steps of converting the mechanical power of the engine to and from electrical power results in added losses. These losses reduce the efficiency gains from operating the engine at a steady state. Also, the addition of the generator adds to the volume and mass of the powertrain.

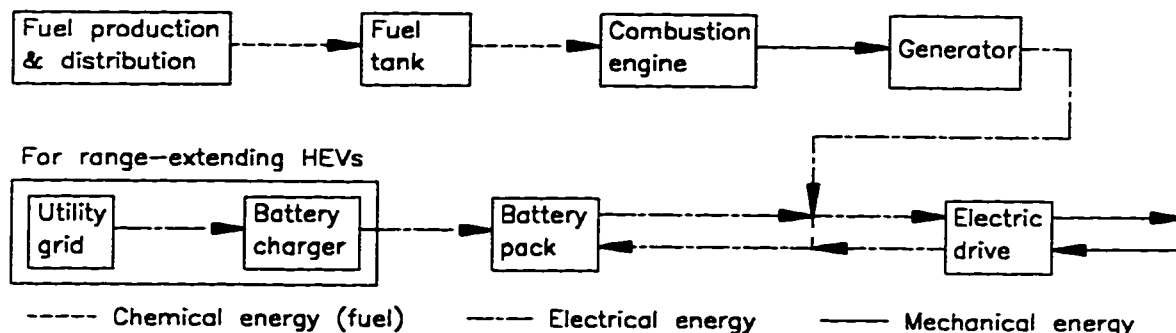


Figure 2-2. Energy flow in a series hybrid electric vehicle

The general premise of a range-extending HEV is that it operates as an electric urban commuter vehicle and a fuel-consuming long distance highway vehicle. It produces zero local emission in urban areas where smog problems are most severe while also

retaining the long range capability of a conventional vehicle. A large battery pack is needed for commuting. For a compact sized HEV, about 12 kW-h of electrical energy storage is required to travel 60 km on a standard urban driving cycle [17]. A battery charger is used to recharge the battery from the electric utility grid. The electric motor is the primary propulsion system for urban driving so it must be sized to give adequate peak performance regardless of the powertrain configuration. The engine is employed to extend the range of the HEV when the battery is depleted and is often called an auxiliary power unit (APU). To minimize engine size and mass, the HEV can be designed to operate as a power-assist hybrid in the range-extending mode.

While a hybrid vehicle is generally heavier than a comparable conventional vehicle due to the additional vehicle components, the additional capabilities provided by these components can allow an HEV to operate more efficiently and produce less pollution, if properly designed. HEVs are expected to provide the greatest benefits in urban traffic conditions where conventional vehicles operate with low efficiency and produce high emissions due to cold starting, long periods of idling, and transient power demands.

2.2. Energy storage

Energy storage is one of the most serious challenges facing hybrid electric vehicles. A vehicle can store electrical energy in electrochemical batteries and chemical energy as a fuel. As with pure electric vehicles, the low energy storage per unit volume (energy density) and per unit mass (specific energy) of currently available batteries make a hybrid vehicle heavier and larger than a comparable combustion powered vehicle. High energy capacitors (ultracapacitors) and flywheels with integrated electric drives can also be used to store electrical energy. These devices have high specific power (around 800 W/kg), but have low specific energy (less than 15 W-h/kg) [18, 19]. Therefore, their use will be generally limited to power-assist HEVs.

An additional challenge for hybrid vehicles is the storage of a second energy source for the engine. Storing a familiar fuel such as gasoline or diesel can be relatively easy compared to storing electrical energy. Some other fuels can pose considerable

difficulties in storage but have advantages over gasoline and diesel in reduced emissions or long term supply.

2.2.1. Electrochemical batteries

The electrical energy storage devices most familiar to the general public are electrochemical batteries. Unfortunately, the best commercially available batteries on today's market store less than 1% of the energy available from the same mass of gasoline. This is not unexpected since a battery usually carries all the reactants involved in the electrochemical reaction. With gasoline or other combustion fuel, the vehicle carries only the fuel used in the combustion reaction. The air used in the reaction, which is several times the mass of the fuel, is simply taken from the atmosphere. New developments and improvements in battery technology will continue to expand the range of potential applications for batteries. These advancements will contribute to improved performance of electric and hybrid vehicles.

Typical performance ratings of specific power and energy are given in Table 2-3 for three potential near-term electric vehicle batteries. Higher specific energy reduces the mass of the vehicle for the same amount of stored energy. Lower vehicle mass decreases energy consumption and increases vehicle range. Higher specific power improves the performance of the vehicle (i.e., better acceleration).

Table 2-3. Typical specifications of current battery types†

Battery	Specific power (W/kg)	Specific energy (W-h/kg)	Energy efficiency (%)	Cycle life
Advanced lead-acid	130, 250 to 400‡	35 to 50	65	500, 750‡
Nickel-cadmium	200	50 to 65	65	1000, 2000‡
Nickel-metal hydride	200	70 to 90	90	1000

† Discharge rate not specified in references [20, 21]. C/3 rate is commonly used for EV batteries.

‡ References give significantly different values

Published specifications can vary even for a given type of battery [20, 21]. In the design of an electrochemical battery, a compromise is generally made between specific power and specific energy (i.e., increasing specific power results in a decrease in specific energy). Specifications will also vary when manufacturers use different test procedures to

determine performance ratings. In actual vehicle use, conditions tend to be more severe (i.e., higher discharge rates) than in battery performance tests, resulting in lower values of specific energy.

Lead-acid (Pb-acid) batteries are produced in large numbers; virtually every automobile manufactured today uses a lead-acid battery to start its combustion engine. The advanced Pb-acid battery designs for electric vehicles offer a substantial increase in specific energy over that of normal Pb-acid batteries (22 W-h/kg to 29 W-h/kg [22]) and sealed maintenance-free deep cycle batteries have been designed for electric vehicle applications. However, lead-acid batteries still have relatively low energy density compared to other types of batteries. The advantages of lead-acid battery technology stem from its long history. It is well developed and continues to improve, and the infrastructure to produce, distribute, and recycle a large number of batteries at a reasonable cost already exists. For these reasons, lead-acid batteries will likely have a prominent role in near-term electric vehicles.

The nickel-cadmium (Ni-Cd) electrochemical cell was developed near the beginning of the twentieth century; however, widespread use of Ni-Cd batteries did not begin until after the middle of the century when extensive development was done for military applications [23]. Today, rechargeable Ni-Cd batteries are widely used in a multitude of applications, including portable electronics and cordless power tools. High capacity cells are available for electric vehicle applications. Ni-Cd batteries offer better performance and greater durability than Pb-acid batteries. Specific energy is 40% greater, specific power is 54% higher, and Ni-Cd cells can be cycled 2.7 times more than Pb-acid cells. In spite of the performance advantages, the use of Ni-Cd batteries in large-scale applications like electric vehicles has been limited due to their much higher purchase cost: about Can\$3.10/W-h compared to about Can\$0.95/W-h for lead-acid batteries.

Nickel-metal hydride (Ni-MH) is a relatively new battery technology with development proceeding since the 1970s [24]. In recent years, Ni-MH batteries have begun replacing Ni-Cd batteries in applications for portable electronics. Ni-MH batteries offer a comparable specific power to Ni-Cd batteries. Specific energy is twice that of Pb-acid batteries and 43% more than Ni-Cd batteries, and energy efficiency is 38% higher.

Recently, sealed maintenance-free cells have been designed and manufactured for prototype electric vehicles. A realistic commercial cost for electric vehicle Ni-MH batteries is difficult to determine as this technology is still under development.

Many other battery types are being investigated for use in electric vehicles [25, 26, 27]. However, early production electric vehicles will likely use a type of battery that is well developed and in common use, such as the lead-acid battery.

2.2.2. Fuels

Gasoline and diesel, both derived from petroleum, are used to fuel almost all automotive vehicles that are currently on the road. The popularity of gasoline and diesel fuels stem from their high energy content and their liquid state under normal atmospheric conditions. Table 2-4 lists the typical specific energy for a number of fuels. As was discussed in Chapter 1, petroleum is inexpensive and abundant, but it is a non-renewable resource and oil prices will eventually rise as reserves are consumed. Other fuels may then become attractive alternatives. Hybrid vehicles could shift the dependency of land transportation away from petroleum by using an alternative fuel and electricity not generated from the combustion of petroleum derivatives.

Table 2-4. Typical specifications of fuels

Fuel	Specific energy‡		On-board specific energy conventional steel tank		On-board specific energy lightweight composite tank	
	(MJ/kg)	(kW-h/kg)	(MJ/kg)	(kW-h/kg)	(MJ/kg)	(kW-h/kg)
Gasoline	44.0	12.2	41	11	43	12
Diesel	43.2	12.0	40	11	42	12
Methanol	20.0	5.56	18.6	5.0	19	5.3
Ethanol	26.9	7.47	25	6.9	26	7.2
Natural gas†	45	13	5.4	1.6	15	4.2
Hydrogen†	120.0	33.33	1.4	0.39	4.6	1.3

† Compressed to 20 MPa (200 atm)

‡ Based on lower heating value of the fuel [28]

Methanol and ethanol have been suggested as alternative fuels to reduce petroleum consumption. They generally reduce exhaust emission, although methanol fueled engines may produce more formaldehyde emissions than gasoline fueled engines. On a unit mass basis, gasoline and diesel contain about twice as much energy as methanol and 60% more

energy than ethanol. The two alcohol fuels, like the two petroleum-derived fuels, are in the liquid state under normal atmospheric conditions. This makes storage, transportation, and distribution of these fuels relatively easy. Ethanol is normally produced by fermenting agricultural crops such as grain, corn, or sugar cane so it can be considered a renewable resource. Unfortunately, current production methods are very energy intensive. Research in new production techniques may make ethanol a viable fuel sometime in the future. Methanol can be produced more economically than ethanol by using methane as a feedstock. At least three major car manufacturers have produced flexible fuel vehicles (FFVs) capable of operating on methanol/gasoline blends of up to 85% methanol.

Natural gas contains about the same amount of energy per unit mass as gasoline and diesel, while hydrogen contains almost three times more. These two fuels offer benefits in terms of reduced pollution and as an alternative energy supply to petroleum. Natural gas is a low emission fuel due to its simple molecular structure. Hydrogen is theoretically pollutant free with only water as a reaction product (except in high temperature reactions involving air where NO_x may be formed). The major challenge with using these gaseous fuels is on-board storage due to their extremely low densities. To store enough fuel within a reasonable volume for a vehicle requires a high pressure tank or the fuel must be cooled and stored in a cryogenic tank. With either scenario, the mass of the storage unit becomes the dominating factor in the overall specific energy of the fuel stored. Table 2-4 shows that the stored specific energy of the gaseous fuels improves considerably when lightweight fuel tanks are used. However, specific energy remains lower than for liquid fuels.

2.3. *Powertrain components*

The powertrain in a hybrid vehicle must be able to convert the electrical and chemical energy stored in the vehicle to mechanical work for propulsion. Electric motors are normally used to convert electrical energy to mechanical energy and can also be operated as generators to recover energy by regenerative braking. The conversion of the chemical energy in a fuel to another form is traditionally done by a heat engine. Other

devices are used in some special applications and these devices may be used in future hybrid vehicles.

2.3.1. Electric drive systems

An electric drive system refers to the combination of an electric motor and motor controller. Since the flow of energy through the electric motor is controlled by a controller designed specifically for the motor, the two components can be considered as a single system. AC induction and brushless DC drive systems appear to be in the forefront for use in electric vehicles. Recent designs offer both high efficiency and specific power.

Tractive drive applications require an electric drive system with variable speed and torque and it is desirable to have maximum torque at zero speed and a monotonic decrease in torque with increasing speed [29]. DC motors have traditionally been used in this application. They have suitable torque-speed characteristics and an inexpensive controller can be used since their speed can be adjusted by simply changing the effective supply voltage. AC motors are generally lighter, less expensive to manufacturer, and require less maintenance than conventional DC motors. However, the controllers for AC motors which convert the DC power from the battery to AC power (inverters) have been large, heavy, and expensive compared to controllers for DC motors in the past. Improvements in high-power transistors and microprocessors have reduced the cost, size, and weight of AC motor controllers. AC induction drive systems have achieved an efficiency of 90% and a specific power in the range of 670 W/kg* [30].

The advancements in power electronics that have benefited AC motor controllers have also been applied to DC drive systems. High power electronic switching circuitry in motor controllers have been used to replace the commutator and brushes in a DC motor. In a brushless DC permanent magnet drive system, the speed of the motor is controlled by both the voltage and the frequency of the electrical power supplied by the motor controller. This type of drive system offers high specific power (up to 840 W/kg* [31]) due to the use of high strength rare earth permanent magnets and high-power transistors. Peak efficiency above 90% has been reached and part load efficiency is generally above

* Calculated from continuous output power and includes mass of both motor and controller.

70% [31]. Part load efficiency is extremely important since vehicles are generally not operated a full power.

2.3.2. Fuel energy conversion systems

The second half of a hybrid powertrain must extract the chemical energy contained in a fuel. Reciprocating piston internal combustion (IC) engines are widely used to accomplish this task in automotive vehicles; almost all motor vehicles are powered by IC engines: either a spark ignition (SI) Otto-cycle engine or a compression ignition (CI) diesel cycle engine. However, gas turbines or fuel cells may be used in future HEVs after further research and development.

IC engines have significant advantages in terms of the low production cost and technological refinement that come from decades of research, development, manufacturing, and consumer use. As a result, these engines will likely be used in most early hybrid vehicles. An IC engine can be used to mechanically propel a parallel HEV or it can be used in conjunction with a generator to produce electricity in a series HEV. As described earlier in the section on hybrid vehicle design, engine size can be reduced because the electric drive system can be used to supply peak power. A smaller engine can be run more efficiently at higher loads and needs only to supply the average power. A series hybrid allows the engine to run at a true steady state, while the engine must run at varying speeds in a parallel hybrid. The engine in a series hybrid could thus operate more efficiently, but additional losses would occur when converting the mechanical output of the engine to electric power.

Gas turbine (GT) engines are successfully used to power aircraft, large compressors, and generators. The advantages of GT engines include long life, lightweight, and smooth power output. Emissions can be readily controlled since steady combustion occurs in a GT engine and a GT engine can be designed to use a variety of fuels. Unfortunately, a GT engine has low efficiency when used at partial loads or at varying speeds which are common in automotive driving cycles. A GT engine in a series HEV could run at its optimum operating point and it could be directly connected to a compact high power generator to make a small lightweight powerplant.

The product from the operation of a hydrogen-oxygen fuel cell is pure water. Thus, these fuel cells represent an opportunity to build zero local emission HEVs. As in a battery, an electrochemical reaction occurs in a fuel cell. However, a fuel cell is constantly supplied with reactants like a combustion engine, while a battery carries a fixed mass of reactants. The chemical energy stored in the hydrogen fuel is converted to electrical energy with an efficiency of 50-60% [32]. Fuel cells have been used extensively and successfully in spacecraft and have potential for future series configuration hybrid electric vehicles. A number of test projects of fuel cell powered buses have been conducted successfully, but further improvements in specific power are required before fuel cells become practical for a significant market of motor vehicles. Also, estimated production cost of fuel cells with current technology, US\$200/kW to US\$300/kW, is high compared to internal combustion engines, about US\$30/kW [33].

2.4. Battery charging system

Battery chargers are an integral part of pure electric vehicles and range-extending HEVs. If an electric vehicle is to be successful, an efficient battery charger is needed to minimize energy consumption and the charger must be designed to meet the charging requirements of the battery pack. A vehicle with a high capacity battery pack will need a high power battery charger in order to fully charge the battery in a reasonable amount of time. A variable output power level is required to prevent overheating or excessive water consumption in the battery during the later stages of the charging cycle.

Battery charger development is focused on solid state designs. Advances in power electronics allow the design of light weight and compact solid state battery chargers. Solid state chargers can be programmed to follow complex charging strategies which may be required by some batteries. The power quality of large electrical loads is a serious concern for electric utility companies [34]. Solid state chargers can be designed with near unity power factor and low electrical line noise.

2.5. Summary of chapter

This chapter has discussed the general design of hybrid electric vehicles. A general system of classifying hybrid electric vehicles based on how energy is used in the vehicle

was presented. The remainder of the chapter then examined some common components that can be used in HEVs. It should be noted that continuing research and development of vehicle components will improve future performance. The research described in this dissertation focused on the performance of a range-extending HEV and compares it to a similarly sized combustion-powered vehicle currently in production.

3. Experimental research

One of the University of Alberta's hybrid electric vehicles, the Hybrid Electric Research Vehicle, was used in the research work done for this thesis. A data acquisition system (DAS) was installed in the HRV to monitor the vehicle's performance. Data was collected during the Hybrid Vehicle Evaluation Project when the HRV was used in Edmonton Power's service fleet. Following the HVE Project, further experiments were done at the U of A in 1996. In addition, the HRV was also tested on a chassis dynamometer by Environment Canada at its laboratory in Ottawa, Canada. This chapter describes the design of vehicle, the data acquisition system, and the tests performed on the vehicle.

3.1. *Design of hybrid electric research vehicle*

The HRV, shown in Figure 3-1, is based on a production 1992 Escort wagon manufactured by Ford Motor Company of Dearborn, USA. It was converted from a conventional gasoline powered automobile to a range-extending parallel hybrid electric vehicle for the 1993 HEV Challenge student competition. The conversion of the HRV was described in detail by Duckworth et al. [35]. A major rebuild was required to prepare the car for the HVE Project with Edmonton Power and the Government of Canada. The work included the installation of a new electric drive system and lead-acid battery pack, and the construction of a new battery charger.



Figure 3-1. The Hybrid Electric Research Vehicle

3.1.1. Hybrid electric powertrain

When the HRV was originally designed and built during 1992 and 1993, a parallel hybrid configuration was chosen. All the major powertrain components (electric motors, motor controllers, internal combustion engine, coupling mechanism, and transmission) were integrated within the engine bay. The same general layout, shown in Figure 3-2, was retained when the HRV was rebuilt for the research project.

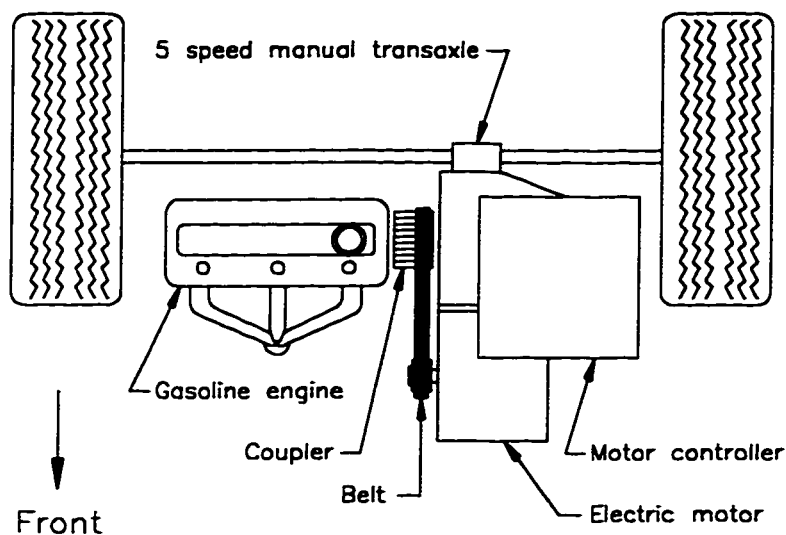


Figure 3-2. Physical arrangement of hybrid powertrain in the HRV

The electric drive system in the HRV consists of a brushless permanent magnet electric motor and a matching solid state motor controller manufactured by Unique Mobility, Inc. of Golden, USA. The combined mass of both components is 38.1 kg and the system is rated with a maximum continuous output of 32 kW (43 hp) at 6 600 rpm, giving it a continuous power to weight ratio of 0.84 kW/kg. Peak efficiency of the system is 91% when operating at rated power. In urban driving, high peak power is required for acceleration. Under intermittent operation the electric motor can supply substantially more power, about 50 kW for up to 1 minute out of every 3 minutes of use (i.e., at a 33% duty cycle). The motor is rated for a maximum speed of 7000 rpm. The tachometer in the driver's instrument panel was modified to indicate the speed of the electric motor since it always rotates when the vehicle is being driven.

The internal circuitry of the motor controller incorporates a closed loop speed control system, and a regenerative braking feature to recover kinetic energy by operating the motor as a generator. One input to the controller provides a signal indicating the desired speed, and another input the indicates the desired regeneration current. The controller uses pulse width modulation (PWM) to vary the power to or from the motor based on the two signal inputs.

The auxiliary power unit in this parallel hybrid is a 1.0 L gasoline fueled engine with electronic throttle body fuel injection. This four stroke, three cylinder engine model is normally found in a 1992 Swift manufactured by Suzuki Motor Corporation of Hamamatsu, Japan. It has a mass of 62 kg and a rated maximum power of 41 kW (55 hp) at 5700 rpm, giving it a power to weight ratio of 0.65 kW/kg. The engine and the calibration of the engine control module (ECM) are essentially stock. Minor modifications were made to facilitate installation in the vehicle. The air filter was changed and the distributor drive shaft shortened to provide space for other parts in the engine bay. Also, the wiring harness was rebuilt to integrate it with the wiring of the Escort chassis. A new exhaust pipe was installed from the exhaust manifold to the muffler and included a catalytic converter. These changes should not affect the general performance characteristics of the engine.

The coupling mechanism, or coupler, combines the mechanical power of the electric motor and combustion engine. The coupler used in the HRV is based on the U of A's second generation design described by Checkel et al. [36]. The coupling mechanism, shown in Figure 3-3, is located between the engine flywheel and the stock clutch, which is inside the bell housing of the transmission. The coupler is permanently connected to the electric motor through a toothed belt. The coupler and motor pulleys give the motor a drive speed ratio of 1.4:1 (i.e., the electric motor turns 40% faster than the coupler).

A sprag clutch inside the coupler mechanically connects the combustion engine to the transmission. The function of the clutch in the coupler is similar to the clutch in the hub of a bicycle. An analogy can be drawn between the HEV and a bicycle with an electric motor connected to the drive wheel. If the cyclist does not pedal, the electric

motor turns the wheel. When the cyclist does pedal, power is transmitted once the rotational speed of the pedals matches that of the wheel. In the hybrid electric vehicle, the combustion engine fills the role of the cyclist. If the engine is not running, the electric motor turns the coupler. When the engine is started, power is transmitted through the coupler once the speed of the engine matches that of the coupler.

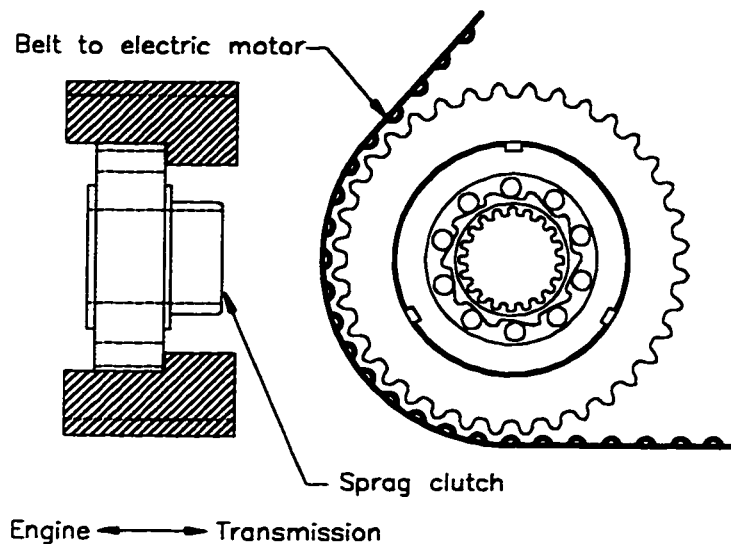


Figure 3-3. Simplified drawing of coupling mechanism

In the HRV, the parallel powertrain configuration allows three possible modes of operation. Either the electric motor or the internal combustion engine can propel the vehicle independently (EV mode or ICE mode, respectively). Alternatively, power from both systems can be combined to propel the vehicle (hybrid, or HEV mode). Ideally, when the vehicle is driven in the hybrid mode, the control system should actively vary the balance of power from the electric motor and gasoline engine depending on the vehicle's operating conditions and the amount of energy stored in the battery pack. However, such a load sharing system is not simple to implement. The limited time and resources available for the project did not permit the development of a complex control system. This was not considered a major problem. As a range-extending hybrid, the HRV would operate mainly as an electric vehicle with the combustion engine employed after the battery pack was depleted. Therefore, the two powerplants were used independently.

In EV mode, electrical power to the internal combustion engine is disabled. A potentiometer connected to the accelerator pedal sends a voltage signal to the motor controller indicating the desired motor speed. A second potentiometer connected to the brake pedal sends a voltage signal to the controller indicated the desired amount of regenerative braking. The hydraulic brakes are activated slightly after the regenerative brake is activated as the brake pedal is pressed. Both the regenerative and the hydraulic brakes proportionally increase with pedal travel.

In ICE mode, electrical power is supplied to the engine so it can be started and run. The power output of the combustion engine is controlled by a cable from the accelerator pedal to the engine throttle, as in a conventional automobile. However, the voltage signal from the accelerator potentiometer is disabled which effectively eliminates any propulsive torque from the electric motor. The operation of the regenerative and hydraulic brakes remains unchanged.

HEV mode is essentially a combination of both EV and ICE modes. The accelerator pedal controls the output of the electric motor through its potentiometer, and controls the output of the engine through the throttle cable. The braking system remains the same as in the other modes.

In HEV mode, the balance of power from the electric motor and engine depends on the position of the accelerator pedal, and the vehicle speed and transmission gear ratio which determine the rotational speed of the motor and engine. When the vehicle is driven at a steady speed on level ground, the engine produces enough torque to propel the vehicle without the assistance of the electric motor. The accelerator pedal is generally in a position where the desired speed signal from the potentiometer is less than the actual rotating speed of the electric motor. Therefore, the motor controller does not supply any electrical power to the motor. When the driver wishes the vehicle to accelerate, the accelerator pedal is depressed. The small engine does not produce enough torque to accelerate the vehicle quickly, especially when the transmission is in a high gear (low numerical gear ratio). When the desired speed signal from the potentiometer rises above the actual motor speed, the controller supplies electrical power to the motor to help accelerate the vehicle.

The operating mode is set by a multi-pole rotary switch mounted in the dashboard that is connected to a set of relays. Setting the position of the mode switch directs the relays to enable or disable the appropriate components for each mode of operation.

3.1.2. Energy storage and distribution

Energy storage is a major challenge for electric vehicles because of the low energy storage density of batteries as was discussed in Chapter 2. A range-extending hybrid must provide enough battery capacity to supply the energy needed for a typical day of driving. In addition, there must be space to store fuel for extended range travel.

In the HRV, electrical energy is stored in a 290 kg lead-acid battery pack. The pack consists of fourteen conventional deep cycle 12 VDC lead-acid modules. These modules are normally used as batteries for recreational vehicles (RVs) and are not specifically designed as traction batteries. However, they are designed for deep discharges and were donated for test purposes by a DC Solutions of Edmonton, Canada. The fourteen modules are connected in series supplying a nominal battery pack voltage of 180 VDC when fully charged.

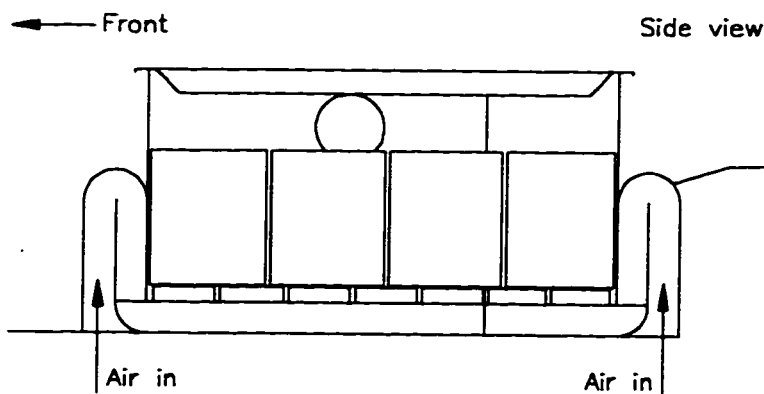


Figure 3-4. Side section of battery box in the vehicle

The modules are housed in a battery box, shown in Figure 3-4, that is located in the space originally used for the rear passenger seat and the stock fuel tank. The layout of the fourteen lead-acid modules within the battery box is shown in Figure 3-5. An induced draft ventilation system is used to draw cooling air through the battery box and remove

any undesirable gases generated by the batteries. A DC brushless fan is mounted on the driver and passenger sides of the box. Air is drawn from underneath the vehicle, through the battery box, and leaves the vehicle through an opening in each of the rear side doors. The fans are powered when the main switch that controls battery power is turned on or the vehicle is being charged. The air flow induced by the fans is sufficient to clear battery gases (i.e., hydrogen, odour, etc.) and provide a small amount of cooling. There is no active thermal management strategy during vehicle operation.

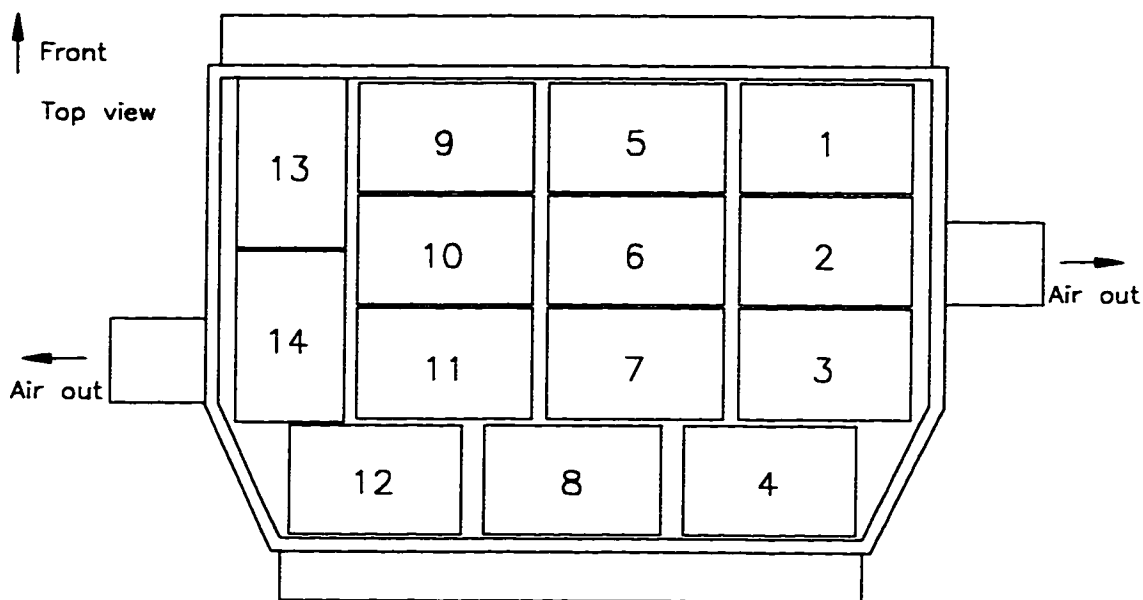


Figure 3-5. Arrangement of 12 VDC lead-acid modules in the battery box.

Figure 3-6 shows the high voltage electricity distribution system in the vehicle. The main switch is a small, high capacity circuit breaker switch mounted on the front of the battery box between the passenger seats. Energy from the battery pack passes through this switch to supply the operating components of the vehicle. The motor controller controls the flow of electrical power to the electric motor which then provides tractive force. A socket for connecting the batter charger was installed in the right rear quarter panel, opposite the normal gasoline filling point. The DC/DC converter powers the vehicle's low voltage (12 VDC) components (i.e., headlights, cooling fan, etc.) when the engine alternator is not in operation. An electric resistance heater uses electricity from the

traction battery pack to heat the coolant flowing through the vehicle's heater core to warm the interior. The actual heater power varies with the battery pack voltage, but it is nominally 1.5 kW. The electric heater is connected to the stock interior heating system, and coolant is circulated by a 12 VDC electric pump.

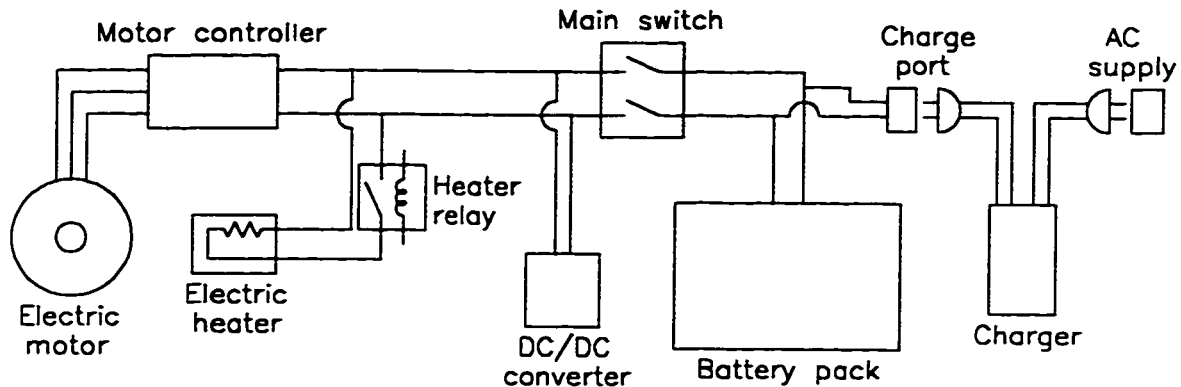


Figure 3-6. Schematic of the HRV high voltage system

The spare tire was taken out of the vehicle to provide space for fuel storage under the rear cargo area. An aluminum tank stores approximately 40 L of gasoline for the internal combustion engine. An immersed fuel pump in the gasoline tank supplies fuel for the 1.0 L engine through the vehicle's original fuel lines and fuel filter.

3.1.3. Battery charger

The HRV uses a solid state charger designed at the U of A by Dale Ulan. The charger was built as a separate unit from the HRV but is normally carried in the vehicle. It is compact in size and has a mass of 9.83 kg. The power electronics section of the charger uses commercially available power supply modules from Lambda Electronics (Canada) Inc. of Montreal, Canada.

The electrical arrangement of the modules is shown in Figure 3-7. The electrical noise (EMI) filter module protects the battery charger from undesirable electrical signals that may be present in the AC power from the utility grid. The power factor correction (PFC) module converts the AC input power to a regulated 360 VDC supply. The PFC module will accept input power between 85 VAC and 265 VAC; however, all the research

experiments were performed using a nominal 110 VAC supply. At this input voltage, the rated typical efficiency of the PFC module is 90%. If the input voltage was increased above 170 VAC, the rated typical efficiency would rise by 4% to 94%. Each of the six DC/DC converter modules takes power from the 360 VDC bus and converts it to a variable 11.2-33.6 VDC power. The DC/DC converter modules provide electrical isolation between the input and output of the battery charger for electrical safety. Their outputs connected in series and are adjusted by a feedback control loop to provide the appropriate charging voltage. An auxiliary DC/DC converter module provides 12 VDC power to operate the battery box ventilation fans and the DAS while charging. This module also powers the internal control circuitry of the battery charger.

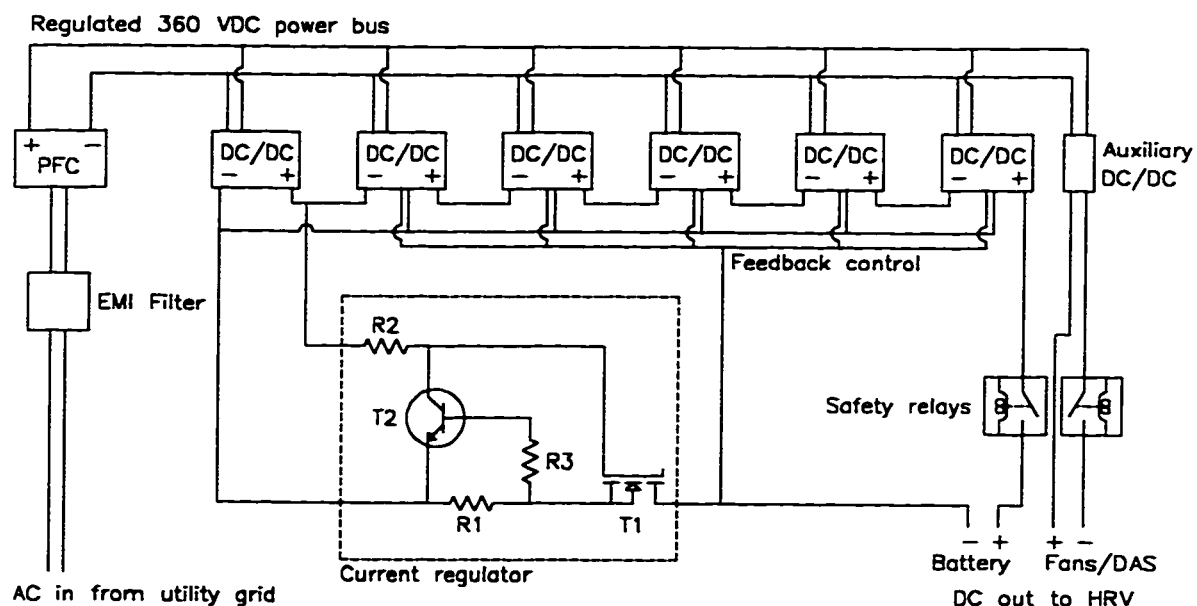


Figure 3-7. Simplified schematic of the HRV battery charger power electronics

A linear current regulator is used to control the battery charging current. The feedback loop to the DC/DC converter modules acts to maintain a constant voltage drop across the current regulator. An insulated gate bipolar transistor (IGBT), T1, adjusts the current by acting as a variable resistor^{*}. Its resistance is determined by its gate voltage.

^{*} A metal-oxide-semiconductor field-effect transistor (MOSFET) is normally used in this application; however, both an IGBT and a MOSFET have been successfully used in the battery charger.

A transistor, T2, measures the charge current by the voltage drop across a resistor, R1. T2 adjusts the current through a second resistor, R2, which changes the IGBT gate voltage. A third resistor, R3, is used to appropriately scale the input voltage to the base of T2.

To illustrate the operation of the current regulator, consider what happens when the charging current increases slightly above the design conditions. The voltage drop across R1 increases which increases the base voltage of T2. T2 will allow more current to flow through R2, lowering the gate voltage to the IGBT. The IGBT resistance will increase to reduce the charge current; thus completing the feedback control of the charging current.

The battery charger's control circuitry and logic were developed by students at the U of A. The charger is programmed to perform safety checks before and during charging. Before charging will begin, a high electrical voltage ($>150\text{VDC}$) must be present at the output terminals, which indicates that the charger is connected to the vehicle. Also, the charger verifies that the on-board DC/DC converter is off, which indicates that the main battery power switch is in the off position. While charging, the control circuitry continuously monitors and adjusts the charging current. If the current exceeds programmed limits, a fault is indicated. The charger will shut down and safety relays will disconnect the output completely. A current that is too high indicates a short circuit, and a current that is too low indicates an open circuit condition such as the charger output cable being unplugged.

The charger is programmed to provide a two stage charging process for the lead-acid battery pack. The control circuitry commands a relay that switches potentiometers connected to the base of transistor T2 (Figure 3-7). Each potentiometer supplies a different amount of current to T2 corresponding to a different charge rate. The potentiometers were adjusted to give the desired charge rate in each stage of the charging process. Figure 3-8 shows the output of the charger during a sample charge. The first stage is a 4.5 A constant current charge. The charger switches from the first stage (high charge rate) to the second stage (trickle charge) when the battery voltage reaches a pre-set voltage or a maximum time limit has passed. It then slowly charges the batteries for an

additional amount of time. For the HRV, the trip voltage was set at 200 VDC, the maximum first stage time was set at 9 h, and the trickle charge time was set at 3 h.

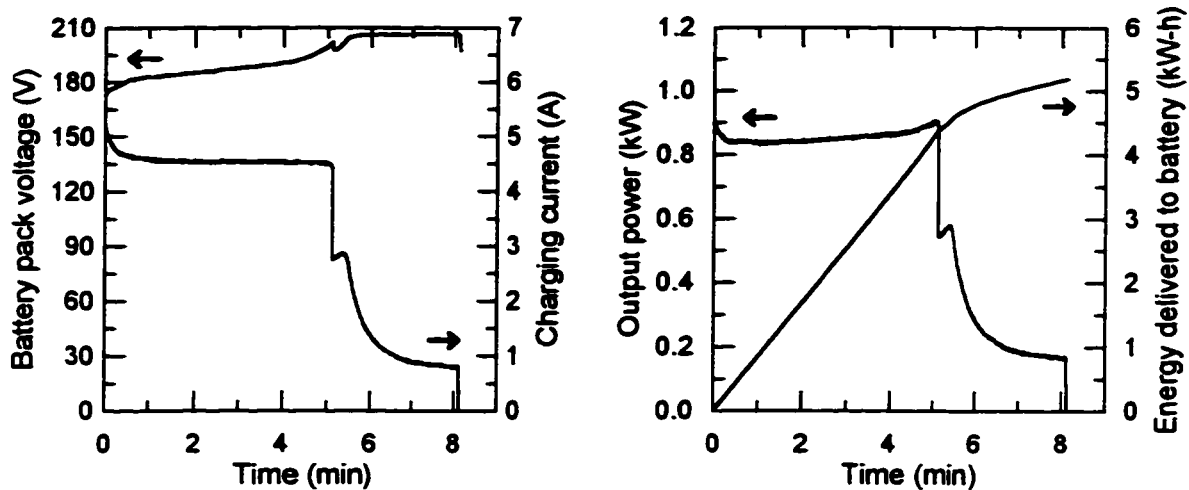


Figure 3-8. Sample charge routine

The design of the battery charger with PFC module gives it a power factor greater than 0.95 and a total harmonic distortion of less than 5% at full load. From a 110 VAC supply, the charger can produce a variable nominal output of up to 10 A (maximum current) or 200 VDC (maximum voltage), with a maximum power of 900 W. The energy efficiency of the battery charger and of other vehicle components were measured in the research work and the results are presented and discussed in Chapter 4.

3.1.4. Other vehicle modifications

For safety considerations, additional changes were made to the vehicle's brakes, chassis, and suspension. In EV mode, engine vacuum is not available to operate vacuum-boosted power brakes. The HRV uses a direct hydraulic system in conjunction with regenerative braking of the electric motor. The stock vacuum boost assembly was removed and the master cylinder bolted to the fire wall. The pivot point of the brake pedal was moved to give the driver more mechanical advantage which keeps pedal effort to a reasonable level. Regenerative braking by the electric motor provides additional braking assist, and the modifications to the hydraulic system allow adequate braking

performance when regenerative braking is not available (i.e., transmission in neutral, clutch pedal depressed, or a system failure).

The vehicle also required some structural modifications. The additional weight of the battery box attached to the floor could cause the roof to collapse in the event of a rollover. A roll-bar was installed with a main hoop supporting the roof and braces to the rear suspension mounts. The roll-bar protects the vehicle occupants and increases the structural stiffness of the vehicle. Stiffer and longer coil springs were installed to maintain adequate ground clearance with the increased vehicle weight. Three point seat belts were installed to replace the five-point racing harnesses that were required when the vehicle was built for the HEV Challenge.

3.2. *Data acquisition system*

To monitor the energy consumption of the HRV, a data acquisition system was purchased from Sigma TecSystems, Inc. of Tampa, USA. The DAS consists of an IBM PC compatible computer with a built-in analogue to digital (A/D) converter and signal conditioning circuitry. The computer supplies power to and receives analogue signals from various sensors located throughout the vehicle. The DAS consumes about 16 W of electricity under normal conditions. Electricity for the DAS comes from the on-board DC/DC converter when the vehicle is driven, and from the battery charger when the vehicle is charged. A small 12VDC lead-acid battery is used for backup power if one of the primary power sources fails. This system was used to collect data during the HVE Project and the experiments performed at the U of A. Environment Canada used their data acquisition system to collect data during the dynamometer testing performed at their facility.

A utility energy (kW-h) meter was installed at the vehicle's parking stall at Edmonton Power to measure the electrical energy used by the battery charger for charging the battery pack. Readings from the meter were recorded in a logbook along with other readings from the vehicle and driver comments. When the vehicle was tested at the U of A, an AC power meter was connected to the DAS to monitor the power consumption of the battery charger.

3.2.1. Data acquisition computer and sensors

The data acquisition computer has sixteen single-ended analogue inputs. Four channels have signal conditioning circuitry dedicated for thermistor type temperature sensors. A built-in frequency to voltage (F/V) converter attached to another channel is used to measure vehicle speed. The eleven remaining channels are available for other sensors and special digital inputs turn the system on and off automatically. A floppy disk holds the software that controls the DAS. Data were stored in a compressed binary format on the floppy disk. One data file was created for each day of operation.

The DAS was configured by modifying a computer file on the floppy disk. This configuration file allowed the user to calibrate the DAS for each sensor's zero offset and sensitivity. The file also allowed the user to set the sampling rate and the channels to record for both driving and charging events. To keep the data files at a reasonable size, the DAS was set to sample once per second during driving events. When charging the batteries, the DAS was set to sample once every 30 s as vehicle variables change much more slowly. A sample data file is included in Appendix A.

The analogue inputs have low-pass filters with a cut-off frequency of 5 Hz to remove electrical noise. Electrical noise was a concern since the large transient electrical currents are present in the hybrid electric vehicle. Shielded cable was used extensively to minimize interference. The speed data were digitally filtered to remove noise spikes in the signal.

Table 3-1 lists the vehicle variables that were used to determine energy consumption. For safety reasons, all measurements of the high voltage system were electrically isolated from the vehicle's low voltage system which is grounded to the chassis. Battery pack voltage was measured with an isolation amplifier which supplied an isolated low voltage signal to the computer. The amplifier was located in the battery box and connected to the main output terminals of the battery pack. Hall Effect transducers were used to measure battery pack, charging, and accessory currents. One of the two wires connecting the battery pack with the main switch was placed through the battery pack current transducer. Similarly, one of the two wires connecting the charge port to the battery pack was placed through the charging current transducer and one of the two wires

supplying power to the DC/DC converter for accessories was placed around the accessory current transducer. To measure vehicle speed, the stock vehicle speed sensor in the transmission was connected to the DAS.

Table 3-1. Measured vehicle parameters for determining energy consumption

Measured parameter	Transducer make	Transducer model	Normal operating range	Measurement uncertainty
Battery pack voltage	Analog Devices	AD202JN	90 VDC to 220 VDC	±1.8 VDC
Battery pack current	Sigma TechSystems	n/a	-110 A to 300 A	±3.4 A
Accessory current	MICRO SWITCH	CSLA1CD	0.60 A to 12.6 A	±0.075 A
Charging current	MICRO SWITCH	CSLA1CD	0.55 A to 5.0 A	±0.053 A
Vehicle speed	Ford	stock	0 km/h to 100 km/h	±0.65 km/h
Utility grid power	Ohio Semitronics	WM-951	280 W to 1300 W	±2.1 W

With these measurements, the electrical energy flows for the HRV components and the distance traveled during a driving cycle could be determined. The formulae used to calculate these values and associated uncertainties from the measured parameters are given in Appendix B. The uncertainty varies among the calculated values due to the different measurement uncertainties involved and the different duration of each cycle. For energy calculations involving battery pack current transducer measuring relatively low currents (i.e., regenerative braking), the uncertainty was as high as 2.5% of the calculated energy value. For all other energy values and for the distance traveled by the HRV, the uncertainty is less than 1% of the calculated value.

Additional operating parameters were monitored but not required in the energy consumption analysis. Thermistors in the battery box measured the temperature of the ambient air entering the box and the temperature of the air within the box. Two thermistors in the vehicle's interior measured the cabin temperature. Another isolation amplifier measured the electric motor speed signal from the motor controller, and an accelerometer was mounted in the car to measure fore and aft acceleration. The driving mode (EV, HEV, or ICE) was determined from a simple transducer that varied its output voltage with position of the mode switch.

3.2.2. Vehicle logbook

A logbook of the vehicle's use was kept and it proved to be useful during the HVE Project because of problems with acquiring vehicle speed data. Table 3-2 gives the items recorded in the logbook. Odometer readings were used to determine the total distance traveled by the vehicle and the distance traveled using only the electric drive system. The kW-h meter measured the electrical energy supplied to the charger.

Table 3-2. Information recorded in logbook

Date of trip
Name of operator
Odometer reading at start of trip (km)
Odometer reading at end of trip (km)
Distance traveled in electric mode (km)
kW-h meter reading at start of charge
kW-h meter reading at end of charge
Estimated cargo and passenger weight (kg)
Gasoline added, if any (L)
Comments

3.2.3. Data collection problems

During the course of the HVE Project, consistently collecting complete data was a major challenge. The DAS was delivered late and some of its accompanying sensors were missing. Ultimately, suitable sensors had to be purchased through a local supplier. Also, the DAS documentation did not adequately describe the installation and set-up of the system. Vehicle speed data could not be obtained because an undocumented internal setting for the F/V converter was not properly set inside the DAS. This problem was eventually resolved after testing and repeated discussions with the Sigma TecSystems' technical support staff.

Problems with the battery voltage and current sensors were found during field testing. The battery voltage sensor failed early in the year and it was replaced with a locally available isolation amplifier. The high current Hall Effect current sensor used to measure the current through the battery pack had insufficient resolution for measuring the

low current during charging. A low current Hall Effect current sensor was installed on the charging line.

The storage floppy was regularly replaced with a new disk. However, it was difficult to predict when a new disk was needed due to variations in vehicle use. Occasionally, data were lost when the disk became full.

One difficulty with using the logbook was that the drivers would forget to fill in the desired information. For example, no record was made in the logbook of gasoline being added to the vehicle during the year. As Edmonton Power uses a cardlock system for vehicle fuel, the amount of fuel used by the car was obtained from the accounting system; however, the vehicle may have been filled with fuel from outside suppliers. Readings from the utility energy meter were also sporadic.

Due to these measurement problems, the data collected during the HVE Project proved to have very limited usefulness. In the experiments performed at the U of A following the HVE Project, these problems were corrected and complete data were obtained. The analysis of vehicle performance presented in Chapter 4 and Chapter 5 will primarily use the data from the U of A experiments.

3.2.4. Calibration

A thorough calibration of the DAS was not done at the start of the Hybrid Vehicle Evaluation Project due to the late delivery of the DAS and time limitations in preparing the vehicle. The voltage and current sensors were linear according to the suppliers; therefore, during the course of the HVE Project, only routine two or three point calibrations were performed whenever the vehicle was returned to the U of A for maintenance or repair. Following the conclusion of the HVE Project, a thorough calibration was performed on the five key in-vehicle sensors used to measure energy consumption: battery pack voltage, battery pack current, accessory current, charge current, and vehicle speed. A brief discussion of the sensor calibration is given below. More detailed information regarding the calibration can be found in Appendix C.

The calibration of the five in-vehicle sensors confirmed that they all had good linearity. Linear regressions of the calibration data for the sensors had correlation

coefficients greater than 0.999. Among the five sensors, errors between 0.5% to 2.9% were observed in the sensitivity calibration. The DAS calibration file was adjusted to correct for these errors, and a correction factor was applied to process existing data. Offset errors were also found in the calibrations. All corrections for offset errors were performed during data processing since it was previously observed that the Hall Effect sensors exhibited some offset drift from day to day. At the end of every event the zero offset of the current sensors could be determined after the main switch was turned off.

The AC power meter used to measure the power consumption of the battery charger in the experiments carried out at the U of A was also calibrated. It also exhibited good linearity with a correlation coefficient again greater than 0.999. However, the percentage error at low power was as high as 6.7%. To obtain better accuracy with the meter, the data collected in experiments were corrected by performing linear interpolations between calibration data points during data processing.

3.3. Operation

Two of the main objectives of the research work were to determine energy consumption and component efficiencies for a hybrid electric vehicle. Energy use was measured using standard dynamometer tests as well as on-road measurements. The standard dynamometer tests give a good indication of how the HEV compares with other vehicles on which the same tests are performed. The on-road measurements give an indication of operating conditions in actual use and how actual use affects vehicle performance compared with the standard tests.

During the HVE Project, the vehicle spent just over 11 months in service. Edmonton Power received the HRV in January, 1995. Apart from the two months spent at Environment Canada and time for maintenance and repairs, the vehicle was in Edmonton Power's fleet until December, 1995. Following the HVE Project, the HRV returned to the U of A where further testing was performed.

3.3.1. Hybrid Vehicle Evaluation Project

During the HVE Project, the HRV was normally used by the Edmonton Power group responsible for servicing and replacing residential electric meters. Driving trips

were generally under light urban traffic conditions during normal working hours. The annual mileage was 2187 km which is quite low for a commercial vehicle. The operators drove the car in EV mode for about 70 % of the distance. Typical monthly mileage while working in Edmonton was only 190 km. It was used on about 90 days so average daily mileage was 19 km. The low annual mileage for the HEV can be partially explained by the availability of alternate vehicles. For urban driving, the car is under-powered in ICE mode and the engine is noisy in either ICE or HEV modes. The drivers had other vehicles available so the HRV tended to be only used on days when short trips were needed.

For this dissertation, the data collected during the HVE Project was only used to determine the tractive energy requirements in typical urban driving in Edmonton, Canada. The usefulness of the data was limited due to the problems described in Section 3.2.3. The primary source of data was the experiments performed at the U of A after the completion of the HVE Project.

3.3.2. Dynamometer testing

In the later half of February, 1995, the HRV was sent to Ottawa, Canada, where it underwent a series of tests conducted by Environment Canada. The HEV was tested for over 200 km on standard certification type dynamometer tests. The tests focused primarily on the efficiency and range of the electric drive system as the calibration of the gasoline engine ECM had not been optimized for the hybrid vehicle. Range and energy consumption were measured at ambient temperatures of 20 °C, -5 °C, and -15 °C. Emissions and fuel consumption of the combustion engine were also measured on the Urban Dynamometer Driving Schedule (UDDS) and the Highway Fuel Consumption Test (HWFCT) cycle [37]. The U of A's other hybrid vehicle, *HEV II*, was tested prior to the HRV allowing a comparison of the two vehicles.

3.3.3. Controlled field testing at the University of Alberta

Following the HVE Project and the calibration of the key sensors related to energy consumption, a series of experiments were performed to determine the variation in vehicle performance with varying amounts of charge energy. The amount of charge energy was increased starting from about 1 kW-h. After each charge cycle, the HRV was charged and

then driven to its maximum range. Several tests were performed at each charge level to check for repeatability and to account for variations in traffic conditions and weather. To minimize variations in the experiments, the same driver performed all the tests and the vehicle carried the same mass of cargo. The driver drove conservatively in an attempt to find the best realistic range in urban traffic conditions. These experiments were the primary source of data for determining the energy consumption and efficiency of vehicle components.

3.3.4. Vehicle maintenance and repairs

As an experimental car, the HRV was reasonably reliable. During the HVE Project, there was only one incident, a large coolant leak, that required the car to be towed back to its parking area at the Edmonton Power service centre. All of the vehicle's other trips were completed without any major failures. Minor maintenance and repairs were performed during weekends to allow Edmonton Power the greatest possible use of the vehicle.

During the year, one major repair was made to the hybrid powertrain. In late July, after 1400 km of service, loud powertrain noises were heard when the engine was run. On inspection, it was found that the sprag clutch inside the coupler had failed. A spare coupler was installed and the car was placed back in service. The coupler was known to be a weak link in the powertrain; however, the resources needed to re-design it were not available.

Other minor work included securing a loose boot on a constant velocity joint, fixing a loose wire that caused intermittent engine operation, and installing a heat shield around the catalytic converter.

The battery pack required occasional maintenance. The lead-acid modules are a conventional flooded design. The electrolyte level was checked periodically. Water was not required until the end of the year. One of the batteries was removed and cleaned in July as electrolyte residue on the battery casing was causing a ground fault. Another battery had a corroded terminal and was cleaned. In August, all the battery cases and terminals were cleaned to remove electrolyte residue and corrosion. In general, the

maintenance that was performed was related to the escape of electrolyte through the battery vents during charging. A vehicle with sealed low water loss batteries would require much less maintenance.

Repairs were needed to the electric heating system, DC-DC converter, and front suspension. In January, 1995, the heater control system and a coolant leak were repaired. The heater control system had a design defect. The electric heating system overheated, causing the coolant leak. The DC-DC converter failed while the car was being tested by Environment Canada and it was replaced. The ball joint of the left front MacPherson suspension was also replaced during 1995 because the rubber grease seal was torn.

In general, the vehicle repairs should not have affected the data collected during the HVE Project. No repairs were needed during the U of A experiments. Vehicle performance was affected when the electrolyte levels in the battery pack were low. The data affected by the low electrolyte levels were not used in the analysis of vehicle performance.

3.4. Chapter summary

A production Escort wagon was converted to a range-extending HEV with a parallel powertrain configuration. A DAS was installed in the vehicle to measure various operating parameters during on-road experiments. A year long field trial, the HVE Project, was conducted in a commercial fleet to determine actual in-use driving conditions. Dynamometer tests based on standard test cycles were performed to provide comparative data with other vehicles. Finally, controlled on-road experiments were completed to determine the effect of varying amounts of charge energy on vehicle performance. The data collected with the DAS during the on-road experiments allows electrical energy flows and the distance traveled by the HRV to be determined with good accuracy. Uncertainties are no more than 2.5% of the calculated values and in most cases, less than 1%.

4. Energy consumption analysis

In this chapter, the energy consumption and the efficiency of vehicle components will be discussed. Knowledge of vehicle and component efficiencies is needed to properly predict energy demand, determine areas of potential improvement, and assess the possible impact of replacing conventional vehicles with HEVs. The main focus of the energy consumption analysis will be on the electric drive system. It is of paramount importance in a range-extending hybrid since it independently propels the vehicle during most normal driving. The major electrical components are connected in series as shown in Figure 4-1. Any component energy loss multiplies the demand for electrical energy. Thus, the efficiency of each component involved in the transfer and use of electrical energy is critical. Since the energy consumption and efficiency varies with operating conditions, driving cycles and their influence on tractive energy requirements will be discussed first. The energy flow in the vehicle components will then be examined.

4.1. *Driving cycles and results of standard tests*

Energy consumption in a vehicle depends strongly on how the vehicle is operated, generally called the driving cycle. Driving cycles are described in terms of the velocity of the vehicle over a period of time. Standard driving cycles, also called test schedules, have been developed to test combustion fueled vehicles using chassis dynamometers for compliance with emission regulations and to estimate fuel consumption. The driving cycle used to certify most vehicles currently operating in North America is the United States 1978 Schedule, shown in Figure 4-2. This cycle is known as the 1978 Federal Test Procedure schedule (FTP-78) since it was adopted in that year. The schedule defines the speed of a vehicle at every second over a 2477 s (41 min 17 s) duration test. It consists of 22 min 52 s (1372 s) of driving followed by a 10 min (600 s) hot soak with the vehicle turned off and ends with a repeat of the first 8 min 25 s (505 s) of driving.

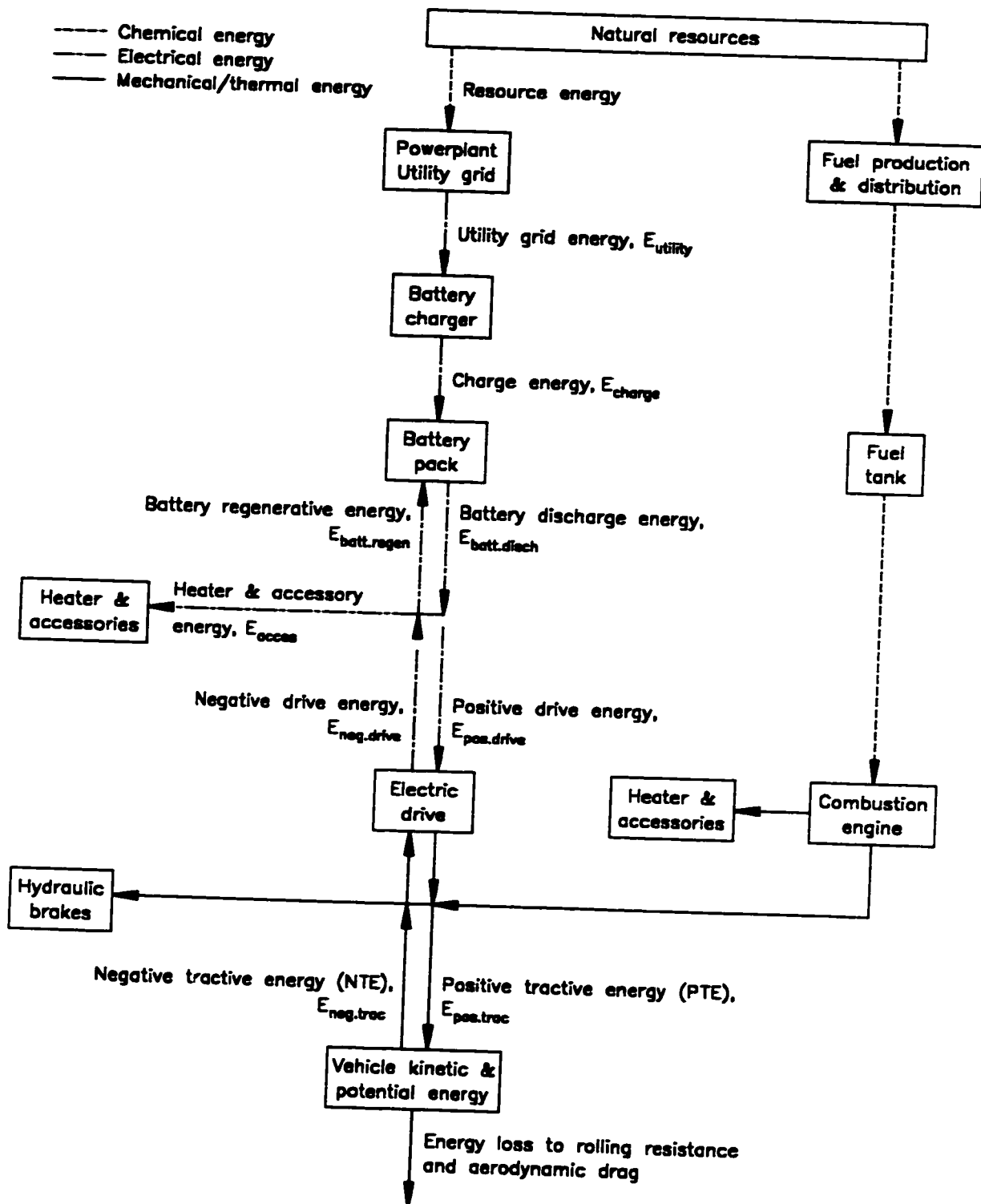


Figure 4-1. Energy flow in the Hybrid Electric Research Vehicle

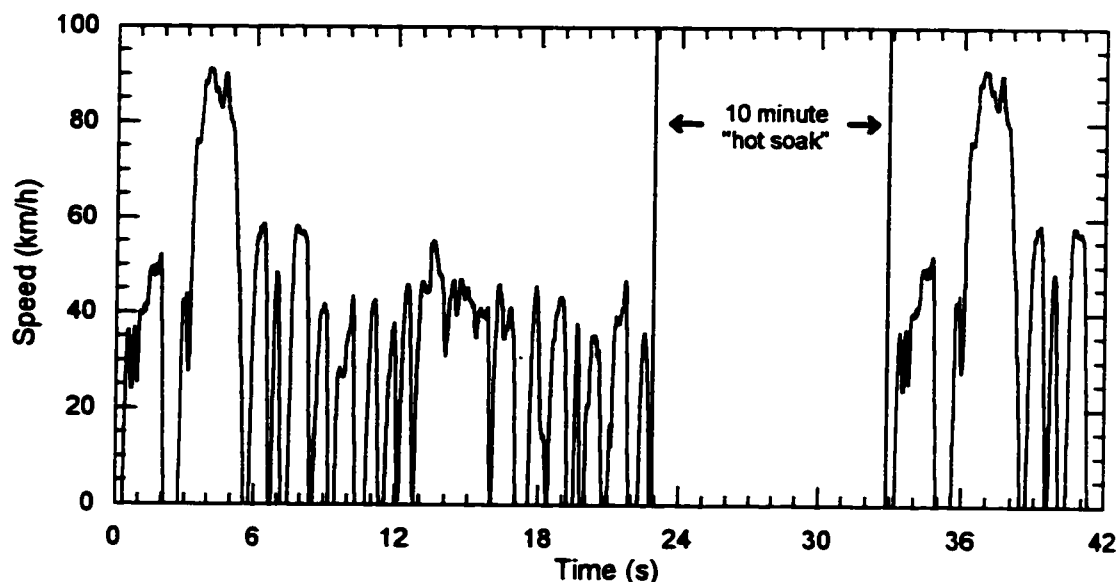


Figure 4-2. 1978 Federal Test Procedure driving schedule [37]

The HRV and U of A's second hybrid vehicle, *HEV II*, were both tested by Environment Canada for energy consumption and emissions using the FTP-78 driving schedule. *HEV II* was also tested at the 1995 HEV Challenge in the HEV mode. The results of the dynamometer tests have been described by Souligny [38, 39], and Duoba and Larsen [40]. A summary of the findings is given in Table 4-1.

Table 4-1. Dynamometer test results

Vehicle	Vehicle mass (kg)	Fuel consumption (L/100 km)	Utility grid energy consumption† (kW-hr/100 km)
1994 Ford Escort wagon	1260	8.69	-
HRV (HEV mode)	1430	8.81	9.4
HEV II (ICE mode)	1480	8.56	-
HEV II (HEV mode)‡	1480	8.98	0

† Electricity consumption is measured as AC power from utility grid into the battery charger. Battery storage efficiency estimated at 65% and battery charger efficiency estimated at 70%.

‡ 1995 HEV Challenge Emissions Event: the fuel consumption measurement was adjusted to account for the electrical energy used from battery. The vehicle mass setting on the dynamometer was about 135 kg too high. Also, the car stalled three times during test due to a problem with the transmission clutch.

Fuel consumption for the hybrid vehicles is similar to the stock 1994 Escort. The HRV and *HEV II* would normally be expected to have higher fuel consumption since their masses are 13.5% and 17.5%, respectively, more than the stock Escort. However, the

effect of the extra mass was offset by using the smaller 1.0 L engine at more efficient operating conditions. The HRV (HEV mode) required 8.81 L/100 km of gasoline, 1.38% more than the stock Escort, and an additional 9.4 kW-h/100 km of electrical energy (the energy equivalent to 1.0 L/100km of gasoline)*. This higher energy consumption can be attributed to the fuel enrichment provided by the engine control module. The ECM in the HRV had the stock calibration which was designed for a vehicle with a mass of only 775 kg. The ECM in *HEV II* was recalibrated to improve efficiency in the 1480 kg hybrid vehicle. *HEV II* (ICE mode) required 8.56 L/100 km, or 1.50% less fuel than a stock 1994 Escort wagon, which has a 1.9 L gasoline fueled engine. At the 1995 HEV Challenge, *HEV II* (HEV mode) was inadvertently tested with the inertial mass adjustment on the dynamometer set too high by about 135 kg (8.5% of the vehicle mass) [40]. This caused higher fuel consumption, but the measurement of 8.98 L/100 km is only 3.34% greater than a stock Escort.

The FTP-78 schedule was developed from studies of urban driving patterns in the area of Los Angeles, USA during the 1960's. It is meant to represent typical daily commuter driving. However, the actual on-road driving cycle of a vehicle in other urban areas, such as a medium sized Canadian city, can vary considerably from the standard test cycle. Also, the capabilities of a vehicle may influence how it is driven. For example, drivers of electric vehicles may alter their driving habits knowing the range limitations of the vehicle. Therefore, data from actual on-road driving are needed to determine the possible effects of introducing electric vehicles. The remainder of this chapter will focus on the on-road testing of the HRV performed during the HRV Project and at the U of A. The available data set was insufficient to determine on-road fuel consumption; therefore only the on-road electrical energy consumption will be discussed in the remainder of this chapter.

* Gasoline: lower heating value, LHV = 44.0 MJ/kg, density, $\rho = 0.75$ kg/L, from John B. Heywood, Internal Combustion Engine Fundamentals, (New York: McGraw-Hill, 1988), p. 915

4.2. Tractive energy requirements of the HRV

The mechanical energy transmitted through a vehicle's tires is called the tractive energy. In a laboratory, tractive energy can be measured with a chassis dynamometer; however, measuring the tractive energy directly during normal on-road driving is very difficult. As an alternative, tractive energy can be estimated from other measurements using a vehicle dynamic model.

4.2.1. Tractive energy analysis

In accordance with Newton's Second Law of Motion, the acceleration of a vehicle is proportional to the difference between the tractive force and the resistive forces, as shown in Figure 4-3. Alternatively, the tractive force can be defined as the force applied on the road by the vehicle to overcome the resistive forces and to accelerate the vehicle. The resistive forces are those caused by aerodynamic drag, rolling resistance, and gravitational force when climbing a grade:

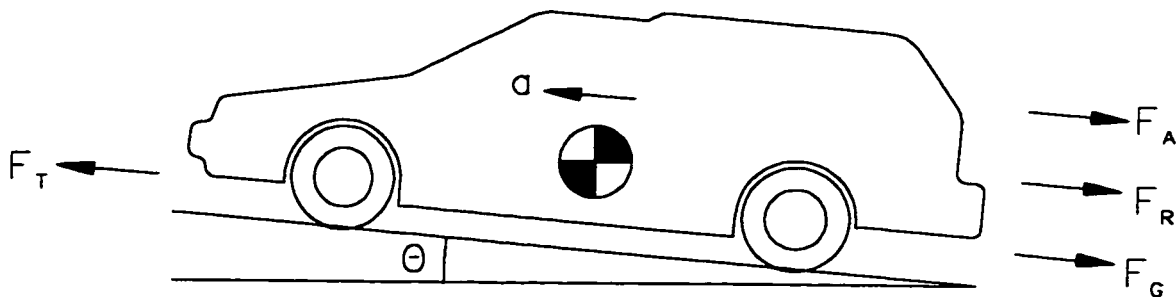


Figure 4-3. Kinetics of a vehicle in motion

$$F_T = (F_A + F_R + F_G) + m \cdot a \quad (4.1)$$

where

- F_T is the tractive force (N)
- F_A is the aerodynamic drag force (N)
- F_R is the rolling resistance force (N)
- F_G is the grade resistive force (N)
- m is the mass of the vehicle (kg)
- a is the acceleration of the vehicle (m/s^2)

$$F_A = \frac{1}{2} \cdot C_D \cdot A \cdot \rho \cdot v^2 \quad (4.2)$$

where C_D is the aerodynamic drag coefficient
 A is the frontal area of the vehicle (m^2)
 ρ is the density of the air (kg/m^3)
 v is the speed of the vehicle (m/s)

$$F_R = C_R \cdot m \cdot g \cdot \cos \theta \quad (4.3)$$

where C_R is the rolling resistance coefficient
 g is the gravitational constant (9.807 m/s^2)
 θ is the inclination of the road surface (rad)

$$F_G = m \cdot g \cdot \sin \theta \quad (4.4)$$

The inclination of the road is small under most normal driving conditions in Edmonton, Canada. This allows the use of approximations in Equations 4.3 and 4.4: $\cos \theta \approx 1$ and $\sin \theta \approx \theta$. Tractive power is calculated from the tractive force and velocity:

$$P = F_T \cdot v \quad (4.5)$$

where P is the tractive power (W)

Tractive energy is then calculated by integrating the tractive power:

$$E = \int_{t_s}^{t_f} P \cdot dt \quad (4.6)$$

where E is the tractive energy (J)
 t is time (s)
 t_s is the time at the start of the trip (s)
 t_f is the time at the end of the trip (s)

These formulae were incorporated in a computer program, *HEV_SIM*, written by Checkel [41]. The program calculates the HRV's tractive energy from the data collected by the DAS. Similar models have been used by Checkel [42], Sovran and Bohn [43], and Griffith [44]. For this study, the resistive forces were calculated at each instant using Equations 4.2 to 4.4 and the HRV properties given in Table 4-2. The aerodynamic drag coefficient was quoted by the original vehicle manufacturer during the 1993 Hybrid Electric Vehicle Challenge student competition. The rolling resistance coefficient was

estimated based on typical values for vehicles. A conservative estimate was used because the vehicle is normally driven on short trips and, therefore, tire and bearing temperature is generally low, leading to higher rolling resistance. The vehicle's frontal area was calculated in accordance with SAE Recommended Practice J1263:

$$A = 0.8 \cdot W \cdot H \quad (4.7)$$

where W is the vehicle width (m)
 H is the vehicle height (m)

The vehicle mass used in the model included an average passenger and cargo mass of 115 kg (250 lb). The air density of 1.12 kg/m^3 was calculated from assuming that air is an ideal gas. A pressure of 94.0 kPa, the mean barometric pressure for Edmonton, Canada, and a temperature of 20.0°C were used in the calculation.

Table 4-2. Specifications of the Hybrid Electric Research Vehicle

Specification	Value	Source
Aerodynamic drag coefficient	0.38	supplied by Ford Motor Company
Rolling resistance coefficient	0.013	estimated
Frontal area	1.85 m^2	measured per SAE J1263
Vehicle mass	1430 kg	measured
Vehicle mass with cargo	1545 kg	estimated

An accelerometer was mounted in the vehicle to measure the longitudinal acceleration of the vehicle parallel to the road surface. The inclination of the road surface could then be determined using the difference between the measurements from the accelerometer and the vehicle speed sensor:

$$\theta = \sin^{-1} \left[\frac{1}{g} \cdot \left(a_{\text{accel}} - \frac{dv}{dt} \right) \right] \quad (4.8)$$

where a_{accel} is acceleration measured by the accelerometer (m/s^2)

Unfortunately, the accelerometer used in the HRV was adversely affected by the high voltage electrical systems in the vehicle and did not produce reliable measurements. Since inclination information was not available, it was assumed in the tractive energy analysis that the vehicle traveled on level roads. This assumption should not greatly affect the

overall values of tractive energy. The vehicle returned to the same parking location for charging and, hence, there was no net change in the vehicle's potential energy over each trip cycle. Also, the terrain in and around the city of Edmonton is relatively flat so the effect of any non-linearities between climbing and descending hills should be small.

The HRV data acquisition system measured vehicle variables at 1 s intervals. To calculate tractive force with Equation 4.1, the linear acceleration of the vehicle was approximated from the rate of change in the velocity data:

$$a_i = \left. \frac{dv}{dt} \right|_{t_i} \approx \frac{v_{i+1} - v_{i-1}}{2 \cdot \Delta t} \quad (4.9)$$

where Δt is the sampling time interval (1 s)

Tractive power was calculated using Equation 4.5. The positive and negative tractive energies were then determined by simple numerical integration:

$$E_{pos.trac} \approx \sum_{i=1}^n (P_i \cdot \Delta t), \text{ for all } P_i > 0 \quad (4.10)$$

where $E_{pos.trac}$ is positive tractive energy (J)

P_i is the tractive power at each sampling interval (W)

$$E_{neg.trac} \approx \sum_{i=1}^n (|P_i| \cdot \Delta t), \text{ for all } P_i < 0 \quad (4.11)$$

where $E_{neg.trac}$ is negative tractive energy (J)

The positive tractive energy (PTE) is the mechanical energy that the powertrain must supply to propel the vehicle through the driving cycle. The negative tractive energy (NTE) is the mechanical energy that the powertrain and hydraulic brakes must absorb during the driving cycle. The NTE represents the maximum available energy for regenerative braking.

The vehicle dynamic model provides a method of calculating the positive and negative tractive energies for a vehicle from a set of speed and time data. As a basis for comparison, the model was used to calculate the tractive energies for the HRV in the FTP-78 driving cycle. The results are given in Table 4-3. The powertrain must provide a total of 8.43 MJ of PTE during the driving cycle. The powertrain and hydraulic brakes

must absorb 2.85 MJ of NTE. The specific tractive energies can be determined by dividing the tractive energies by the distance traveled during the cycle, 17.76 km. The specific positive tractive energy (SPTE) is 0.475 MJ/km and the specific negative tractive energy (SNTE) is 0.161 MJ/km. Since electrical energy is commonly measured in the watt-hour unit^{*}, equivalent values in this unit are also given in the table. In the remainder of this dissertation, energy measurements will generally be expressed in the watt-hour unit.

Table 4-3. Estimated tractive energy for the HRV in the FTP-78 test cycle

	Tractive energy		Specific tractive energy	
	(MJ)	(kW-h)	(MJ/km)	(kW-h/km)
Positive energy	8.43	2.34	0.475	0.132
Negative energy	2.85	0.792	0.161	0.045

4.2.2. Tractive energy results

The speed-time data collected by the data acquisition system in the HRV allow the vehicle dynamic model to calculate the positive and negative tractive energies for on-road use. Figure 4-4 shows the calculated PTE for 47 driving cycles of varying distance. The data points are from the experiments performed at the U of A and the same driver performed all the tests. As expected for cycles with similar driving conditions, the data points indicate a linear relationship between the PTE and the distance traveled. However, there is a moderate amount of scatter about the least-squares linear regression line. The uncertainties involved in the linear curve fit can be determined using some basic statistical methods shown in Appendix D. The uncertainties used in this dissertation are based on a 95% confidence interval. The intercept of the linear fit with the energy axis occurs at 0.039 ± 0.111 kW-h. The value of the intercept should be zero; however, the offset can be accounted for by the uncertainty in the intercept calculation due to the scatter in the data.

The PTE requirements for the on-road driving cycles can be compared to the FTP-78 energy requirement, which is also shown in Figure 4-4. The required PTE to travel 17.76 km during on-road use was 1.94 ± 0.24 kW-h compared with 2.34 kW-h on

^{*} 1 watt-hour (W-h) = 3600 joules (J)

the FTP-78 driving cycle. The slope of the linear curve fit indicates the SPTE required by the vehicle: 0.107 ± 0.006 kW-h/km compared with 0.132 kW-h/km on the FTP-78 driving cycle. These values indicate a 17% to 19% lower energy requirement for the U of A on-road tests than for the FTP-78 cycle. On-road energy consumption is expected to be lower because road traffic in Edmonton, Canada, is generally uncongested and the HRV was driven conservatively (i.e., low acceleration).

An alternative method is available to estimate the average specific energy for the vehicle. The specific energy is calculated for each individual cycle. The mean of these values is then determined. The SPTE values for each cycle are plotted in Figure 4-5. The mean of these values is 0.109 ± 0.002 kW-h/km, which agrees reasonably with the value of SPTE from the linear regression.

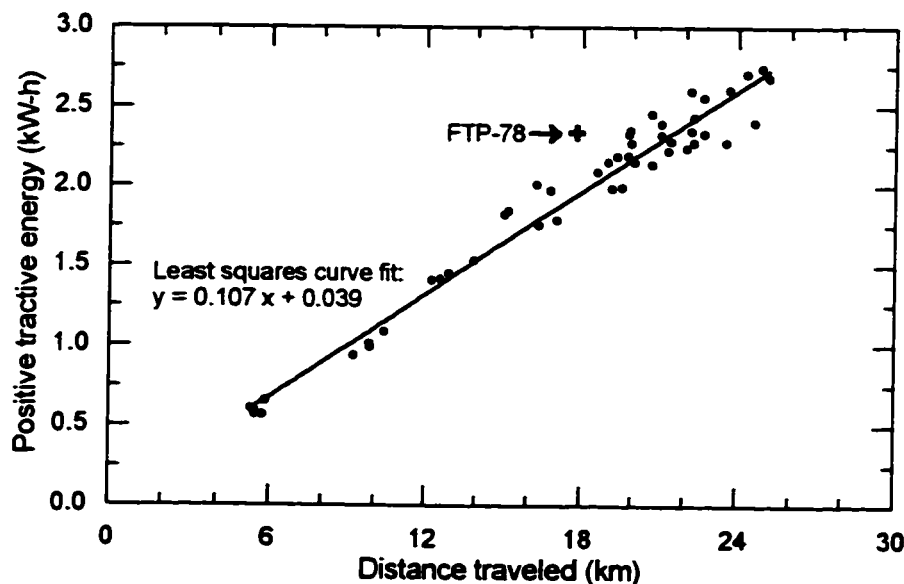


Figure 4-4. Positive tractive energy during U of A tests

The data collected during fleet operation with Edmonton Power indicated a similar PTE requirement to the U of A data. Due to problems with vehicle speed measurement, the data set for tractive energy analysis contained only twenty-one complete trips. Figure 4-6 shows the PTE values for the valid data set. Again, the data points indicate a linear relationship. From the linear curve fit, the SPTE was found to be 0.111 ± 0.005 kW-h/km and the predicted energy required for a 17.76 km trip was 1.99 ± 0.12 kW-h. The SPTE

values for the twenty-one data points in the Edmonton Power data set are plotted in Figure 4-7. The mean value of the data set is 0.115 ± 0.005 kW-h/km.

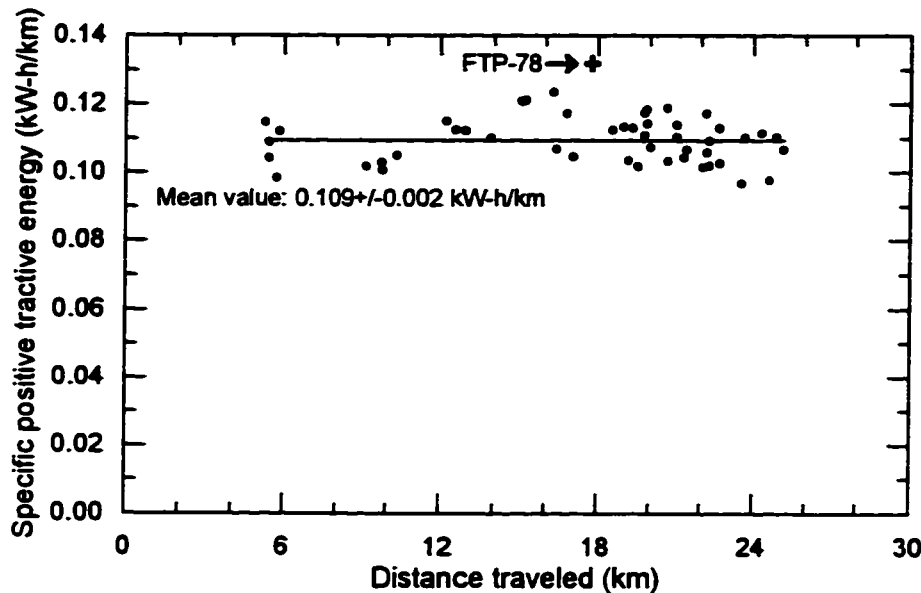


Figure 4-5. Specific positive tractive energy during U of A tests

The HRV was used by a few different of drivers during its time with Edmonton Power. The data set can be sorted by vehicle operator and examined for variations in energy requirements. While caution must be taken when interpreting the results due to the limited number of data points for each driver, a general observation can be made. Different symbols are used for each driver in Figure 4-6 and Figure 4-7. Table 4-4 gives the SPTE values calculated from linear curve fits of each driver's data points. The uncertainties in the values of SPTE are considerably greater than for previous estimates due to the small number of data points and in the case of Driver 3, the close proximity of the data points in terms of the length of trips. Despite the uncertainties, the data suggest that the vehicle requires significantly more tractive energy when used by Driver 1. This is seen most clearly in Figure 4-7 where the data points for Driver 1 are generally higher than for the other drivers.

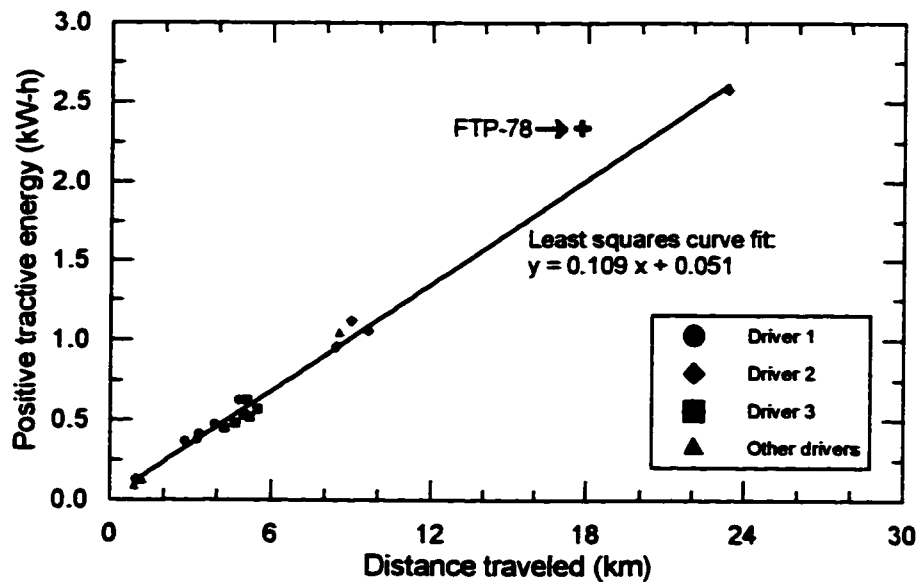


Figure 4-6. Positive tractive energy during Edmonton Power tests

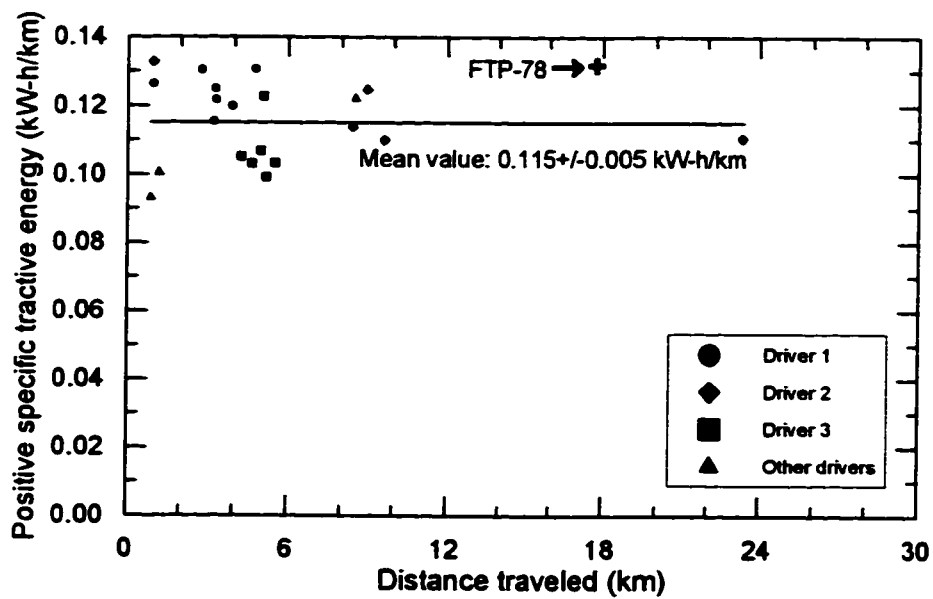


Figure 4-7. Specific positive tractive energy during Edmonton Power tests

Table 4-4. Estimated specific positive tractive energy for three different drivers

Driver	Number of data points	Length of trips (km)	Specific positive tractive energy (kW-h/km)
1	7	0.97 to 4.79	0.127±0.020
2	5	0.96 to 23.2	0.109±0.012
3	6	4.26 to 5.18	0.109±0.135

The NTE calculated by the vehicle dynamic model is the energy that is absorbed by the powertrain and hydraulic brakes during the driving cycle. This energy represents the maximum energy available for regenerative braking. The amount of electrical energy actually produced from regenerative braking will be examined in Section 4.3.

Figure 4-8 gives the NTE in the experiments performed at the U of A. Urban driving conditions in Edmonton are such that the NTE on any given 17.76 km trip is comparable to, but lower than, the FTP-78 test cycle. The NTE during the FTP-78 cycle was estimated to be 0.792 kW-h. This value is within the uncertainty of the NTE from the linear curve fit, 0.637 ± 0.196 kW-h, but 24% higher. Also, the SNTE for the FTP-78 cycle, 0.045 kW-h/km, is 41% higher than the value predicted by the curve fit, 0.032 ± 0.005 kW-h/km. The intercept of the linear regression line with the NTE axis occurs at 0.071 ± 0.089 kW-h. The SNTE values for the forty-seven driving cycles from the U of A tests are plotted in Figure 4-9. A number of cycles have specific negative tractive energies that are similar to the FTP-78 cycle, but the cycles tend to have a lower specific energy. The mean value is 0.036 ± 0.002 kW-h/km, 20% lower than for the FTP-78 cycle.

The data set from the Edmonton Power fleet trials is shown in Figure 4-10 and Figure 4-11. The NTE values in this data set are generally greater than in the U of A data set. The slope of the linear fit in Figure 4-10 indicates a NTE of 0.035 ± 0.004 kW-h/km and the mean value in Figure 4-11 indicates a NTE of 0.043 ± 0.004 W-h/km. The difference between these two values is a result of the distribution of the length of trips. The large group of data points for trips less than 12 km have higher specific energies and influence the mean value. The single data point located at 23.2 km has lower specific energy and influences the slope of the curve fit. Without this single data point, the NTE

indicated by the curve fit becomes 0.040 ± 0.007 kW-h/km, which agrees more closely with the mean estimate of SNTE.

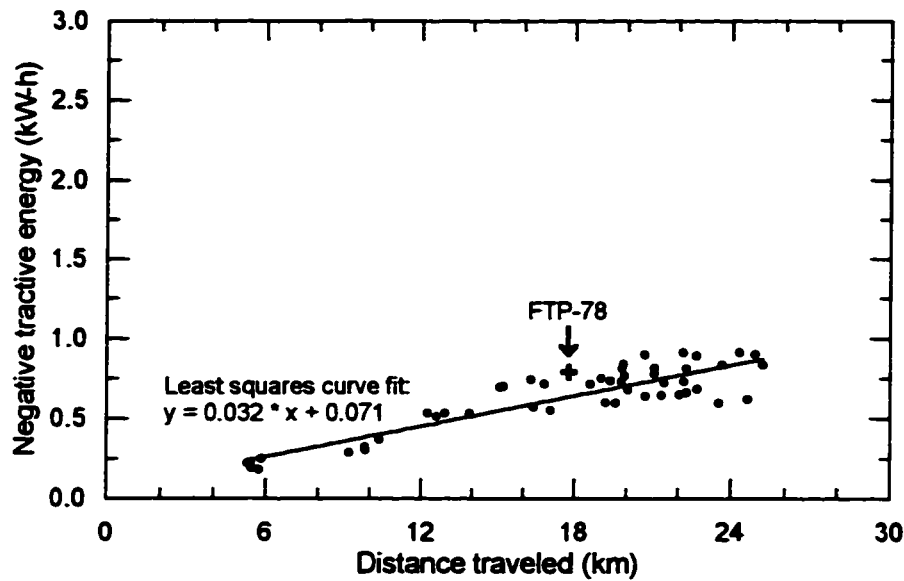


Figure 4-8. Negative tractive energy during U of A tests

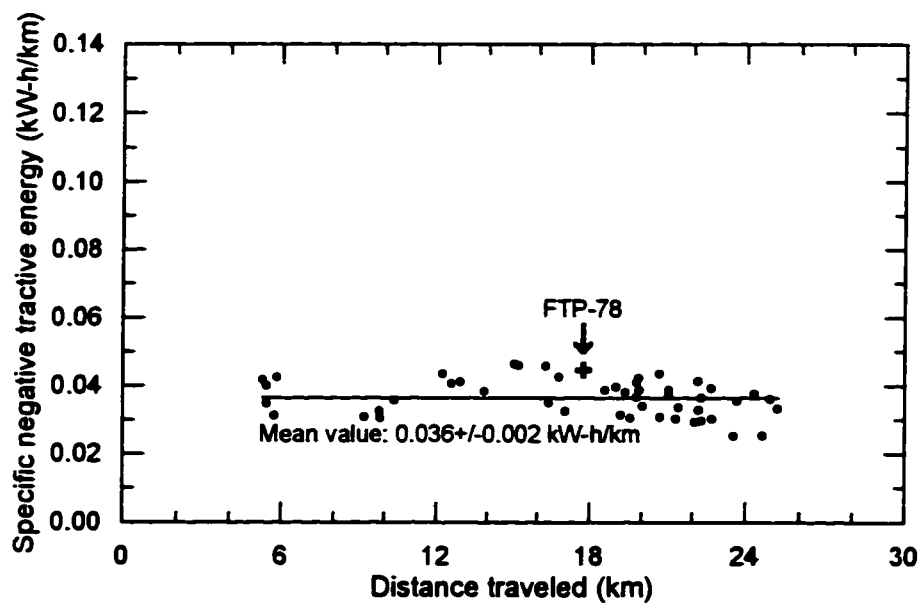


Figure 4-9. Specific negative tractive energy during U of A tests

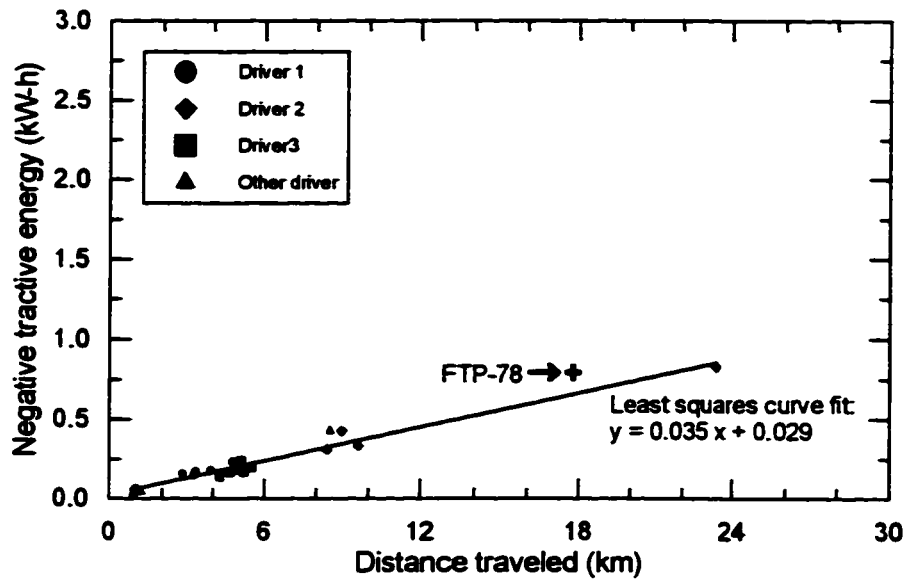


Figure 4-10. Negative tractive energy during Edmonton Power tests

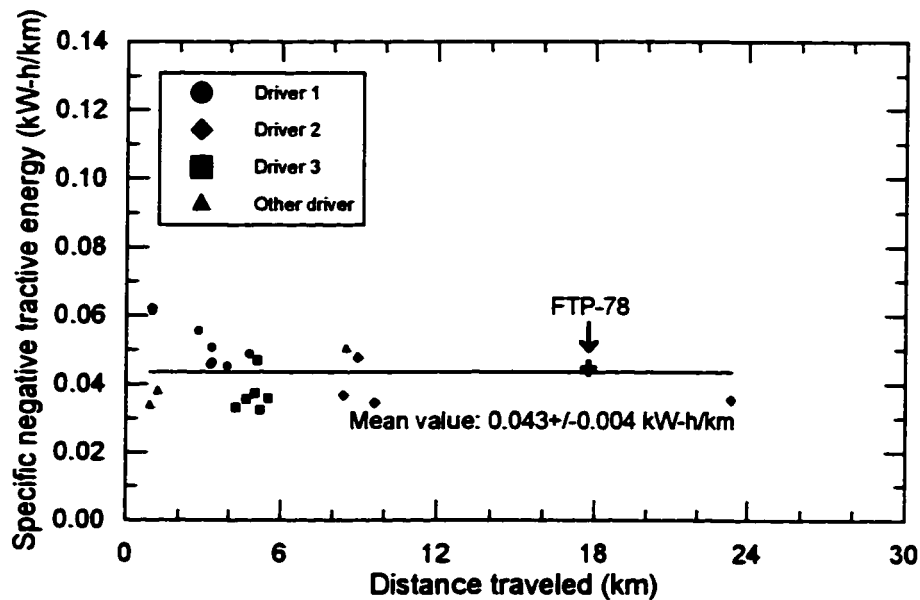


Figure 4-11. Specific negative tractive energy during Edmonton Power tests

Urban driving conditions in Edmonton (as experienced by the HRV) are generally less strenuous than in the FTP-78 cycle. The data indicated positive tractive energies up to 20% lower in on-road tests of the same distance and negative tractive energies up to 30% lower. The NTE available for regenerative braking is approximately 30% of the PTE

required to propel the vehicle in typical driving cycles. The specific energy required to propel the vehicle remains relatively constant. However, there is some indication that shorter trips require higher specific energy. This is not surprising since drivers are more likely to drive conservatively on long trips due to electric range limitations. Conversely, drivers are less concerned about conserving energy on short trips and, therefore, are more likely to drive aggressively. Also, vehicle warm-up would increase specific energy consumption for short trips. (There may also be a correlation between short trips in intense urban conditions and longer trips in suburban cruising conditions. However there are insufficient data to examine this hypothesis.)

The tractive energy analysis indicates that driving cycles during the Edmonton Power fleet service required slightly more energy than driving cycles during the U of A tests. However, the tractive energies were comparable. Thus, the remaining analysis of the HRV performance will focus on the data collected during the U of A experiments. These experiments were performed by the same driver under similar driving conditions, so it was expected that correlations in the data would be more readily apparent.

4.3. Powertrain performance analysis

The instrumentation in the HRV measures battery pack voltage and the flow of electrical current to and from the battery pack. It also monitors the electrical current to accessory loads. The flow of electrical current to the electric drive system was determined by subtracting the electrical current used by the accessories from the electrical current flowing out of the battery pack.

$$I_{pos.drive} = I_{batt.disch} - I_{access} \quad (4.12)$$

where $I_{pos.drive}$ is the electrical current flowing to the electric drive system (A)

$I_{batt.disch}$ is the electrical current flowing out of the battery pack (A)

I_{access} is the electrical current used by the vehicle accessories (A)

Similarly, the electrical current produced by regenerative braking was determined by adding the electrical current returned to the battery pack and the electrical current used by the accessories.

$$I_{neg.drive} = I_{batt.regen} + I_{access} \quad (4.13)$$

where $I_{neg.drive}$ is the electrical current produced by regenerative braking (A)
 $I_{batt.regen}$ is the electrical current flowing to the battery pack from regenerative braking (A)

The flow of electrical power was then calculated by multiplying the current flow by the battery pack voltage. Knowing the power flow to each component, the respective energy values are determined by numerical integration similar to Equations 4.10 and 4.11.

4.3.1. Powertrain energy

The positive drive energy is the electrical energy supplied to the motor controller to produce PTE. The values of positive drive energy for the U of A on-road tests are shown in Figure 4-12. As with the tractive energy graphs in Section 4.2, a linear relationship appears between energy and distance traveled. The slope of the linear curve fit indicates the specific positive drive energy required by the motor controller: 0.160 ± 0.007 kW-h/km.

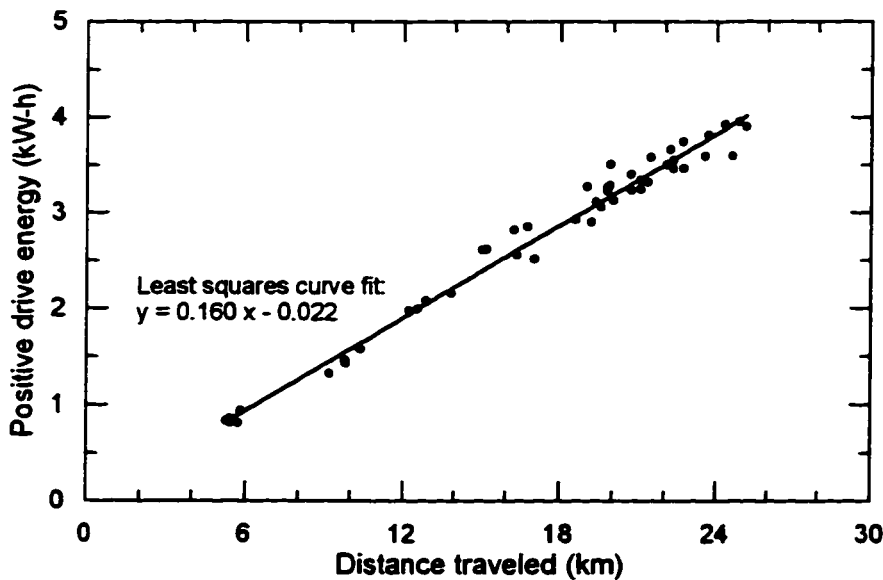


Figure 4-12. Positive drive energy, $E_{pos.drives}$, used by electric drive system during U of A tests

The negative drive energy is the electrical energy produced by the drive system from regenerative braking. Figure 4-13 shows the values of negative drive energy for the U of A on-road tests. Again, a linear relationship is present. The specific negative drive energy is 0.019 ± 0.004 kW-h/km. Regenerative braking returned about 12% of the electrical energy required to drive the powertrain.

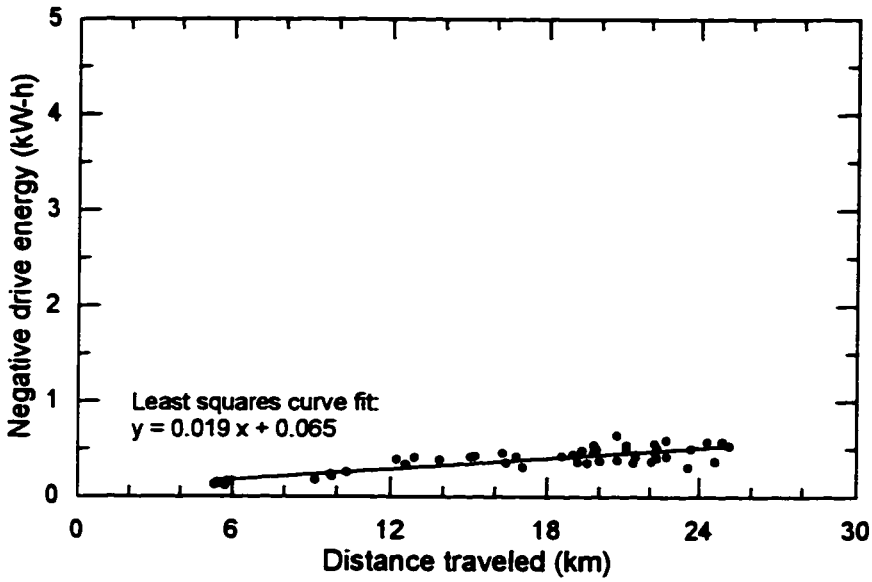


Figure 4-13. Negative drive energy, $E_{neg.drive}$, produced by regenerative braking during U of A tests

4.3.2. Powertrain efficiency

The powertrain drive efficiency measures the performance of the electric drive system in producing mechanical tractive energy from electrical energy:

$$\eta_{drive} = \frac{E_{pos.trac}}{E_{pos.drive}} \cdot 100\% \quad (4.14)$$

where η_{drive} is the powertrain drive efficiency (%)
 $E_{pos.trac}$ is the PTE estimated by the vehicle dynamic model (kW-h)
 $E_{pos.drive}$ is the electrical energy supplied to the drive system (kW-h)

The regenerative braking efficiency measures the performance of the drive system in using the available mechanical tractive energy to produce electrical energy:

$$\eta_{regen} = \frac{E_{neg,drive}}{E_{neg,brac}} \cdot 100\% \quad (4.15)$$

where η_{regen} is the regenerative braking efficiency (%)
 $E_{neg,drive}$ is the electrical energy produced by regenerative braking (kW-h)
 $E_{neg,brac}$ is the NTE estimated by the vehicle dynamic model (kW-h)

Separate efficiency values are used to evaluate the difference in performance between operating the drive system as a motor and as a generator. When stopping, tractive braking energy is divided between the regenerative and hydraulic braking systems. As a result, the effective regenerative braking efficiency is dependent on driving conditions and driver behavior. Gradual stops are accomplished with only regenerative braking and give high regenerative braking efficiency; sharp stops require the assistance of friction braking and result in low regenerative braking efficiency.

Figure 4-14 and Figure 4-15 show the powertrain drive and regenerative braking efficiencies, respectively, for the U of A data set. The mean powertrain drive efficiency was $68.8 \pm 0.7\%$ and the data points also fall in a narrow band near the mean. The mean regenerative braking efficiency was $62.7 \pm 1.6\%$ and there is a considerable variation in the regenerative braking efficiency among the driving cycles.

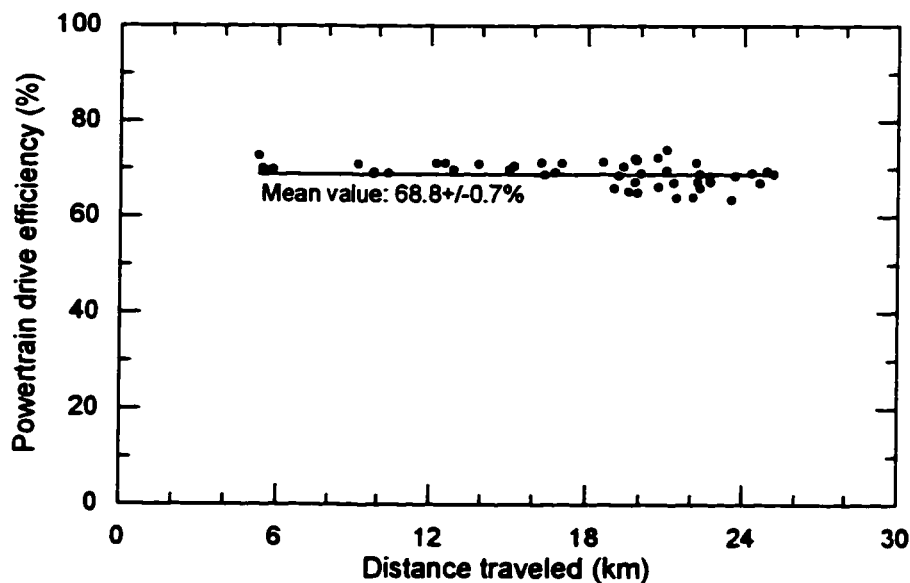


Figure 4-14. Powertrain drive efficiency, η_{drive} , during U of A tests

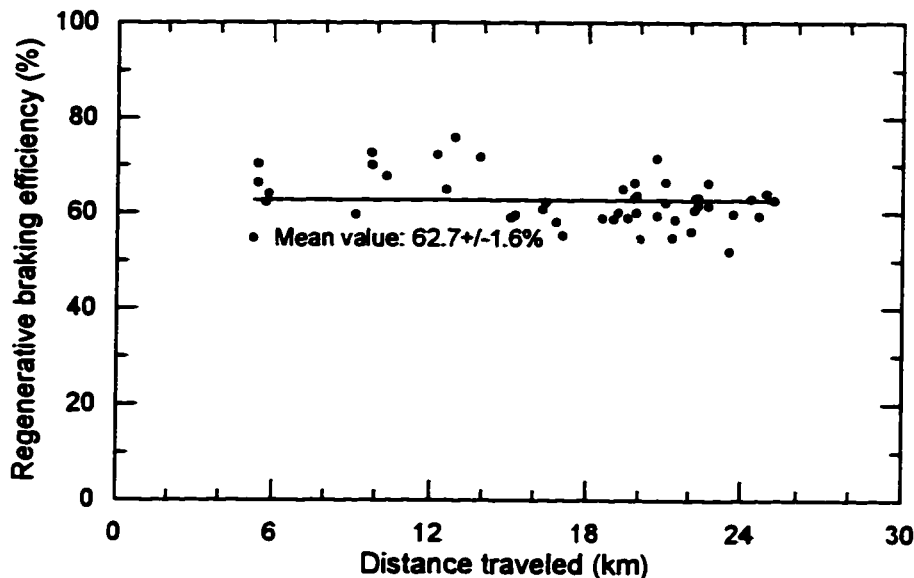


Figure 4-15. Regenerative braking efficiency, η_{regen} , during U of A tests

4.4. Vehicle accessory load

The energy required to operate vehicle accessories (i.e., components not required to produce tractive forces) is normally small compared to the tractive energy. However, when the vehicle is used at extreme temperatures, the energy consumed by a cabin heater or air conditioner can be significant.

While the HRV was equipped with a cabin heater for winter operation, the data gathered during fleet service with Edmonton Power did not provide a clear picture of accessory energy requirements at cold temperatures. For 45 driving cycles from April through December, 1995, the time-averaged accessory power over each cycle and the average ambient temperature are shown in Figure 4-16. The HRV was predominately used at temperatures above -5°C when the cabin heater was not needed; the mean of the data points is 0.411 kW. The drivers were hesitant to use the vehicle in cold weather because of the limited electric range coupled with the noise and vibration produced by the combustion engine.

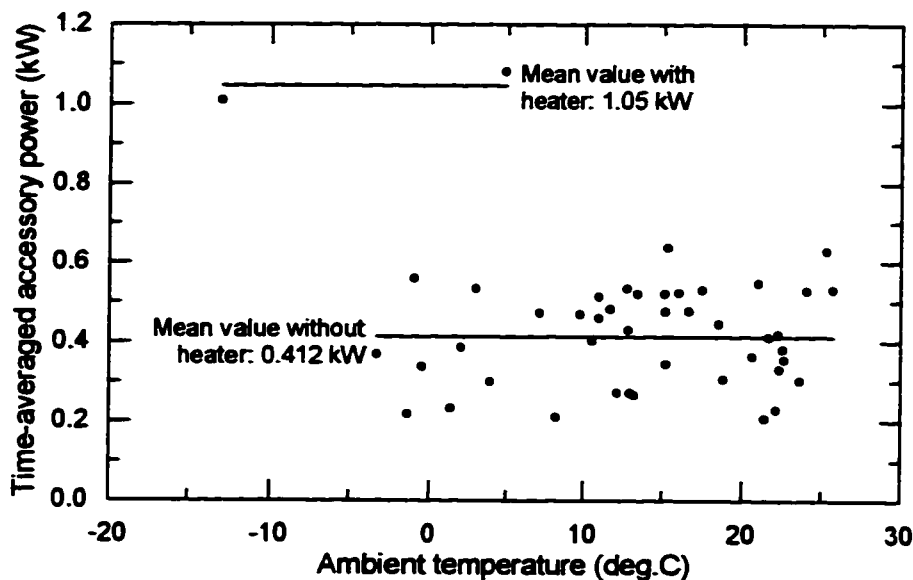


Figure 4-16. Average accessory power and ambient temperature during fleet service with Edmonton Power

The data from the U of A on-road tests indicate that the amount of energy consumed by the accessories is linearly dependent on the time that the HRV was in use. Figure 4-17 shows the energy consumed during the 47 driving cycles in the data set. Two linear relationships appear; the slopes of which indicate two rates of energy consumption. The lower rate of energy consumption, 0.185 ± 0.006 kW, represents the power required to operate the basic vehicle accessories: items such as the battery pack and electric motor cooling fans, turn signals, stop lamps, driver instrumentation, and trickle charging of the 12VDC engine starting battery. The higher rate of consumption, 0.357 ± 0.018 kW, occurred during night time driving when the vehicle's exterior lights (headlights and parking lights) were also used. The ambient temperature was relatively warm during the U of A tests so the cabin heater was not used in this data set.

Alternatively, the average accessory power during each trip can be plotted against the duration of each trip as shown in Figure 4-18. The two different accessory power levels are apparent. The mean value using the minimum vehicle accessories is 0.183 ± 0.002 kW and the mean with the exterior lights turned on is 0.342 ± 0.003 kW. Both of these results are in reasonable agreement with the accessory power values determined from Figure 4-17.

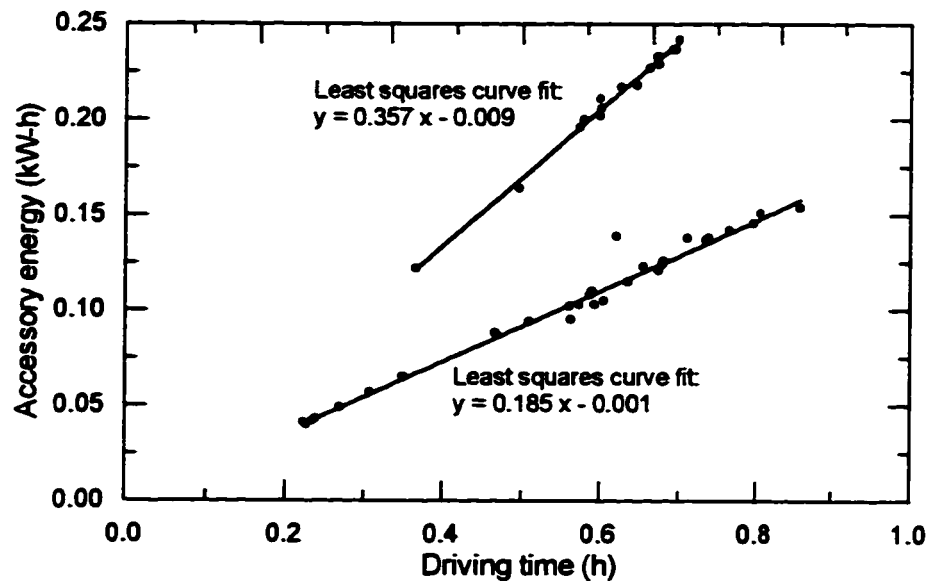


Figure 4-17. Accessory energy during U of A tests

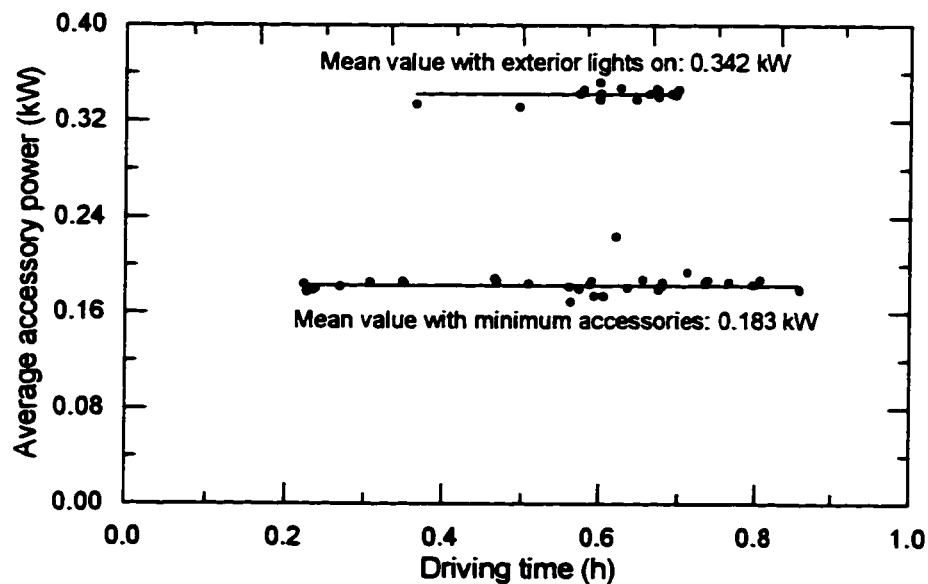


Figure 4-18. Average accessory power during U of A tests

The electrical energy consumption of the drive system and the accessories can be compared if an estimate is made of a typical average vehicle speed in urban driving. In this case, an average speed of 30 km/h will be used. The specific positive energy consumed by the drive system was estimated to be about 0.160 kW-h/km. The average

electrical power required by the drive system, 4.8 kW, is obtained from multiplying the specific energy by the average speed. The positive drive system and accessory power requirements for three situations are given in Table 4-5. The accessories consume a relatively small portion (<10%) of the total electrical power supplied by the battery pack in warm weather. At low ambient temperatures, the cabin heater and fan would increase the total electrical load. The power required would depend on the ambient temperature; however, an average accessory power of 1.2 kW would not be an unreasonable estimate. At this level, the accessories would be 20% of the total energy consumption.

Table 4-5. Electrical power requirements

	Minimum accessories		Exterior lights on		Heater and lights on	
	Power (kW)	Percent of total	Power (kW)	Percent of total	Power (kW)	Percent of total
Positive drive power	4.8	96.3	4.8	93.3	4.8	80
Accessory power	0.183	3.7	0.342	6.7	1.2	20
Total power	5.0	100	5.1	100	6.0	100

The energy required to heat a vehicle in cold weather must be addressed if electric and hybrid vehicles are to be used areas like Canada and the northern United States. Further research is needed to better measure the energy requirement and the effects on vehicle range and efficiency.

4.5. Battery performance analysis

4.5.1. Battery energy

The most serious problem facing electric vehicles is the low energy storage density of batteries. Although the specific energy consumption of an electric vehicle is low, the energy storage density of a battery pack is extremely low compared with gasoline. After including the mass of a fuel tank, pump, and lines, the specific energy storage density of gasoline is typically about 40 000 kJ/kg, or 11 000 W-h/kg. The maximum measured battery capacity of the HRV during the course of the research was 7.05 kW-h (on the Highway Fuel Consumption Test Cycle at Environment Canada's laboratory). The mass of the battery pack, not including the battery box, was approximately 290 kg giving a

specific energy density of 24.3 W-h/kg or 87.5 kJ/kg. (Published values suggest a specific energy density between 22 W-h/kg and 29 W-h/kg for conventional lead-acid batteries [22], so the measured performance is typical.) The maximum battery capacity gave only 0.219% of the energy density of gasoline.

After one and a half years of light use, the observed maximum battery capacity decreased to 4.04 kW-h, corresponding to a specific energy density of 13.9 W-h/kg. Possible reasons for this decline include battery degradation from deep discharges and improper charging (overcharging or undercharging). As discussed in Chapter 2, lead acid batteries have a relatively short useful life (500 to 750 cycles). Williams [45] estimated that 258 kW-h of energy is required in the production of each kW-h of storage capacity of an advanced lead-acid battery with a specific energy of 40 W-h/kg. Thus, although it was not evaluated in this research, the energy to manufacture a vehicle component can be significant to the lifetime energy efficiency.

The given HRV battery capacities are the observed capacities ($E_{\text{batt,disch}}$); the measured maximum energy discharged from the battery before charging is required. The observed capacity in use is slightly greater than the actual capacity since regenerative braking supplies some energy to the battery during vehicle use. Figure 4-19 illustrates how regenerative braking affects the observed battery capacity. In this example, the battery has an actual maximum capacity of 60 units of energy. To recharge the battery, 100 units of energy (E_{charge}) must be supplied by the battery charger. Without regenerative braking the observed capacity is the same as the actual capacity. If regenerative braking is used and it returns 15.2% of the energy leaving the battery, ($E_{\text{batt,regen}}$), the battery can supply a total of 66 units of energy (assuming the battery has a constant energy storage efficiency of 60%). The observed capacity of the battery is now 66 units. Although the observed capacity is affected by the energy recovered from regenerative braking, it is a valid measure of battery capacity from a practical point of view. It indicates the amount of energy available for use in the vehicle, and, hence, is directly proportional to vehicle range.

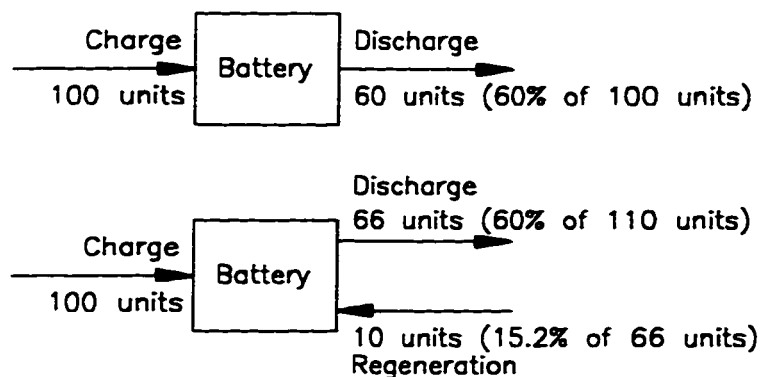


Figure 4-19. Effect of regenerative braking on observed battery capacity

In the experiments conducted at the U of A, a number of consecutive charge and driving cycles were performed. The amount of charge energy was increased starting from a 1 kW-h charge until the maximum observed battery capacity was reached. After each charge, the vehicle was driven until the battery was discharged to a point where it could not supply adequate operating voltage to the motor controller on acceleration. Since this point is subject to variability in operating conditions, a number of tests were performed at each level of charge to ensure the test results were reasonably consistent. A total of 46 good test points were obtained*. To evaluate battery performance, the observed battery capacity has been plotted against energy supplied to the battery in Figure 4-20. The battery required a minimum of about 7.25 kW-h of energy to reach the maximum observed battery capacity of 4.04 kW-h.

The main concern of the vehicle operator is the amount of energy that the charger must provide to recharge the battery, since this energy is purchased from the electric utility grid. In Figure 4-21, the observed battery capacity is plotted against only the charge energy. About 6.75 kW-h of electrical energy was required from the battery charger to obtain the maximum observed battery capacity.

As discussed in the last two sections, the SPTE and powertrain drive efficiency are relatively constant. Therefore, vehicle range is expected to be proportional to the observed battery capacity. Also, the relationship between vehicle range and charge energy

* The battery electrolyte level was low during one test resulting in a significant drop in battery capacity. The data from that test were not used in the analysis.

is expected to be similar to the relationship shown in Figure 4-21. The maximum vehicle range is about 25 km, as shown in Figure 4-22.

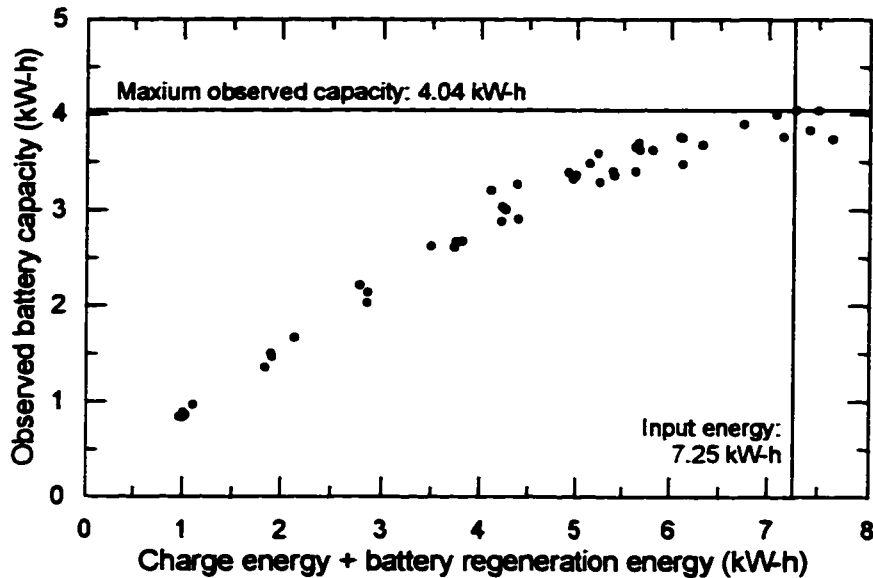


Figure 4-20. Observed battery capacity during U of A tests ($E_{\text{batt.disch}}$, as a function of input energy, $E_{\text{charge}} + E_{\text{batt.regen}}$)

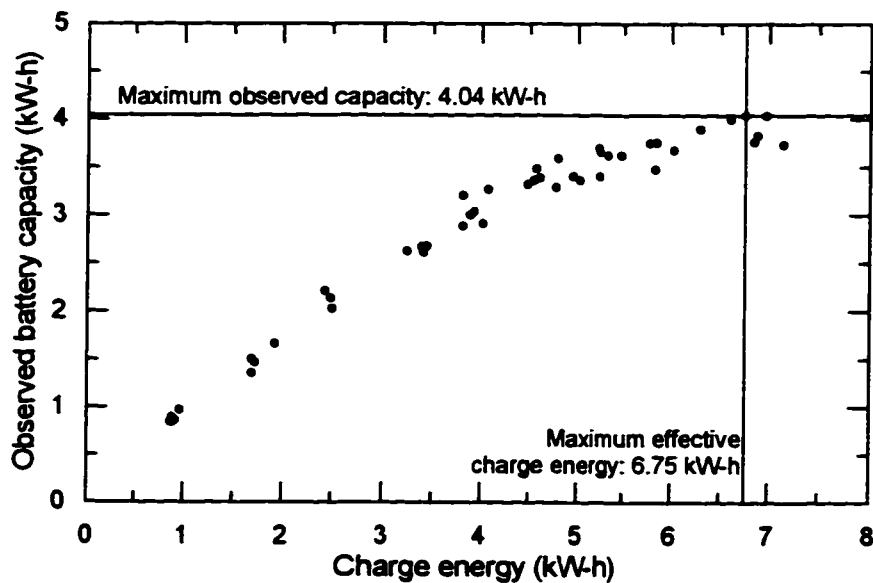


Figure 4-21. Observed battery capacity during U of A tests ($E_{\text{batt.disch}}$, as a function of charge energy, $E_{\text{charge}} + E_{\text{batt.regen}}$)

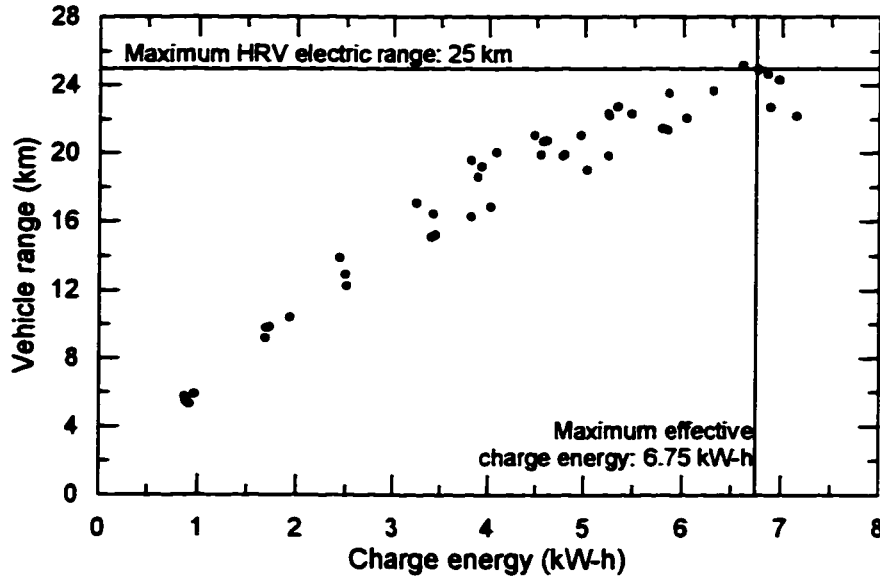


Figure 4-22. Vehicle range for varying levels of charge energy, E_{charge}

4.5.2. Battery efficiency

To evaluate the performance of the battery pack, the battery's actual energy storage efficiency (η_{batt}) is defined as the energy the battery pack supplies during the driving cycle divided by the energy that the battery receives from the charger and regenerative braking:

$$\eta_{\text{batt}} = \frac{E_{\text{batt.disch}}}{E_{\text{charge}} + E_{\text{batt.regen}}} \cdot 100\% \quad (4.16)$$

where η_{batt} is the energy storage efficiency of the battery (%)
 $E_{\text{batt.disch}}$ is the energy discharged from the battery (kW-h)
 E_{charge} is the energy supplied by the charger to the battery (kW-h)
 $E_{\text{batt.regen}}$ is the energy returned to the battery by regenerative braking (kW-h)

This is the true storage efficiency of the battery pack and is the most useful. There are two alternative measure of battery energy storage efficiency. From the point of view of the vehicle operator, the energy recovered by regenerative braking is "free". Therefore, an observed battery efficiency ($\eta_{\text{obs.batt}}$) is defined as the energy supplied by the battery pack during the driving cycle divided by the energy that the charger must supply to the

battery (i.e., the useable energy that the vehicle receives divided by the energy the operator must pay for):

$$\eta_{obs.batt} = \frac{E_{batt.disch}}{E_{charge}} \cdot 100\% \quad (4.17)$$

where $\eta_{obs.batt}$ is the observed energy storage efficiency of the battery (%)

This observed efficiency could be greater than 100% under certain conditions, as shown in Figure 4-23. In this hypothetical case, the vehicle has a battery with an actual efficiency of 85%. The vehicle also operates efficiently so regenerative braking is able to return 19.6% of energy leaving battery. The observed battery capacity would be 102 units of energy for a charge energy of 100 units; therefore, $\eta_{obs.batt}$ would be 102%. η_{batt} remains at 85% with or without regenerative braking. $\eta_{obs.batt}$ is affected by the design of the vehicle and the driving cycle so it is not as useful as η_{batt} .

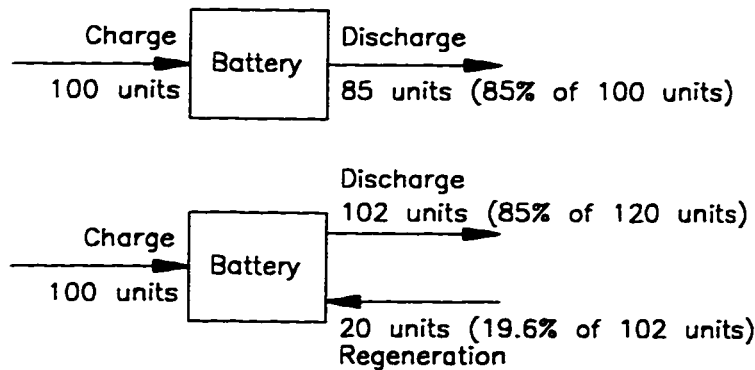


Figure 4-23. Effect of regenerative braking on observed battery performance

Another alternative measure of battery efficiency arises from electric vehicle instrumentation practices. Frequently, vehicles are equipped with meters that simply measure the net battery output (i.e., the discharge energy less the regenerated energy). A net energy storage efficiency ($\eta_{net.batt}$) is then calculated by dividing the net battery output by the charge energy:

$$\eta_{net.batt} = \frac{(E_{batt.disch} - E_{batt.regen})}{E_{charge}} \cdot 100\% \quad (4.18)$$

where $\eta_{net.batt}$ is the net energy storage efficiency of the battery (%)

While the calculation is very simple, $\eta_{net.batt}$ has little value. η_{batt} is the best indicator of battery performance and $\eta_{obs.batt}$ is useful when examining the battery pack as a part of a particular vehicle system. For the illustration given in Figure 4-23, all three measures of efficiency give the same battery efficiency (85%) without regenerative braking. The addition of regenerative braking does not change η_{batt} but does change $\eta_{obs.batt}$ and $\eta_{net.batt}$. $\eta_{obs.batt}$ increases to 102%, reflecting the increase in energy available for producing tractive power. However, $\eta_{net.batt}$ decreases to 82%. Thus, $\eta_{net.batt}$ does not represent the real performance of the battery like the η_{batt} , nor does it represent the positive benefits of regenerative braking like $\eta_{obs.batt}$. $\eta_{net.batt}$ will not be used in the following discussion of battery performance.

The actual energy storage efficiency of the HRV battery pack as measured during U of A testing is shown in Figure 4-24. η_{batt} varied from about 85% when operating at low states of charge (SOC) down to about 55% for full charge cycles. The SOC refers to how much energy is stored in the battery relative to its maximum capacity (i.e., how “full” it is); a fully charged battery is at a 100% SOC. The data indicate that a battery at a low SOC can store electrical energy more efficiently than a battery at a high SOC.

The observed energy storage efficiency of the battery pack, shown in Figure 4-25, varies from about 94% down to about 58%. At low states of charge the battery can more efficiently store energy from regenerative braking. Therefore, the increase in $\eta_{obs.batt}$ over the actual efficiency is greater at low charge levels (about 9%) and less at high charge levels (about 3%).

The energy storage characteristics of the battery pack discussed in this section lead to an important conclusion about the operation of an electric vehicle. An inherent compromise must be made between high energy efficiency and long driving range, which is clearly shown in Figure 4-26. Very high energy efficiency can be achieved when the vehicle is operated at low states of charge; however, vehicle range will be extremely

limited and battery life is adversely affected. The vehicle can have a much greater range by charging the battery to a higher SOC, but efficiency will drop substantially.

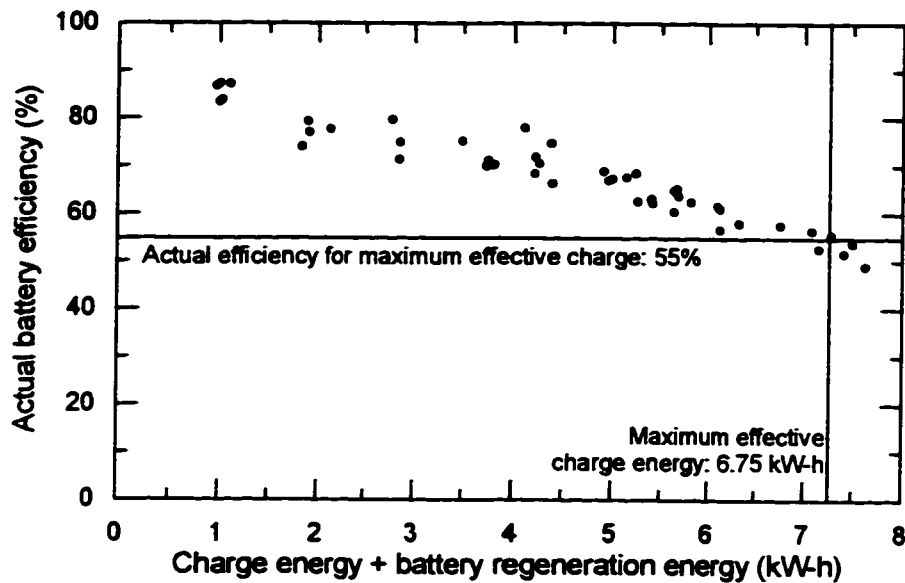


Figure 4-24. Actual battery efficiency, η_{batt} , during U of A tests

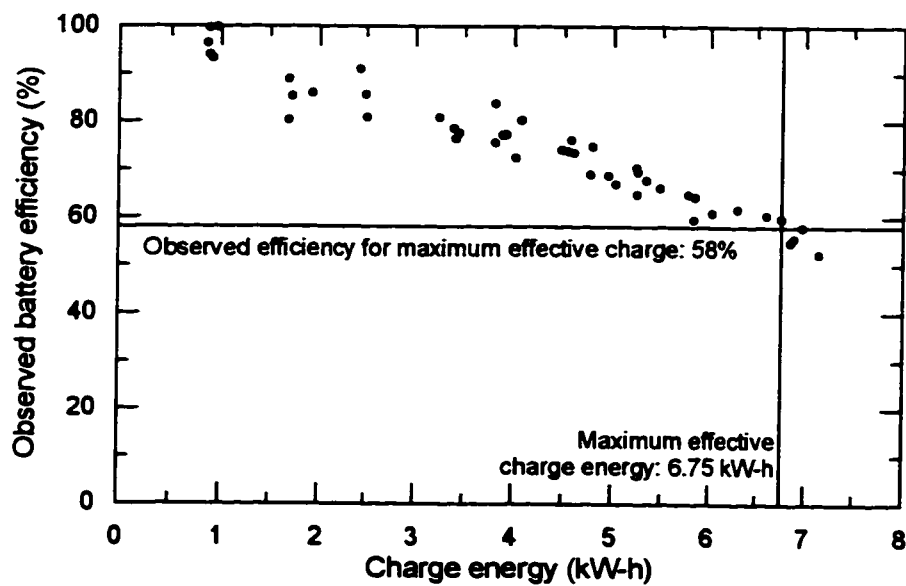


Figure 4-25. Observed battery efficiency, $\eta_{\text{obs. batt}}$, during U of A tests

The charge efficiencies shown in Figure 4-26 were measured by completely discharging and recharging the battery in successive cycles. Hence, each charge cycle began at a low SOC. If charge cycles were started from a high SOC, lower battery efficiencies would be expected. In actual service, the operator normally maintains the vehicle at a high state of charge even when the vehicle is used for only very short trips. This keeps the vehicle prepared for long trips, but adversely affects vehicle efficiency. In fact, the in-use battery efficiency would be expected to be at or below the full charge efficiency of 58%.

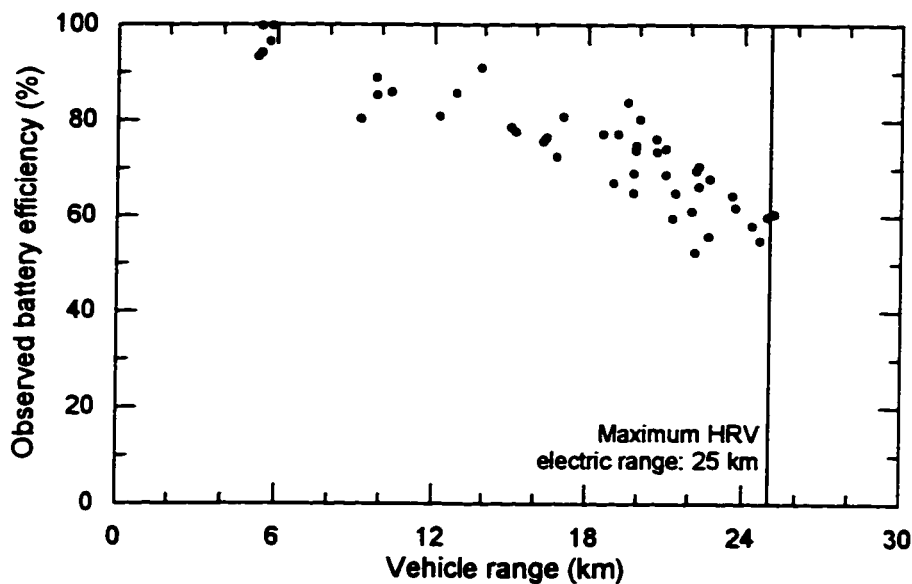


Figure 4-26. Observed battery efficiency, $\eta_{\text{obs.batt}}$, for various vehicle ranges during U of A tests

4.5.3. Temperature effects

In the cold temperature tests conducted by Environment Canada, the electric range of the car decreased dramatically from 27.4 km (at 20°C) to 5.6 km (at -15°C). In these tests, the vehicle was placed at the test temperature for 12 h to 24 h, allowing the battery temperature to drop after it had been charged at room temperature. During field operation with Edmonton Power the vehicle was parked and charged indoors so the

battery pack remained relatively warm throughout the year. As shown in Figure 4-27, over about 8 months of vehicle operation, the battery temperature only ranged between 12°C and 31°C while the ambient temperature ranged between -12°C and 26°C. The heat capacity of the battery pack is large, the driving range is short, and heat is generated internally during discharge. Therefore, the battery temperature only decreased moderately during trips in cold ambient temperatures and performance was not greatly affected.

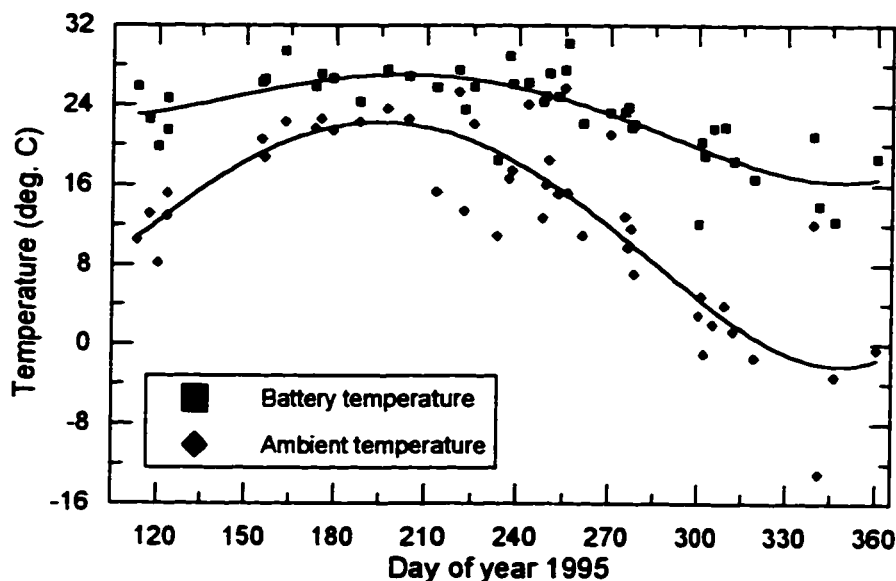


Figure 4-27. Battery pack and ambient temperature during in-service tests with Edmonton Power

The decrease in the performance of lead-acid batteries at low temperatures is well known and temperature gradients within large battery packs can also significantly affect performance [46, 47]. Thus, thermal management and its effects on maintaining battery performance would be important topics of research for vehicles parked outdoors. Battery performance is also affected by other service conditions, such as the rates of charge and discharge. Performance tests that simulate conditions encountered in electric vehicle applications are needed to characterize battery performance [47].

4.6. Battery charger energy and efficiency

In analysis of electric vehicle performance, the battery charger is an important component. The energy used in a pure electric vehicle or normally used in a range-extending HEV originates from the electric utility grid and must pass through the battery charger to be stored in the traction battery. Thus, the efficiency of the battery charger is very important to the overall consumption of the vehicle. The instantaneous efficiency of the battery charger is determined by the ratio of output power to input power:

$$\eta_{i, \text{charger}} = \frac{P_{\text{charge}}}{P_{\text{utility}}} \cdot 100\% \quad (4.19)$$

where $\eta_{i, \text{charger}}$ is the instantaneous efficiency of the battery charger at a specific time and charge rate (%)
 P_{charge} is the output power from the battery charger (W)
 P_{utility} is the input power required by the battery charger (W)

The energy efficiency of the battery charger for a given charge cycle is determined from the ratio of output energy to input energy:

$$\eta_{\text{charger}} = \frac{E_{\text{charge}}}{E_{\text{utility}}} \cdot 100\% \quad (4.20)$$

where η_{charger} is the energy efficiency of the battery charger over a charge cycle (%)
 E_{utility} is the energy the charger uses from the electric utility grid (kW-h)

While charging the HRV, the battery charger supplies power to run the battery pack ventilation fans, about 8.7 W, and to operate the data acquisition system, about an additional 16 W. The electrical power for these auxiliary components was not included as a part of the battery charger's output in determining efficiency, since they do not directly contribute to vehicle propulsion.

4.6.1. Performance variation while charging

The instantaneous efficiency of the HRV battery charger during the course of a 12 h charge is shown in Figure 4-28. For the first 4.6 h, the charger delivers 4.5 A of DC

current and is operating near its maximum power output (900 W). The efficiency of the battery charger is over 70% during this period. When the battery reaches its maximum charging voltage (205 V), the charger reduces its power output to limit water loss in the battery. At this point, the charger has delivered about 3.9 kW-h or 58% of the energy required for a full charge. By the end of the charge cycle, the output power has dropped to about 170 W and the instantaneous efficiency has dropped to about 52%. A part of this efficiency drop is due to the power for the auxiliary components, about 25 W, which contributes to the demand for utility power but not to the charger output power. (If this power was included in the charger output, the charger's instantaneous efficiency would increase by about 2% at high output power and 8% at low output power.)

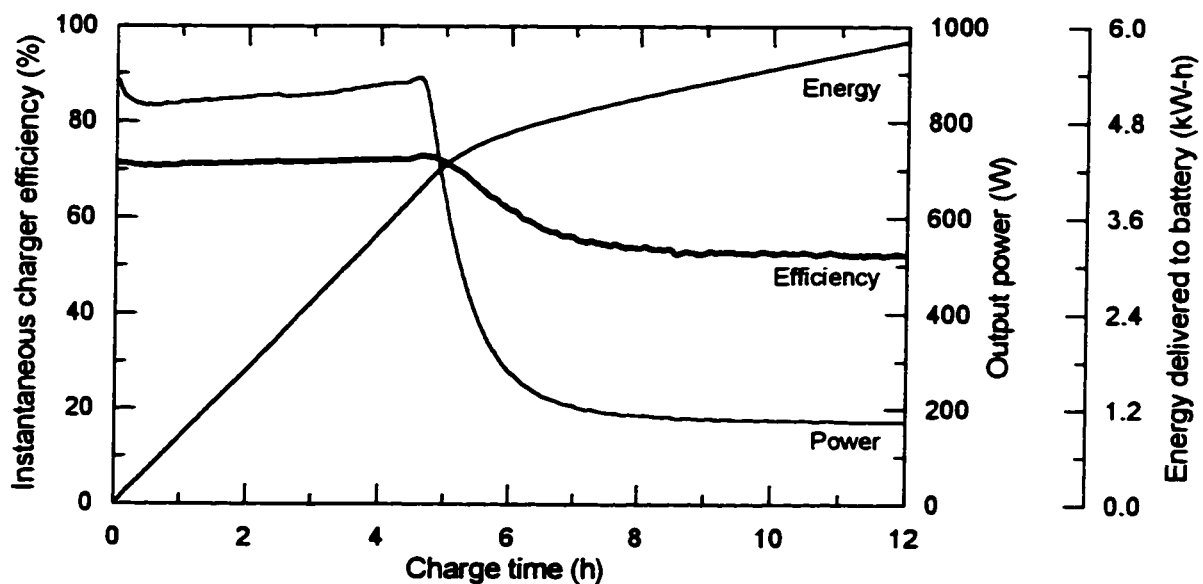


Figure 4-28. Typical battery charger performance over a 12 h charge

Figure 4-29 compares the battery charger's instantaneous efficiency with its output power for the same 12 h charge as shown in Figure 4-28. The small "hook" on the right hand end of the curve occurs over the first 4.6 h of charging. The efficiency increases with the rising output power and with the rising charging voltage. The charger reaches a peak efficiency of 73% at an output of 895 W. The long curve from the maximum output power down to 170 W corresponds to the period from 4.6 h to 12 h. Here, the output

voltage remains essentially constant, but the efficiency decreases with the decreasing charging current and power.

With a peak efficiency of 73%, the HRV battery charger performs reasonably well, considering the fact it is assembled from components not specifically designed for this application as described in Section 3.1.3. Battery chargers designed as complete integrated units should be able to obtain higher efficiencies. For example, one company rates the full power efficiency of their electric vehicle chargers from 85% for a 1.5 kW charger to 93% for a 25 kW charger [48]. However, part load efficiency is also critical since a substantial fraction of the charge is delivered at less than full power. To properly evaluate the energy efficiency of a charger over a charge cycle a complete efficiency/power curve is required.

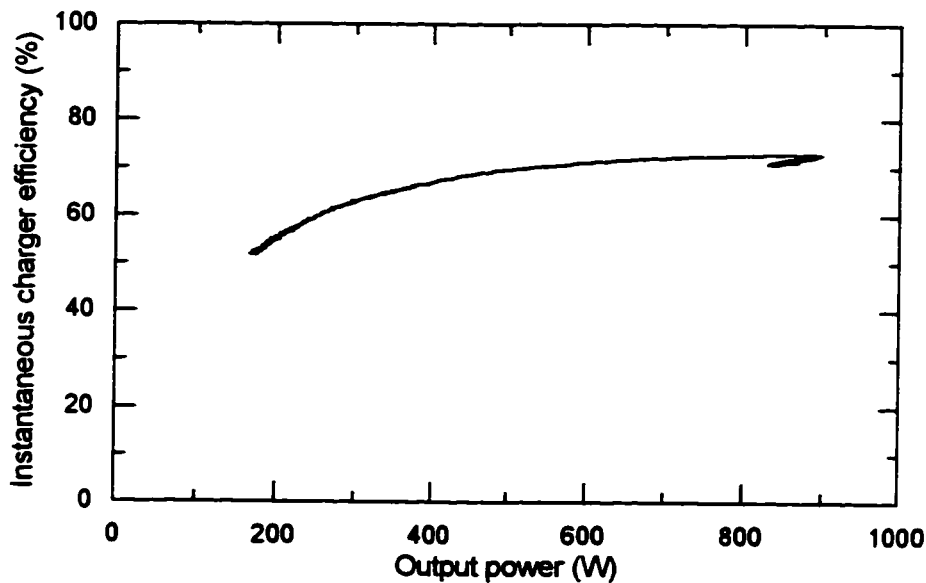


Figure 4-29. Instantaneous battery charger efficiency, $\eta_{i, \text{charger}}$, as a function of output power, P_{charge}

4.6.2. Performance variation among charge cycles

The energy efficiency of the battery charger for a charge cycle, η_{charger} , depends on the amount of energy delivered during the charge. The energy efficiencies measured in the U of A tests are shown in Figure 4-30 as a function of the charge energy. For charge

cycles beginning at a low SOC, the energy efficiency of the charger remains relatively constant, $70.5 \pm 1.0\%$, up to a charge energy of about 5 kW-h. The energy efficiency decreases at higher levels of charge. For a full charge of 6.75 kW-h, the energy efficiency is 64% and 10.5 kW-h of energy is required from the utility grid, as shown in Figure 4-31.

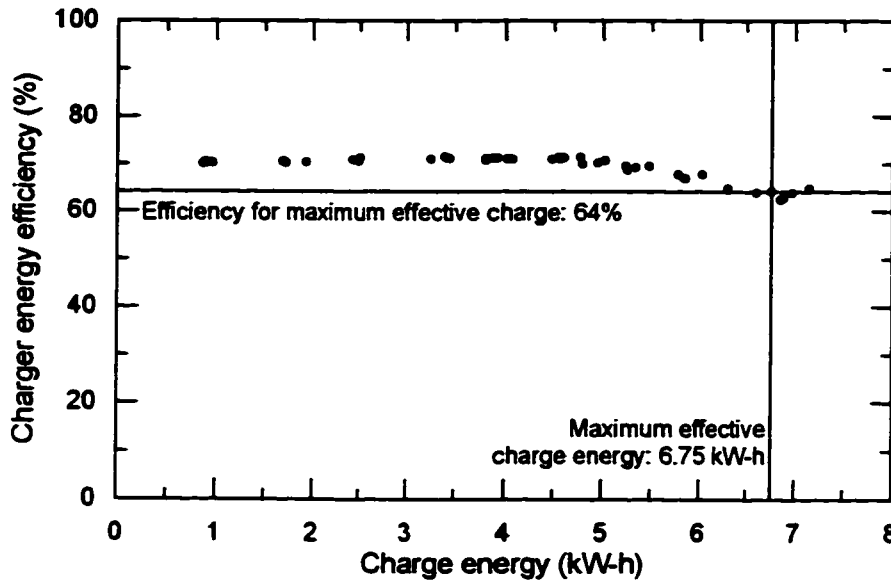


Figure 4-30. Battery charger energy efficiency, η_{chargers} as a function of charge energy, E_{charge}

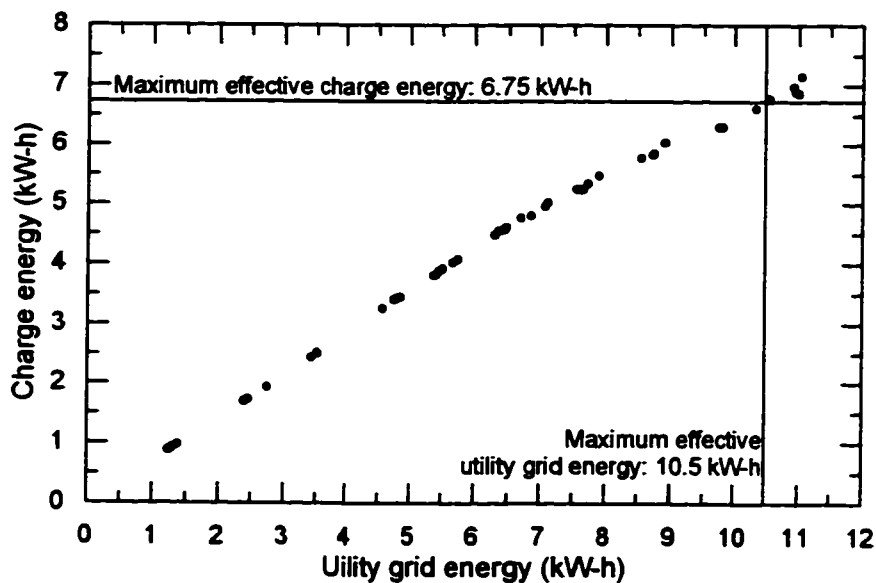


Figure 4-31. Charge energy, E_{charges} produced from utility grid energy, E_{utility}

As noted earlier, the battery always started from a low SOC in this data set. Therefore, the battery charger could run at a high level of power and efficiency for low charge levels. At higher levels of charge, the battery charger must reduce its output power to protect the batteries, resulting in lower efficiency. As discussed previously, the vehicle operator would generally try to maintain the battery at a high state of charge in actual service. Hence, the charger would deliver a large portion of the charge at low power and efficiency, resulting in lower in-service energy efficiency.

Since the infrastructure for fast-charging electric vehicles has not yet been developed, the battery charger for the HRV was designed to charge the vehicle from a common 115 VAC electric outlet. Consequently, the charger is relatively small with an output power of about 900 W (1230 W input power). Figure 4-32 shows the amount of energy delivered by the charger to the battery for charge cycles of various duration. The charger may require 18 h or more to supply enough energy to fully charge the battery. Charge time could be reduced by using a battery charger with higher output power (charge rate). However, higher charge rates would generally result in lower battery efficiency (η_{batt}) as more of the charge energy is expended in ohmic heating and water dissociation.

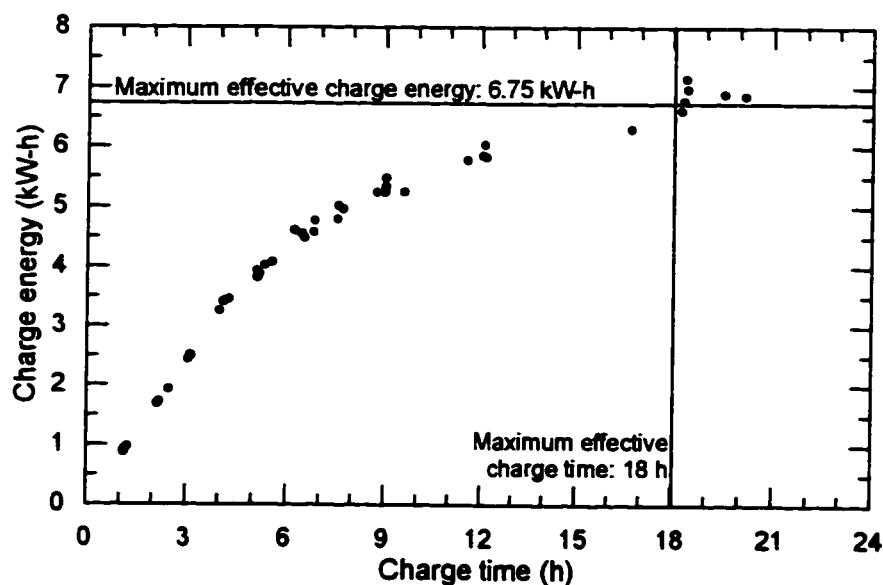


Figure 4-32. Charge energy, E_{charge} , delivered over a range of charge times

4.7. Vehicle energy and efficiency

The overall energy required to operate the HRV as an electric vehicle is the energy supplied by the electric utility grid to the battery charger. Figure 4-33 shows the relationship between vehicle range and the utility energy required for the vehicle to meet that range. The required energy rises with increasing range and approaches a vertical asymptote at the vehicle's maximum range. This corresponds to the point where the battery has reached its maximum capacity and further charging increases energy consumption without increasing vehicle range. After one and a half years of use, the HRV had a maximum electric range of 25 km. Using an optimum charging strategy, this range could be achieved with 10.5 kW-h of utility grid energy, which corresponds to a specific energy consumption of 0.42 kW-h/km.

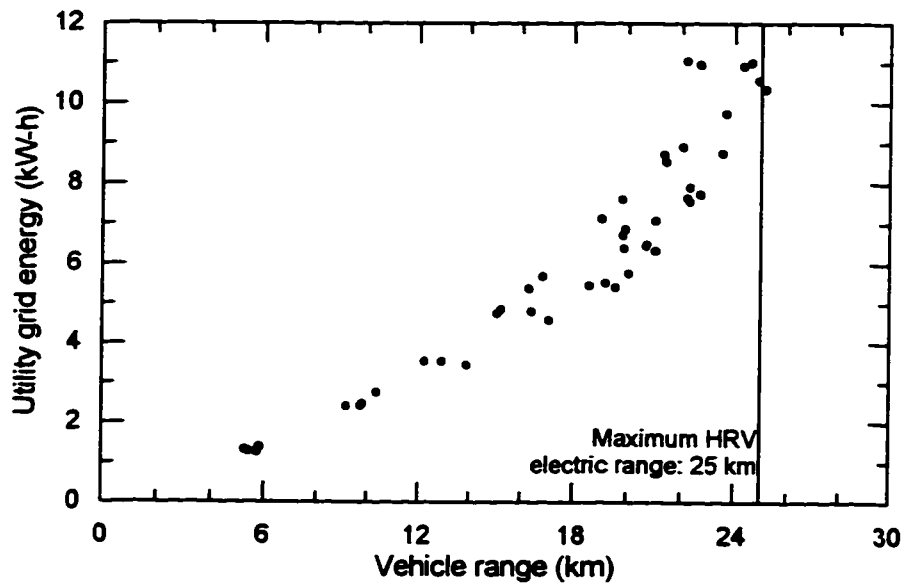


Figure 4-33. Utility grid energy, $E_{utility}$, required to achieve vehicle range

The overall electrical energy efficiency can be defined as the PTE produced to propel the vehicle divided by the energy consumed from the electric utility grid:

$$\eta_{elec} = \frac{E_{pos.trac}}{E_{utility}} \cdot 100\% \quad (4.21)$$

where η_{elec} is the overall electrical energy efficiency of the vehicle (%)

Figure 4-34 shows that a very high electrical energy efficiency can be achieved if the vehicle is only expected to travel a very short distance. However, the electrical energy efficiency of the vehicle decreases as a higher charge is required for longer vehicle range. This trend is determined primarily by the performance characteristics of the battery. The drop in battery charger efficiency at higher charge levels also contributes to the decrease in overall efficiency. However, this drop is due to the reduction in output power which was determined by the charging characteristics of the battery.

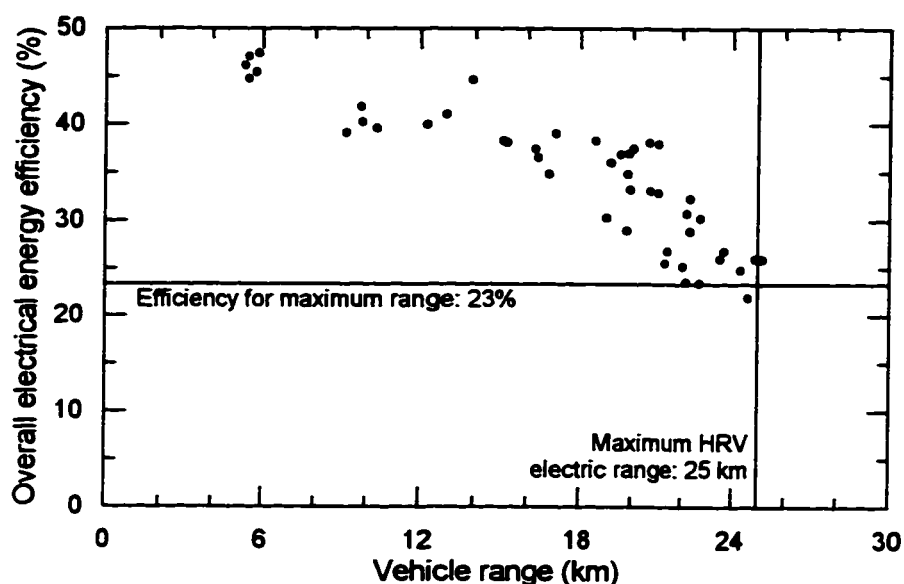


Figure 4-34. Variation in overall electrical energy efficiency, η_{elec} , with vehicle range

The utility grid energy can be expressed in terms of the amount of gasoline containing the equivalent amount of energy (i.e., as the equivalent gasoline energy). Figure 4-35 shows the equivalent gasoline energy consumption of the HRV. The equivalent energy consumption is given as litres of gasoline to travel 100 km; the same unit used in Canada for published government estimates of vehicle fuel consumption. The HRV consumed as little as 2.6 L/100 km of equivalent gasoline energy when a range of only 6 km was required. For its maximum range of 25 km, the HRV consumed 4.7 L/100 km of equivalent gasoline energy. For comparison, the stock 1994 Ford Escort wagon was rated by Transport Canada at a fuel consumption of 8.69 L/100 km on the

FTP-78 test schedule. Since the tractive energy requirement was lower for on-road tests, the on-road fuel consumption of a stock Escort would be expected to decrease slightly.

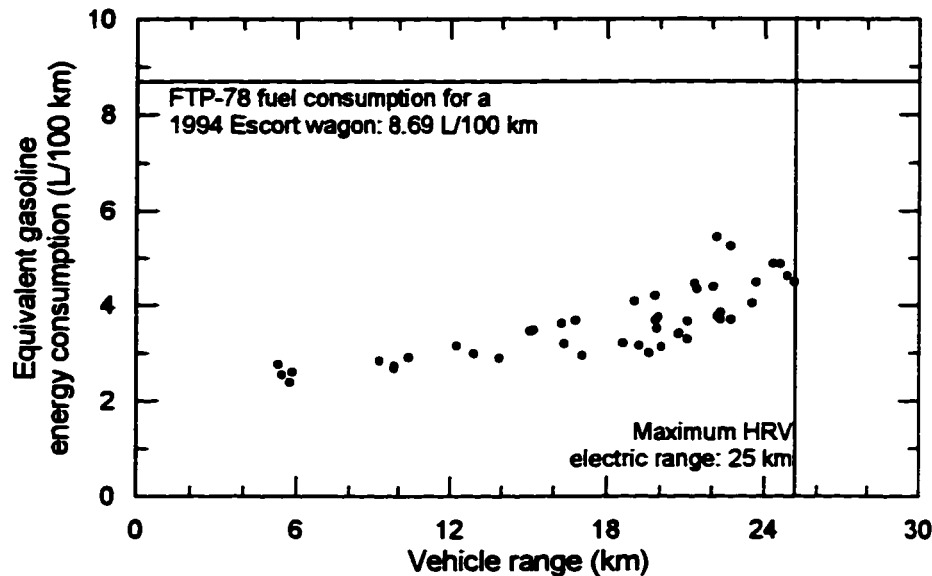


Figure 4-35. Equivalent gasoline energy consumption

The HRV using electrical energy clearly consumed much less energy than a conventional, combustion-powered vehicle. However, the efficiency of the entire energy cycle must be considered, including the efficiency of producing and distributing energy for vehicles, to objectively compare transportation alternatives.

4.8. Resource energy

An HEV using high quality electrical energy can be expected to achieve relatively high efficiencies compared with a conventional automobile utilizing chemical energy. The HRV, when used as an electric vehicle, consumes about half the energy of a conventional automobile. However, the energy efficiencies of processes involved in the production and distribution of vehicle fuels and electricity should also be considered to understand overall consumption of the world's limited energy resources.

The vast bulk of the gasoline and diesel motor fuel in the world is obtained from traditional methods of extracting and refining natural crude oil. Figure 4-36 shows an

estimate of the energy efficiency of supplying gasoline to a service station for consumer use [49].

Gasoline from crude oil		Electricity from coal	
↓ Crude recovery	96.9%	↓ Coal mining	98.1%
↓ Crude transportation	98.9%	↓ Coal transportation	99.0%
↓ Crude refinery	87.4%	↓ Generating plant	33.5%
↓ Gasoline transportation	99.2%	↓ Electricity transmission	92.0%
Service station		Wall outlet	
(Overall efficiency)	83.1%	(Overall efficiency)	29.9%

Figure 4-36. Efficiency of producing and distributing two forms of energy [49]

Evaluating the efficiency of producing and distributing electricity is more complex. Electricity is produced at many generating plants from different natural resources and is distributed across a large network connecting the plants to consumers. The source of electricity when an incremental load is added is dependent on many factors including geographical location, time of day, seasonal variations in energy demand, and generating plant emission regulations. In this analysis of resource energy consumption, a simplifying assumptions was made. It was assumed that an increase in electricity demand from the operation of an electric vehicle would be supplied by a coal-fired generating plant. This would generally be the case for electricity supplied for night charging in Edmonton, Canada [50]. Figure 4-36 shows the estimated production and distribution energy efficiency of electricity generated at a coal-fired generating plant, 29.9%.

The natural resource energy consumption of the research hybrid vehicle and a comparable conventional vehicle can be compared using the estimated production and distribution energy efficiencies for gasoline and electricity. The resource energy consumption given in Figure 4-37 is obtained by applying the efficiencies to the vehicle energy consumption data (Figure 4-35). For short HRV travel distances, the stock Escort and the HRV consume comparable amounts of resource energy. At maximum electric range, the HRV consumes about 45% more resource energy than a similar gasoline vehicle.

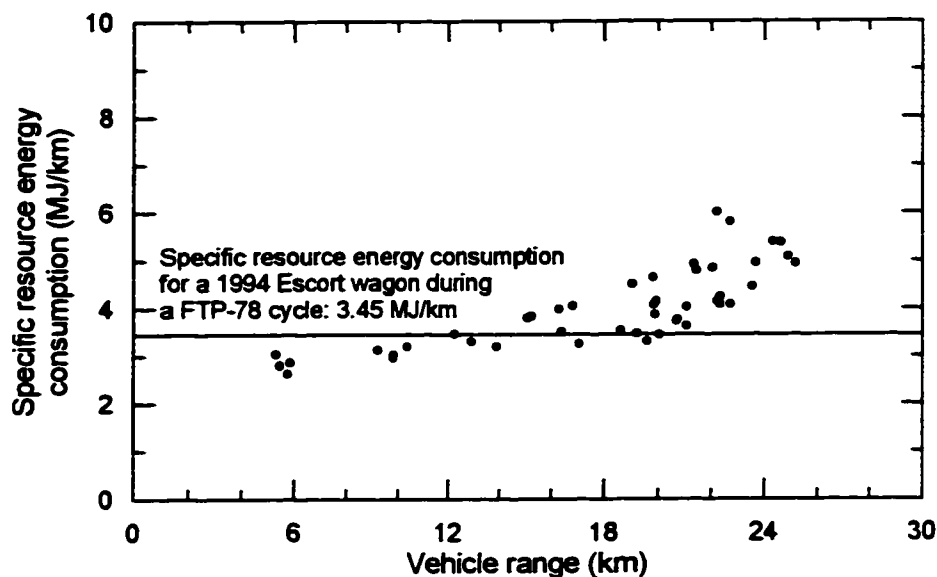


Figure 4-37. Specific resource energy consumption for electricity produced from coal

Although the HRV may consume more resource energy than a conventional vehicle, electric and HEVs still offer resource-related benefits. Petroleum consumption would be reduced by shifting transportation energy use to other, less limited resources such as coal and nuclear power. The limited supply of petroleum could then be used in other applications. These range from non-energy applications such as the production of plastics, to energy used for more demanding purposes such as aircraft. If automotive consumption of gasoline is reduced, refining processes could be modified to produce less gasoline and thus extend long-term supplies.

In the long term, a significant increase in electricity demand due to the use of electric vehicles will result in the construction of new, efficient generating plants. The total system efficiency of in-service vehicles could, thus, be improved without modifying the vehicles. The ultimate success of electric vehicles may depend on the development of efficient and economical methods of generating electricity. These new sources of electricity should also be low polluting or, ideally, pollution-free.

5. Air pollution emissions

The need to reduce urban air pollution is the major driving force behind the development of electric vehicles. As discussed in Chapter 1, the high concentration of motor vehicles in urban areas significantly affects air quality. Electric vehicles produce very little local air pollution and are often called Zero Emission Vehicles (ZEV). However, air pollution may be produced in generating the electricity used by electric vehicles. Similarly, there is pollution associated with the production and distribution of fuel for combustion powered vehicles. To assess the environmental impact of replacing conventional vehicles with HEVs, the emissions associated with the use of HEVs must be compared to those associated with conventional vehicles. The emissions from the entire energy cycle, including the steps in the production and use of energy, must be examined to make an objective comparison.

5.1. Gasoline energy cycle emissions

In Chapter 4, the entire energy cycle was considered (from the extraction of natural resources to the final consumption by the vehicle) to compare two energy cycles. Similarly, the emissions generated in the entire energy cycle should be considered when comparing the air pollution impact of different transportation alternatives. In this section, estimates of the emissions produced in a gasoline energy cycle will be determined for conventional vehicles comparable to the HRV.

Vehicle tailpipe exhaust emissions usually represent the largest source of energy cycle emissions for gasoline fueled vehicles. Table 5-1 compares current and proposed certification standards with the tested emissions of the U of A HEVs and a production Escort wagon. The Escort meets California standards for a transitional low emission vehicle (TLEV). An Escort wagon converted to an HEV should be able to achieve similarly low emission levels. However, in the few emission test sessions available, neither the HRV nor *HEV II* achieved such low emissions, primarily due to lack of testing and optimization.

Table 5-1. Combustion engine exhaust emissions

Vehicle or emissions standard	Vehicle mass (kg)	CO (g/mi)	NO _x (g/mi)	HC (g/mi)	NMHC (g/mi)
US EPA Tier I standard (1994)	-	3.4	0.40	-	0.25
California TLEV standard	-	3.4	0.27	-	0.121
California 1997 ULEV standard	-	1.7	0.20	-	0.039
Stock (new) 1994 Escort wagon†	1260	1.24	0.04	0.12	-
HEV II (ICE mode) †	1480	1.35	0.689	0.268	-
HEV II (HEV mode, SOC corrected)‡	1480	2.16	0.147	(0.255)	0.203
HRV (HEV mode, no SOC correction)†	1430	5.52	1.44	0.42	-

† Emission test results from Environment Canada

‡ Emission test results from 1995 HEV Challenge. The vehicle mass setting on the dynamometer was about 135 kg too high. Also, the car stalled three times during test due to a problem with the transmission clutch. HC value calculated by author from raw test data.

With the data given in Table 5-1, various approaches are available to estimate the average emissions of a combustion vehicle similar to the HRV over its lifetime. An optimistic approach would be to use the measured emission levels for the new 1994 Escort wagon. A conservative approach would be to use the maximum emission levels allowed by government regulations since vehicles must be certified to meet these levels for the first 80 000 km (50 000 mi) of operation [51]. These two approaches will be used to set the limits of the actual lifetime average emission levels, which are expected to be between the levels of the new Escort and US EPA Tier I standards. The results of the HRV and *HEV II* are poor estimates of the lifetime average emissions since the engine calibrations and emission controls are not optimum.

Estimates of air pollution associated with the production of gasoline have been reported by Tyson, et al. [52]. These estimates were used to predict the emissions associated with the production and distribution of regular unleaded gasoline for a conventional vehicle (a 1994 Escort wagon) with a fuel consumption of 8.69 L/100 km. Appendix E describes how these predictions were made. Table 5-2 shows the amount emissions contributed by each step in the energy cycle based on the two approaches for estimating average vehicle emissions. For most pollutants, the end use (vehicle) produces the majority of emissions. Therefore, the total energy cycle emissions are highly dependent on the emission characteristics of the vehicle.

Table 5-2 Estimated gasoline energy cycle air emissions for a conventional vehicle

	CO ₂ (g/mi)	CO (g/mi)	NO _x (g/mi)	HC† (g/mi)	SO ₂ (g/mi)	Particulates (g/mi)
Feedstock production	16.6	0.0093	0.0580	0.0174	0.0035	0.0006
Feedstock transportation	5.45	0.0174	0.0394	0.0185	0.0012	0.0019
Fuel production	32.9	0.0104	0.0789	0.0104	0.0510	0.0027
Fuel distribution	1.51	0.0058	0.0104	0.055	0.0004	0.0004
Subtotal	56.5	0.0429	0.1867	0.101	0.0597	0.0056
End use (new 1994 Escort wagon)‡	322	1.24	0.04	0.12	0.0638	0
End use (US EPA Tier I standards)§	322	3.40	0.40	0.25	0.0638	0
Fuel cycle total (new 1994 Escort wagon)	378	1.28	0.23	0.22	0.120	0.0056
Fuel cycle total (US EPA Tier I standards)	378	3.44	0.59	0.35	0.120	0.0056

† HC and VOC are assumed to be equivalent.

‡ CO₂, CO, NO_x, and HC emissions for 1994 Ford Escort measured by Environment Canada. SO₂ emissions estimated from sulphur content of fuel. Particulate emissions from passenger vehicles not available.

§ CO₂ and SO₂ emissions assumed to be dependent on fuel consumption which is the same as the new Escort for this case. Particulate emissions from passenger vehicles not available.

5.2. Electricity cycle emissions

As discussed in Chapter 4, it is often difficult to determine the source of electricity for charging an electric vehicle. Table 5-3 gives the emissions from a (sweet) natural gas and a coal-fired generating plant to supply 1 kW-h of electrical energy to a consumer in Edmonton, Canada. Average transmission and distribution losses have been included in determining these values. Both generating plants operate on the Rankine cycle using boilers and steam turbines. The boilers are steady combustion devices and emissions of CO and HC should be very low; thus, they are assumed to be negligible in this case. In the regional electricity grid, a coal fired plant is generally used to supply peak power during the late evening and night when demand is normally low. During the day and early evening, additional generating capacity is needed and is usually supplied by a natural gas fired generating plant. The data in Table 5-3 indicate that lower emissions would be produced if electric vehicles were charged during the day. However, it is usually more convenient for vehicle operators to charge at night. Electric utility companies would also prefer night charging since demand is low and electricity can be produced less expensively by the coal fired plant.

Table 5-3. Emissions from typical fossil fueled peak power generating plants in Alberta, Canada†

Fuel	CO₂ (g/kW-h)	NO_x (g/kW-h)	SO₂ (g/kW-h)	Particulates (g/kW-h)
Landfill gas (methane) and sweet natural gas	576	1.19	0.00	0.00
Coal	1095	2.28	6.91	0.16

† Values supplied by EPCOR and include average transmission and distribution losses of 9.725% for Edmonton and Calgary, Canada [50]

An estimate of the utility grid energy required by the HRV to complete the FTP-78 cycle was needed to determine the amount of pollutants produced at the generating plant. Ideally, the required utility grid energy would be determined by driving the HRV on a FTP-78 cycle and then recharging the battery pack. However, such test results were not available. Instead, the performance results from Chapter 4 have been used to estimate the energy consumption of the vehicle.

Figure 5-1 illustrates the method used to estimate the utility energy. The required PTE of 2.34 kW-h was obtained from the vehicle dynamic model. The average powertrain drive efficiency in actual urban driving (68.8% from Figure 4-14) was applied to give 3.40 kW-h of positive drive energy. The vehicle accessories consume 0.126 kW-h of energy over the 0.688 h test period, based on the average accessory power (0.183 kW from Figure 4-18). No optional accessories are used during the test. This gave a total battery discharge energy of 3.53 kW-h. The required charge energy was obtained from Figure 4-21 (or from Figure 4-25 by simultaneously solving for the observed battery efficiency). Similarly, the battery charger energy efficiency and utility grid energy were obtained from Figure 4-30 (or Figure 4-31). These are optimistic estimates of battery and battery charger performance since they assume that the battery pack was only charged to the minimum required capacity to complete a single FTP-78 cycle and not fully charged.

The amounts of each pollutant produced due to the use of the hybrid vehicle were determined by multiplying the electric generation emission factors in Table 5-3 by the required utility energy. Then, the normal units for expressing vehicle emissions (g/mi) were obtained by dividing the amounts of each pollutant over the distance traveled during the test cycle (17.76 km). Table 5-4 gives the resulting emission levels for the HRV. The

air pollution generated from the energy cycles of the HRV and a similar gasoline fueled vehicle can now be compared.

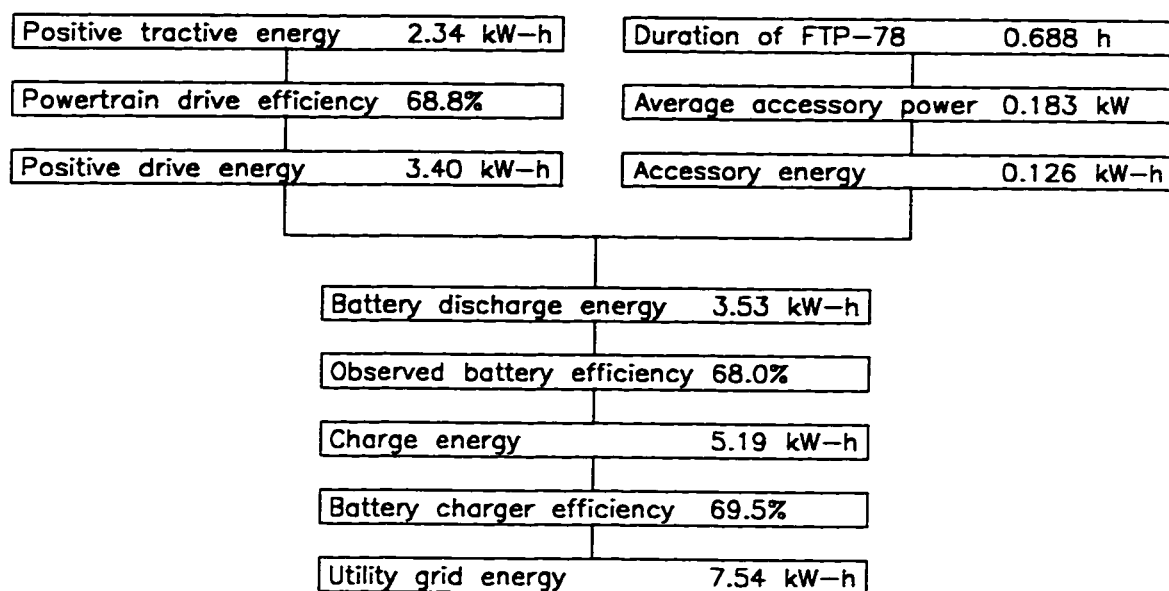


Figure 5-1. Estimated electric energy requirement of the HRV for FTP-78 cycle

Table 5-4. Emissions from producing electricity for the HRV

Charging scenario	CO ₂ (g/mi)	CO (g/mi)	NO _x (g/mi)	HC (g/mi)	SO ₂ (g/mi)	Particulates (g/mi)
HRV day charge (landfill or natural gas)	390	- †	0.80	- †	0.00	0.00
HRV night charge (coal)	741	- †	1.54	- †	4.67	0.11

† Data not available.

Table 5-5 compares the emissions from the HRV energy cycles and those from the gasoline energy cycles. The HRV energy cycles are based on operating the HRV during mild weather in Edmonton, Canada. The energy cycles based on the new 1994 Escort wagon emissions and the US EPA Tier I standards are used to set the lower and upper bounds of the expected lifetime average emissions of a conventional vehicle similar to the HRV. The HRV would produce less air pollution when charged during the day using electricity from a gas-fired plant. However, CO₂ and NO_x emission would still be greater than those from the conventional vehicle energy cycles: CO₂ emissions would be 3%

higher and NO_x emissions from 36% to 248% higher. Under normal circumstances, night time charging of the HRV is expected. In this case, CO₂ emissions would be 96% more than the conventional vehicle energy cycles. NO_x emissions would be from 2.6 to 6.7 times higher than the conventional vehicle energy cycles, SO₂ emissions 38.9 times higher, particulate emissions 19.6 times higher.

Table 5-5. Emission comparison of different vehicle energy cycles

Vehicle energy cycle	CO ₂ (g/mi)	CO (g/mi)	NO _x (g/mi)	HC (g/mi)	SO ₂ (g/mi)	Particulates (g/mi)
HRV day charge (landfill or natural gas)	390	-†	0.80	-†	0.00	0.00
HRV night charge (coal)	741	-†	1.54	-†	4.67	0.11
Conventional vehicle (1994 Escort)	378	1.28	0.23	0.22	0.120	0.0056
Conventional vehicle (US EPA Tier I)	378	3.44	0.59	0.35	0.120	0.0056

† Although no data were obtained for the generation of CO and HC in the HRV energy cycles, emissions of these two pollutants are expected to be lower than from the gasoline energy cycles.

Some benefits of electric vehicles are not reflected by the emission results. The relocation of vehicle emissions to electrical generating plants improves urban air quality since most generating plants are located away from urban areas. Human exposure to pollutants will be reduced and the pollutants are more effectively dispersed in rural areas. Of course, the effects of increased emissions on the environment surrounding a generating plant should also be considered.

Electric vehicles centralize the production of pollutants at a relatively small number of generating plants which could be more easily controlled. Immediate benefits would occur if cleaner and more efficient generating plants were built or more advanced emission control technologies were implemented at generating plants. Generating plant improvements immediately reduce the emissions associated with the operation of all electric vehicles. With conventional combustion automobiles, improvements that affect all vehicles are essentially limited to changes in the fuel formulation. A technological improvement that involves a physical change to vehicles normally requires a complete renewal of the vehicle fleet, which may take over a decade to fully implement. For example, catalytic converters and electronic fuel injection are virtually universal in all new

automobiles; however, a large number of older vehicles still in service do not have these emission reducing technologies.

The results presented here are specific to the HRV. Future production vehicles will need higher efficiencies to lower both electrical energy consumption and air pollution. The introduction of electric and range-extending hybrid vehicles may improve urban air quality; however, it is unlikely to bring great environmental benefits from a global perspective. The emissions produced at the generating plant are directly related to the energy requirements of the HRV. Ultimately, the benefits of these vehicles will depend on improved vehicle efficiency and the development and implementation of low emission methods of generating electricity.

5.2.1. Impact of HRV use on air pollution

A number of conclusions can be made regarding some of the environmental impacts of using the HRV instead of a conventional automobile.

On a global scale, using the HRV charged by a coal-fired generating plant is detrimental to the environment: higher CO₂ emissions contributes to the greenhouse effect and may lead to undesirable global warming; and higher SO₂ and NO_x emission levels will increase the formation of acid rain. The HRV (coal) energy cycle efficiency must be approximately doubled before significant reductions in CO₂ emissions will occur. NO_x, SO₂, and particulate emissions will still remain much higher than the conventional vehicle gasoline fuel cycle unless further emission controls are implemented at the generating plant.

In terms of urban air quality, operation of electric vehicles can lead to significant benefits provided that the exhaust gases from generating plants are dispersed away from urban areas. Urban emissions of all five pollutants would decrease. The removal of NO_x and HC emissions from urban centres would reduce the level of urban smog and air quality would improve in urban areas that experience high levels of CO.

6. Summary and recommendations

In this research project, a data acquisition system was installed in a hybrid electric vehicle belonging to the University of Alberta. The DAS measured a number of operating parameters while the vehicle was driven in actual on-road urban conditions in Edmonton, Canada. During 1995, the HRV was operated by Edmonton Power, an electric utility company, in their vehicle fleet. Further on-road testing was performed by the U of A in 1996. The data collected from these experiments were used to determine the performance of vehicle components, the energy consumption of the vehicle, and the emissions generated in the vehicle's energy cycle.

A hybrid electric vehicle overcomes the range limitations of a pure electric vehicle by employing an on-board fuel and powerplant. The general definition of an HEV can encompass a wide range of vehicle designs. This dissertation evaluated the performance characteristics of a range-extending type HEV with a parallel powertrain configuration. A lead-acid battery pack was used to store electricity. When the battery pack is depleted an internal combustion engine burning gasoline is used to extend the range of the vehicle.

A range-extending HEV is expected to operate in urban areas as an all electric vehicle under normal conditions. Thus, it faces electric range and weight problems due to the low energy storage density of currently available batteries. Improving the technology to store electrical energy remains the key to successfully introducing electric vehicles on a large scale. Batteries with higher energy density would allow more energy to be stored on a vehicle or a reduction in vehicle mass and volume, leading to a lower specific tractive energy requirement. Consequently, driving range would increase while the specific energy consumption from the utility grid would decrease. High energy efficiency batteries would minimize resource energy consumption.

6.1. Energy consumption

An electrochemical battery typically stores less than 1% of the energy available from an equal mass of gasoline. Thus, high efficiency vehicle components are critical to the success of range-extending HEVs and pure electric vehicles. A good energy management strategy that focuses on energy conservation and recovery is also important.

Regenerative braking can significantly extend the range of an electric vehicle. In typical urban driving, about 30% of the tractive energy supplied by the powertrain is available for regenerative braking.

During on-road driving tests in Edmonton, Canada, the powertrain of the HRV converted electrical energy to mechanical tractive energy with an average efficiency of $68.8 \pm 0.7\%$. The regenerative braking system converted mechanical energy back to electrical energy with an average efficiency of $62.6 \pm 1.5\%$. These efficiencies appeared to be independent of the distance traveled. The electric powertrain consumed 0.160 ± 0.007 kW-h of electricity per kilometre that the vehicle traveled and regenerative braking was able to produce 0.019 ± 0.004 kW-h of electricity per kilometre.

The electrical power consumed by vehicle accessories is relatively small (0.183 kW) for daytime driving when no climate controls are required. At a typical average urban driving speed of 30 km/h, the accessory energy consumption would be about 0.0061 kW-h/km. In more extreme climate conditions, where heating (or air conditioning) is required the accessory load can be significant. At a speed of 30 km/h and with the vehicle's lights on and a 1 kW heating load, the accessory energy consumption in the HRV would be about 0.039 kW-h/km, which is 20% of the total energy supplied by the battery.

The 290 kg battery pack in the HRV originally provided an electric range of 35 km to 40 km. After about 1.5 years of light use, the vehicle's electric range was only 22 km to 25 km. The maximum observed battery capacity dropped from 7.05 kW-h to 4.04 kW-h. This degradation of battery capacity is known to occur with lead-acid batteries, especially in applications where the battery is deeply discharged. It is also well known that battery capacity varies with temperature. However, the HRV was parked and charged at an indoor location. Therefore, battery capacity was not greatly affected by decreases in ambient temperature.

The efficiency of the battery was measured when its capacity was 4.04 kW-h. No data were available to determine if the efficiency, like the capacity, varied with age or with temperature. Battery efficiency can be relatively high, around 85%, if the battery is used over a narrow operating range at a low SOC. When the full capacity of the battery is

used, efficiency is only about 55%. Even lower efficiencies would be expected in normal operation when the battery is maintained at high states of charge. A battery pack with a high energy storage efficiency is desirable to minimize energy consumption. Less energy would be needed to recharge the battery and the battery would make better use of the energy available from regenerative braking and extend the vehicle's driving range. Therefore, improving energy efficiency will both reduce energy consumption and improve vehicle range.

A 900 W solid state battery charger was designed for the HRV. The instantaneous efficiency of the battery charger is primarily dependent on the output power level: higher efficiency at higher power. During a typical charge cycle, the charger efficiency varies from about 73% (at an output power of 895 W) down to about 51% (at 170 W). In addition to supplying energy to the battery pack, the charger also operates the battery box ventilation fans while charging; however this secondary function was not included as a part of the charger output for determining its efficiency.

The energy efficiency of the charger over a charge cycle will depend on the charging requirements of the battery pack. For the lead-acid battery pack, the charge power must be reduced when the battery nears its full capacity to prevent overheating and excessive water consumption. The battery charger energy efficiency for a full charge is only 64%. Efficiency would be less in normal operation when charging cycles are started at a significantly SOC. Thus, a significant amount of energy is lost through the battery charger, making it a component that has a large potential for improvement.

Currently, motor vehicles are almost completely dependent on petroleum-based fuels. Electricity can be generated from many energy sources. Thus, range-extending hybrid electric vehicles allow the source of energy used for transportation to be diversified. The total natural resource energy consumed by a range-extending HEV will depend on vehicle efficiency and on the efficiency of the generating plant producing electricity. When electricity demand from the use of HEVs is significant, new efficient generating plants are expected to be built to meet that demand. In the near-term, increases in demand for electricity in North America will be met by existing generating plants. In most areas, the base electricity demand is met by the most economical or least

polluting plants, depending on local regulations. Consequently, peak power is supplied by less economical or more polluting generating plants like those burning coal. With coal as a source of energy, the HRV requires about 5.0 MJ of coal energy per kilometre traveled. A conventional combustion vehicle needs only 3.45 MJ of crude oil energy per kilometre. Unless there is a shortage in the supply of petroleum, hybrid vehicles that consume 40% less energy than the HRV are needed before their use can be justified on an energy basis.

6.2. Pollutant emissions

The main source of energy for the HRV is electricity from the utility grid. Widespread use of HEVs would shift the generation of pollutants from highly populated urban areas to sparsely populated rural areas where generating plants are generally located. The levels of all five common pollutants in the urban centres would decrease, resulting in improved urban air quality. However, if electricity is generated from coal combustion, little or no reductions in air pollution would be realized from a global perspective. Using the HRV instead of a comparable gasoline fueled vehicle would increase emissions of CO₂ (which contributes to global warming) by 96%; NO_x (which contributes to acid rain) by 2.6 to 6.7 times; and SO₂ (which also contributes to acid rain) by 38.9 times. The amount of pollution associated with the use of an electric vehicle depends on the energy required by the vehicle. Improved energy efficiency over that of the HRV and lower generating plant emissions are needed to improve global air quality.

6.3. Future work

The research presented here has led to a number of general conclusions that can be applied to many types of electric and hybrid vehicles; however, many results are specific to the HRV. Further research is needed on other hybrid and electric vehicles and on different components and control strategies.

The energy consumed by accessories is important in a vehicle that has a very limited storage of energy. Large loads like a heater or an air conditioner can have a significant impact on overall energy consumption and vehicle range. Further research is needed to determine the energy requirements of vehicle accessories, especially in areas that experience extremes in temperatures.

Many new types of batteries are under development. These batteries will require extensive in-vehicle evaluations of their performance to determine their suitability for electric vehicles. To predict vehicle performance, the performance characteristics of the battery pack must be known over a range of operating conditions. Standard battery tests which simulate actual in-vehicle conditions must be adopted.

Most published research has focused on battery capacity and power, since these are seen as the primary characteristics limiting the acceptance of electric vehicles in the consumer market. More research is needed on battery energy efficiency as it has a strong influence on resource energy consumption and the generation of air pollutants. Different operating conditions should be investigated to determine their effects on battery efficiency. A single efficiency value is often given for a battery based on a simple (i.e., constant current discharge) test. Such an efficiency value can be misleading. As found in this research, battery efficiency varies considerably with operating conditions. Experiments should be performed to determine battery efficiencies in on-road operating conditions, such as partial discharge and charge at a high SOC. A relatively low efficiency would be expected under these conditions, but measurements are needed to quantify actual battery performance. The effects of fast charging should also be examined and long term testing is needed to determine how energy efficiency is affected by battery age.

References

- 1 John B. Heywood, Internal Combustion Engine Fundamentals, (New York: McGraw-Hill, 1988), p. 5
- 2 Canada, Conservation and Protection, Canada's Greenhouse Gas Emissions: Estimates for 1990, By A.P. Jaques, (Ottawa: Environment Canada, 1992)
- 3 John H. Seinfeld, Atmospheric Chemistry and Physics of Air Pollution, (New York: John Wiley & Sons, 1986), p. 55
- 4 A.J. Haagen-Smit, "Chemistry and Physiology of Los Angeles Smog", Industrial and Engineering Chemistry, Vol. 44, 1952, p. 1342-1346
- 5 Seinfeld, p. 154
- 6 Irvin Glassman, Combustion, 2nd ed., (Orlando: Academic Press, 1987), p. 320
- 7 Ronald J. Gillespie, et al., Chemistry, 2nd ed., (Boston: Allyn and Bacon, 1989), p. 684
- 8 Heywood, p. 567
- 9 Canada, Pollution Data Branch, "1990 Emissions of Common Pollutants for Canada", (Ottawa: Environment Canada, January, 1995)
- 10 Canada, Environment Canada, "Technical Supplement to the Environmental Indicators on Urban Air Quality", (Ottawa: Environment Canada, 1996)
- 11 Canada, Environment Canada, "Air Quality Trends in Canadian Cities, 1979-1992", (Ottawa: Environment Canada)
- 12 Canada, Environment Canada, "National Environmental Indicator Series: Urban Air Quality", (Ottawa: Environment Canada, 1996)
- 13 Canada, Industrial Programs Branch, "International New Vehicle Emissions Standards (Internal Report)", Unpublished report by N. Ostrouchov, (Ottawa: Environment Canada)
- 14 M.D. Checkel, "Appendix D. Vehicle Emission Standards", Vehicle Emissions Project - The City of Edmonton Transportation Master Plan, (Edmonton, AB: City of Edmonton Transportation Department, 1996)

- 15 Canada, Industry Division, Quarterly Report on Energy Supply and Demand in Canada, Vol. 21, No. 2, (Ottawa: Statistics Canada, February 1997)
- 16 Michael Duoba, et al., "Design Diversity of HEVs with Example Vehicles from HEV Competitions", Paper 960736, (Warrendale, PA: Society of Automotive Engineers, 1996)
- 17 V. Yung, et al., "Development of the University of Alberta Entry in the 1995 Hybrid Electric Vehicle Challenge", The 1995 HEV Challenge, SP-1170, (Warrendale, PA: Society of Automotive Engineers, 1996), p. 111-124
- 18 Subhash Narang, et al., "Exceeding DOE mid-term performance with ultracapacitors", Electric & Hybrid Vehicle Technology '95, (Dorking, Surrey: UK & International Press, 1995), p. 131-134
- 19 Thomas W. Grudkowski and Evan C. Polley, "Advanced flywheel technology", Electric & Hybrid Vehicle Technology '95, (Dorking, Surrey: UK & International Press, 1995), p. 138-143
- 20 C.J.T. van de Weijer and R.A.A. Schillemans, "Electric Vehicles; Energy Consumption and the comparison with Other New Vehicle Technologies", Paper VM9606, (The Netherlands: TNO Road-Vehicles Research Institute, 1996)
- 21 Robert Q. Riley, Alternative Cars in the 21st Century, (Warrendale, PA: Society of Automotive Engineers, 1994), p. 227
- 22 Robert U. Ayres and Richard P. McKenna, Alternatives to the Internal Combustion Engine: Impacts on Environmental Quality, (Baltimore: The John Hopkins University Press, 1972), p. 87
- 23 Ayres and McKenna, p. 90
- 24 Riley, p. 235
- 25 Ayres and McKenna, p. 86-108
- 26 Riley, p. 225-244
- 27 T.R. Crompton, Battery Reference Book, 2nd ed., (Warrendale, PA: Society of Automotive Engineers, 1996)

- 28 Heywood, p. 915
- 29 Ayres and McKenna, p. 192
- 30 Ajay Yelne and Kenneth Heitner, "Switched Reluctance Drives for Electric and Hybrid Vehicles", Strategies in Electric and Hybrid Vehicle Design, Paper 960256, SP-1156, (Warrendale, PA: Society of Automotive Engineers, 1996), p. 91-102
- 31 Unique Mobility, Installation and Operating Instructions SR180 Brushless DC Motor CR20-300A Brushless DC Motor Controller, (Golden, CO: Unique Mobility, 1994)
- 32 Riley, p. 244
- 33 Bill Visnic, "Fuel (cells) for Thought", Ward's Auto World, March 1997, p. 141+
- 34 Electric Vehicle Association of Canada, Electric Vehicle Infrastructure Requirements in Canada, (Nepean, ON: EVAC, 1995), p. 54
- 35 V.E. Duckworth, et al., "The University of Alberta Hybrid Electric Vehicle Project Final Technical Report", Innovations in Design: 1993 HEV Challenge, SP-980, (Warrendale, PA: Society of Automotive Engineers, 1994), p. 1-11
- 36 M.D. Checkel, et al., "Development of the University of Alberta Entry in the 1994 HEV Challenge", 1994 HEV Challenge, SP-1103, (Warrendale, PA: Society of Automotive Engineers, 1995), p. 1-14
- 37 "Emission Test Driving Schedules-SAE J1506 Jun91: SAE Information Report", 1993 SAE Handbook, Vol. 3, (Warrendale, PA: Society of Automotive Engineers, 1993), p. 25.140-151
- 38 Canada. Environment Canada, "Emissions and Performance Study of the University of Alberta's Hybrid Vehicle-HEV CAR", Unpublished Report by Michel Souligny, (Ottawa: Environment Canada, 1995)
- 39 Canada, Environment Canada, Emissions and Performance Study of the University of Alberta's Hybrid Vehicle-HEV II, By Michel Souligny, (Ottawa: Environment Canada, 1995)

- 40 Michael Duoba and Robert Larsen, "HEV Dynamometer Testing with State-of-Charge Corrections in the 1995 HEV Challenge", Paper 960740, (Warrendale, PA: Society of Automotive Engineers, 1996)
- 41 M. D. Checkel, Department of Mechanical Engineering, University of Alberta, private communication, 1996
- 42 M.D. Checkel, "Appendix A. Development of Multi-Mode Test Schedule", NGV Conversion Effects on Vehicle Emissions and Fuel Economy, (Edmonton, AB: Alberta Transportation and Utilities, 1992)
- 43 G. Sovran and M.S. Bohn, "Formulae for the Tractive Energy Requirements of Vehicles Driving the EPA Schedules", Paper 810184, (Warrendale, PA: Society of Automotive Engineers, 1981)
- 44 J.T. Griffith, "Measuring energy performance of electric vehicles", Electric & Hybrid Vehicle Technology '95, (Dorking, Surrey: UK & International Press, 1995), p. 148-151
- 45 K.R. Williams, "Energy Analysis and the Electric Car", Paper 760736, (Warrendale, PA: Society of Automotive Engineers, 1976)
- 46 Battery Council International, Battery Service Manual, 10th ed., (Chicago, IL: Battery Council International, 1987), p. 28
- 47 Sandeep Dhameja and Min Sway-Tin, "Traction Batteries - Their Effects on Vehicle Performance", Strategies in Electric and Hybrid Vehicle Design, Paper 970240, SP-1243, (Warrendale, PA: Society of Automotive Engineers, 1996), p. 43-48
- 48 Delco Propulsion Systems, "Delco Electric Vehicle Inductive Charging Systems", (Anderson, IN, Delco Propulsion Systems, 1996)
- 49 Quanlu Wang and Mark A. DeLuchi, "Impacts of Electric Vehicles on Primary Energy Consumption and Petroleum Displacement", Institute of Transportation Studies, July 1991, in Robert Q. Riley, Alternative Cars in the 21st Century, (Warrendale, PA: Society of Automotive Engineers, 1994), p. 206

- 50 Brian Rawson, Environmental Affairs and Sustainable Development, EPCOR, private communication, 1996
- 51 United States, Environmental Protection Agency, "Light-Duty Vehicles and Trucks: Exhaust Emission Certification Standards" in M.D. Checkel, "Appendix D. Vehicle Emission Standards", Vehicle Emissions Project - The City of Edmonton Transportation Master Plan, (Edmonton, AB: City of Edmonton Transportation Department, 1996)
- 52 K. Shaine Tyson, et al., Fuel Cycle Evaluations of Biomass-Ethanol and Reformulated Gasoline, (Golden, CO: National Renewable Energy Laboratory, November 1993), p. 52

Appendix A. Sample data file from the data acquisition system

A sample of the data collected with the data acquisition system (DAS) is given in Figure A-1. The first section of this data is for a charge cycle of 12 h 10 min duration. The first 9 analogue inputs to the data acquisition system (DAS) are sampled 1460 times at 30 s intervals. The second part of the data given is for a driving cycle of 36 min 3 s duration. The first 13 analogue inputs to the DAS are sampled 2163 times at 1 s intervals.

```
hev.275 VEHICLE ID# HEV          VER#: 0   Time= 09:07   Day= 275
EVNT1= 9  EVNT2= 0  CNVTM2= 1  CNVTIME= 30000  DIGIN= 5
Sequenc: 0 1 2 3 4 5 6 7 8
Scale : 0.00 0.00 57.08 30.14 15.33 0.00 0.00 3.23 1.00
Offset : 0.00 0.00 0.00 0.00 0.00 0.00 0.00 6.25 -0.01
0 26.8 22.0 177.62 -6.48 -0.00 19.0 21.0 5.03 6.48
1 26.3 22.1 177.90 -6.18 -0.08 19.1 20.9 5.00 6.39
2 26.3 22.5 178.18 -6.33 -0.00 19.8 21.2 4.97 6.38
3 26.3 22.3 178.46 -6.18 -0.08 20.0 20.8 4.90 6.29
4 26.8 22.1 178.74 -6.33 -0.00 19.5 21.0 4.92 6.29
5 26.3 22.3 178.74 -6.18 -0.08 20.0 20.9 4.87 6.25
6 26.5 22.5 178.74 -6.04 -0.00 19.9 21.0 4.89 6.26
7 26.6 22.3 178.74 -6.18 -0.00 19.7 21.0 4.82 6.20
8 26.6 22.0 179.02 -6.04 -0.00 19.5 21.0 4.84 6.20
.
.
.
1451 27.9 24.3 203.83 -2.36 -0.00 22.5 22.9 0.85 1.63
1452 27.9 24.3 203.56 -2.36 -0.00 22.5 22.6 0.86 1.62
1453 28.0 24.2 203.56 -2.36 -0.08 22.3 23.1 0.86 1.62
1454 27.7 24.3 203.56 -2.36 -0.00 22.3 22.8 0.86 1.63
1455 27.7 24.3 203.56 -2.36 -0.00 22.5 22.8 0.86 1.63
1456 27.7 24.2 203.56 -2.21 -0.00 22.3 22.8 0.86 1.62
1457 27.6 24.3 203.56 -2.21 -0.00 22.1 22.8 0.86 1.63
1458 27.4 24.2 203.56 -2.36 -0.08 22.3 22.9 0.86 1.63
1459 27.6 24.4 195.19 -1.18 0.07 22.3 22.9 0.04 0.67
EOR1: TIME= 21:17 DATE= 275 Digin= 001 TREF= 1.235 GREF= 0.000

VEHICLE ID# HEV          VER#: 0   Time= 21:46   Day= 275
EVNT1= 13 EVNT2= 0  CNVTM2= 1  CNVTIME= 1000  DIGIN= 165
Sequenc: 0 1 2 3 4 5 6 7 8 9 10 11 12
Scale : 0.00 0.00 57.08 30.14 15.33 0.00 0.00 3.23 1.00 1.00 16.87 1.01 6.92
Offset : 0.00 0.00 0.00 0.00 0.00 0.00 0.00 6.25 -0.01 -0.00 0.00 2.47 5.94
0 27.3 21.2 182.36 0.29 -0.00 22.0 22.3 0.20 0.01 -0.00 -2.23 -0.04 1.14
1 27.1 20.6 182.36 0.29 -0.08 22.0 22.6 0.22 0.01 -0.00 -2.39 -0.04 1.14
2 27.3 21.9 182.36 0.29 -0.00 22.0 22.3 0.20 0.01 -0.00 -2.14 -0.04 1.10
3 27.0 20.7 182.08 0.88 -0.08 22.3 22.5 0.25 0.01 0.80 0.25 -0.03 1.41
4 27.3 20.4 182.08 0.74 -0.00 21.8 22.3 0.25 0.01 0.81 0.25 -0.04 1.34
5 27.3 20.4 182.08 0.74 -0.00 21.9 22.3 0.23 0.01 0.81 0.49 -0.04 1.31
6 27.2 19.9 182.08 0.59 -0.08 22.1 22.1 0.23 0.01 0.81 0.49 -0.04 1.31
7 27.2 17.6 179.30 8.54 0.52 21.9 22.5 0.26 0.01 0.81 3.87 0.04 1.37
8 27.2 20.8 178.46 13.54 7.26 21.7 22.7 0.29 0.01 0.81 6.92 0.04 1.31
.
.
.
2154 31.1 18.2 157.82 -1.18 -0.08 11.6 19.4 0.01 0.02 -0.00 -0.08 -0.01 0.00
2155 31.3 18.1 157.54 -1.18 -0.00 11.6 19.3 0.01 0.01 -0.00 -0.17 0.00 0.00
2156 30.9 18.3 157.54 -1.33 -0.00 11.2 19.1 -0.01 0.01 0.00 -0.00 -0.01 0.00
2157 30.9 18.3 157.82 -1.33 -0.00 11.2 19.3 0.01 0.01 0.00 -0.00 -0.00 0.12
2158 30.9 18.1 157.82 -1.47 -0.00 11.5 19.3 0.03 0.01 -0.00 -0.00 0.00 0.00
2159 31.1 18.3 157.82 -1.33 -0.00 11.5 19.1 0.01 0.02 0.00 -0.00 -0.00 0.12
2160 31.3 18.1 157.82 -1.18 -0.00 11.6 19.3 -0.01 0.01 -0.00 -0.17 -0.00 0.00
2161 31.1 18.2 157.82 -1.33 -0.08 11.6 19.0 0.01 0.01 -0.00 -0.08 -0.01 0.00
2162 31.1 18.2 157.82 -1.33 -0.08 11.6 19.0 -0.01 0.01 -0.00 -0.00 -0.01 0.00
EOR2: TIME= 22:23 DATE= 275 Digin= 129 TREF= 1.235 GREF= 0.000
```

Figure A-1. Sample file of data collected

A brief description of the data file format will be presented in this appendix. A more detailed description can be found in the “Operator’s Manual” for the data acquisition system. The first five lines of each section of the data file give information regarding the particular operating cycle (time and day of year when the cycle begins), the sampling interval, and the calibration of each DAS analogue input channel. The sixth and successive lines give the data values of each channel at each sampling interval. The first column lists the interval number and the remaining columns correspond to the values obtained from the analogue input channel listed in the third line “Sequenc(e)” numbers.

Table A-1. Data file format

Channel or “Sequenc(e)” number	Measured parameter	Units of data
0	Battery box temperature	°C
1	Cabin temperature #1	°C
2	Battery pack voltage	V
3	Battery pack current	A
4	Vehicle speed	km/h
5	Ambient air temperature	°C
6	Cabin temperature #2	°C
7	Charging current	A
8	Output voltage of utility grid power meter	V
9	Vehicle operating mode indicator	V
10	Electric motor speed	100 rpm
11	Accelerometer output	G (9.81 m/s ²)
12	Accessory current	A

The “Scale” and “Offset” values are set for each channel in the DAS configuration file. The values allow the measured voltage from each transducer to be converted to the units of the actual parameter of interest. Table A-1 gives the measured parameter for each DAS input channel and the units in which the data is presented in the data file. For example, the output voltage of the battery pack voltage transducer (channel 2) is multiplied by the “Scale” value (57.08) to determine the battery pack voltage. The “Scale” value corresponds to the sensitivity of the transducer: 1 V output per 57.08 V input. A “Scale” value of zero indicates that a thermistor is connected to that channel and a built-in calibration curve is used by the DAS to calculate the measured temperature. The “Offset” value is used when the output voltage of a particular transducer is not equal to zero when the measured parameter is equal to zero.

Appendix B. Uncertainty in calculated electrical energy and distance traveled

The electrical power flowing into a particular component was determined by multiplying the battery voltage with the electrical current flowing into the component.

$$P = V \cdot I \quad (\text{B.1})$$

where P is the electrical power (W)
 V is the battery voltage (V)
 I is the electrical current (A)

Since there is uncertainty in the measured values of battery voltage and electrical current (as given in Table B-1), there is some uncertainty in the calculated electrical power.

$$\delta P = |P| \cdot \sqrt{\left(\frac{\delta V}{V}\right)^2 + \left(\frac{\delta I}{I}\right)^2} = \sqrt{V^2 \cdot \delta I^2 + I^2 \cdot \delta V^2} \quad (\text{B.2})$$

where δP is the uncertainty in the calculated electrical power (W)
 δV is the uncertainty in the measured battery voltage (V)
 δI is the uncertainty in the measured electrical current (A)

The uncertainty in power must be calculated at every sampling interval as both voltage and current will change.

Table B-1. Uncertainties in measurements

Measured parameter	Symbol	Measurement uncertainty
Battery pack voltage	δV	± 1.8 VDC
Battery pack current	δI_{batt}	± 3.4 A
Accessory current	δI_{access}	± 0.075 A
Charging current	δI_{charge}	± 0.053 A
Vehicle speed	δv	± 0.65 km/h
Utility grid power	$\delta P_{\text{utility}}$	± 2.1 W

The amount of electrical energy transferred to a component during each sampling period of the DAS was determined by multiplying the electrical power by the sampling period.

$$e = P \cdot \Delta t \quad (\text{B.3})$$

where e is the electrical energy transferred during a single sampling period (J)
 Δt is the sampling period (1 s for driving cycles, 30 s for charging cycles)

The uncertainties in electrical power and sampling period are propagated in the calculation of electrical energy. The internal clock of the computer has good accuracy and the uncertainty in the sampling period was assumed to be no greater than 0.01 s.

$$\delta e = |e| \cdot \sqrt{\left(\frac{\delta P}{P}\right)^2 + \left(\frac{\delta \Delta t}{\Delta t}\right)^2} = \sqrt{P^2 \cdot \delta P^2 + \Delta t^2 \cdot \delta P^2} \quad (\text{B.4})$$

where δe is the uncertainty in the calculated electrical energy during a sampling period (J)
 $\delta \Delta t$ is the uncertainty in the sampling period (0.01 s)

The total energy transferred during a given driving or charging cycle was determined by numerical integration (i.e., calculating the sum of the electrical energies of each sampling period).

$$E = \sum_{i=1}^n e_i \quad (\text{B.5})$$

where E is the electrical energy transferred during a cycle (J)
 e_i is the electrical energy transferred during the i^{th} sampling period (J)
 n is the number of samples in the cycle

The uncertainty in the calculation of total electrical energy can be determined with the following equation:

$$\delta E = \sqrt{\sum_{i=1}^n \delta e_i^2} \quad (\text{B.6})$$

where δE is the uncertainty in the calculated total electrical energy during a cycle (J)

The uncertainty in each calculated energy value is different because of the different measurement uncertainties of each transducer, the different amount of energy delivered during each cycle, and the different duration of each cycle. In general, the uncertainty in

the calculated energy produced by regenerative braking was less than 2.5% of the energy produced and the uncertainty for all other calculated energy flows was less than 1% of the calculated value.

A similar set of equations was used to determine the uncertainty in the calculated distance traveled by the vehicle.

$$d = v \cdot \Delta t \quad (\text{B.7})$$

where d is the distance traveled during a single sampling period (m)
 v is the measured vehicle speed (converted to m/s)
 Δt is the sampling period (1 s for driving cycles)

$$\delta d = |d| \cdot \sqrt{\left(\frac{\delta v}{v}\right)^2 + \left(\frac{\delta \Delta t}{\Delta t}\right)^2} = \sqrt{v^2 \cdot \delta \Delta t^2 + \Delta t^2 \cdot \delta v^2} \quad (\text{B.8})$$

where δd is the uncertainty in the calculated distance traveled during a sampling period (m)
 δv is the uncertainty in the measured vehicle speed (converted to m/s)

$$D = \sum_{i=1}^n d_i \quad (\text{B.9})$$

where D is the distance traveled during a cycle (m)
 d_i is the distance traveled during the i^{th} sampling period (m)

$$\delta D = \sqrt{\sum_{i=1}^n \delta d_i^2} \quad (\text{B.10})$$

where δD is the uncertainty in the calculated total distance traveled during a cycle (m)

As with the calculated energy values, the uncertainty in each calculated distance traveled is different because of the different velocities in different driving cycles, and the different duration of each cycle. In general, the uncertainty in the calculated distance was less than 1% of the distance value.

Appendix C. Calibration of data acquisition system

Following the Hybrid Vehicle Evaluation Project, a detailed calibration was performed on the data acquisition system (DAS) for the key measurements related to energy consumption. These measurements were battery pack voltage, battery pack current, charge current, accessory current, and vehicle speed. In addition, an AC power meter was calibrated and used for measuring the electrical power consumed by the battery charger from the utility grid. The on-board sensors in the hybrid electric research vehicle (HRV) displayed good linear response. Therefore, the errors present due to the initial simplified calibration were easily corrected in the data analysis, by applying correction factors for the sensor sensitivity and offset.

The uncertainties in measurement were determined from statistical methods in linear regression. An outline of the method used is given in Appendix D

Calibration of voltage measurement

A high voltage power supply and a Fluke 8060A digital multi-meter were used to calibrate the battery pack voltage measurement. The power supply output was varied from 0.00 VDC to 220.2 VDC and the digital multi-meter was used as a standard for comparison. As shown in Figure C-1, the voltage measurement by the DAS had good linearity. The linear regression of the calibration data had a correlation coefficient, r , greater than 0.999. The regression equation showed that the DAS calibration for the sensitivity was 0.5% too high and the zero offset was 2.82 VDC too low. The DAS sensitivity was adjusted in the calibration file and the offset error was corrected during the data analysis. The uncertainty in the measurement of the battery pack voltage between the calibration range was less than ± 1.8 VDC ($\pm 0.82\%$ of upper range limit) with 95% confidence.

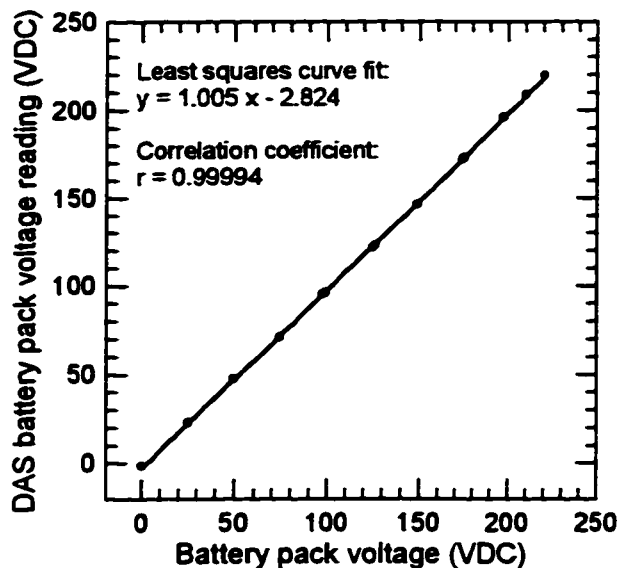


Figure C-1. Calibration curve for measurement of battery pack voltage

Battery current measurement

A calibrated 0 to 500 A shunt and a Fluke 8060A digital multi-meter were used to calibrate the battery pack current measurement. The HRV was driven on a chassis dynamometer at various speeds to vary the battery current draw from about 35 A to 105 A. The voltage drop across the shunt (0.1 mV/A) was measured with the digital multi-meter and used as the standard for determining the actual current. The battery pack current measurement had good linearity as shown in Figure C-2. The linear regression of the calibration data had a correlation coefficient, r , greater than 0.999. The regression equation showed that the DAS calibration for the sensitivity was about 2.9% too high and the zero offset was about 1.097 A too low. The DAS sensitivity was adjusted in the calibration file. It was observed that the measurement displayed a small drift (± 0.5 A) over time. An offset correction was applied during the data analysis of each cycle to account for this error.

The uncertainty in the measurement of the battery pack current between the calibrated range of 25.4 A and 103.0 A is less than ± 1.4 A ($\pm 1.4\%$ of upper range limit) with 95% confidence. During on-road driving, the range of battery pack current was measured between -110 A to 300 A. The calibration range was limited due to difficulty in

maintaining a steady high current for calibration and the inability to apply a driving force to the tires to maintain a steady negative current from regenerative braking. However, it can be reasonably assumed that the Hall Effect current sensor used to measure the battery pack current behaves linearly over its rated operating range. Under this assumption and based on the calibration data, an extrapolation can be made to estimate the uncertainty in the normal current range: less than ± 3.4 A ($\pm 1.1\%$ of upper range limit) with 95% confidence.

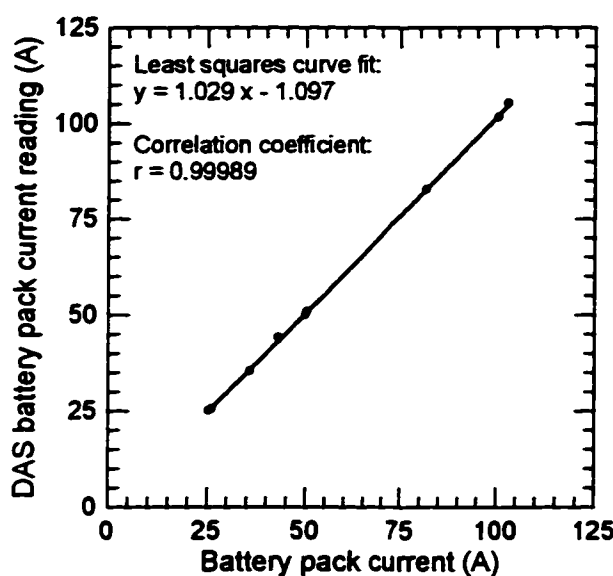


Figure C-2. Calibration curve for measurement of battery pack current

Charge current measurement

A calibrated 0 A to 10 A shunt, a Fluke 8060A digital multi-meter, and a 0 A to 10 A power supply were used to calibrate the charge current measurement. The power supply output was varied from 0.568 A to 5.059 A. The voltage drop across the shunt (10 mV/A) was measured with the digital multi-meter and used as the standard for determining the actual current. The charge current measurement had good linearity as shown in Figure C-3. The linear regression of the calibration data had a correlation coefficient, r , greater than 0.999. The regression equation showed that the DAS calibration for the sensitivity was about 0.5% too high and the zero offset was about

0.022 A too high. The DAS sensitivity was adjusted in the calibration file. It was observed that the measurement displayed a small drift (± 0.05 A) over time. An offset correction was applied during the data analysis of each cycle to account for this error. The uncertainty in the measurement of the charge current in the calibration range is less than ± 0.053 A ($\pm 1.1\%$ of upper range limit) with 95% confidence.

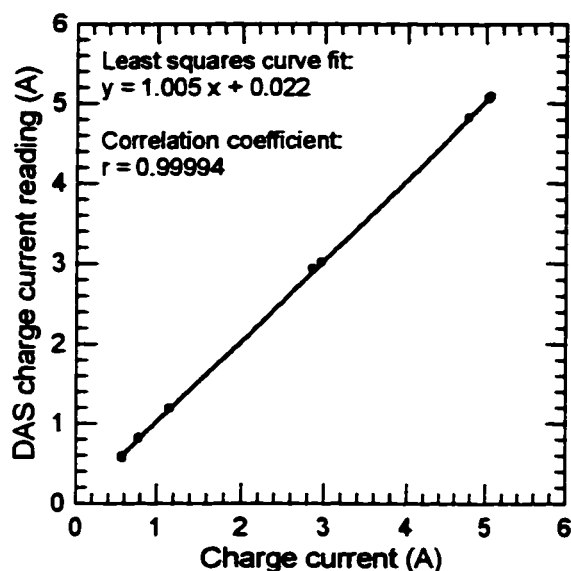


Figure C-3. Calibration curve for measurement of charge current

Accessory current measurement

A calibrated 0 A to 10 A shunt and a Fluke 8060A digital multi-meter were used to calibrate the accessory current measurement. Various accessories were turned on and off to vary the accessory current from 0.684 A to 12.629 A. The voltage drop across the shunt (10 mV/A) was measured with the digital multi-meter and used as the standard for determining the actual current. The shunt was rated for operation up to 20 A for 1 minute, which allowed calibration above 10 A. The charge current measurement had good linearity as shown in Figure C-4. The linear regression of the calibration data had a correlation coefficient, r , greater than 0.999. The regression equation showed that the DAS calibration for the sensitivity was about 0.7% too high and the zero offset was about 0.551 A too high. The DAS sensitivity was adjusted in the calibration file. It was

observed that the measurement displayed a small drift (in a ± 0.12 A range) over time. An offset correction was applied during the analysis of the data collected each day to account for this error. The uncertainty in the measurement of the charge current in the calibration range is less than ± 0.075 A ($\pm 0.59\%$ of upper range limit) with 95% confidence.

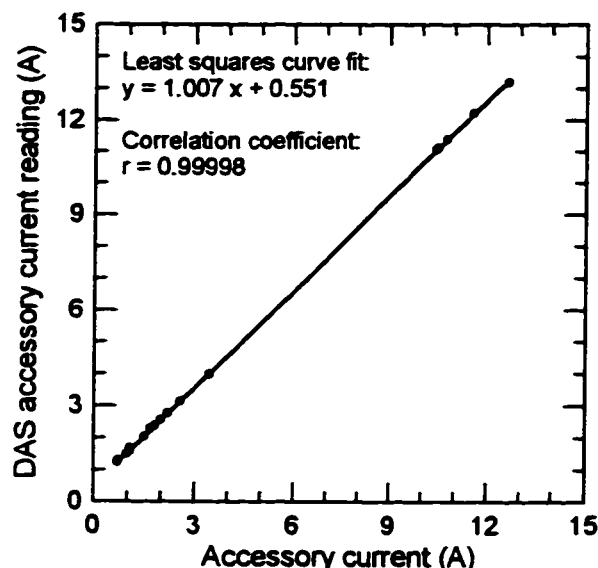


Figure C-4. Calibration curve for measurement of accessory current

Vehicle speed measurement

A Shimpo DT-105 hand digital tachometer was used to calibrate the vehicle speed measurement. The nominal rolling diameter of the tire was measured (1.755 m) and then used to determine the conversion factor from the rotational speed of the tire to the vehicle speed: 0.1053 km/h/rpm. The HRV was driven on a chassis dynamometer at speeds from 0.00 km/h to 101.58 km/h. The rotational speed of the tire, measured with the digital tachometer, was multiplied by the conversion factor to give the standard for the actual vehicle speed. The vehicle speed measurement had good linearity as shown in Figure C-5. The linear regression of the calibration data had a correlation coefficient, r , greater than 0.999. The regression equation showed that the DAS calibration for the sensitivity was about 0.6% too low and the zero offset was about 0.187 km/h too low. The DAS sensitivity and offset was adjusted in the calibration file. The uncertainty in the

measurement of the vehicle speed in the calibration range is less than ± 0.65 km/h ($\pm 0.64\%$ of upper range limit) with 95% confidence.

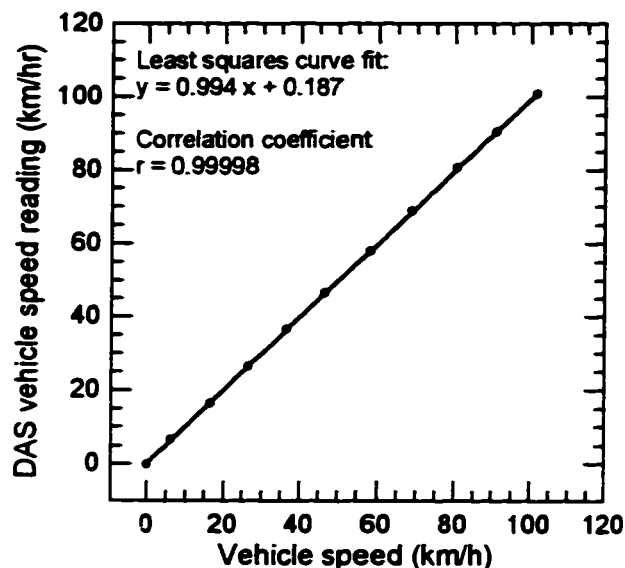


Figure C-5. Calibration curve for measurement of vehicle speed

Calibration of AC power meter

The DAS was used to measure the voltage output of the AC power meter (Ohio Semitronics digital watt meter, model WM-951) to record the power consumption of the battery charger. The output of the meter was calibrated using three digital multi-meters and an electrical resistance load cell. The load cell was adjusted to vary the electrical power passing through the AC power meter from 0.000 W to 1469 W. At each calibration point, the AC voltage and current were measured and multiplied to determine the standard for the actual AC power, and the corresponding voltage output from the meter was recorded. The voltage output from the meter had good linearity as shown in Figure C-6. However, the linear regression of the calibration data was not used to determine AC power during data analysis.

The uncertainty in the measurement of AC power based on the output voltage of the meter is about ± 20 W ($\pm 1.4\%$ of upper range limit) with 95% confidence. When the battery charger is operating at high power it requires about 1200 W of electrical power.

The uncertainty in power measurement is only $\pm 1.7\%$ at this level. However, the charger delivers about half the charge energy at a relatively low power level, consuming about 300 W. The uncertainty in power measurement is $\pm 6.7\%$ at this level. To fully charge the battery pack, the charger operates for about 18 h and consumes 10.5 kW-h of energy. In this case, the uncertainty in power accumulates to give an uncertainty in energy measurement of ± 0.36 kW-h ($\pm 3.4\%$ of the energy consumed), assuming the uncertainty in the sampling interval is negligible.

To reduce measurement uncertainty, a linear interpolation between calibration points was performed in the data analysis with each recorded voltage output from the AC power meter. This procedure accounts for most of the non-linearity in the AC power meter output. If the remaining non-linearity (i.e., the non-linearity between calibration points) is assumed to be negligible, the measurement uncertainty can be estimated from the uncertainty in measuring the output voltage of the AC power meter (± 0.01 V) divided by the maximum sensitivity of the meter (4.8 mV/W). This calculation gives an uncertainty in measuring AC power consumption of about ± 2.1 W.

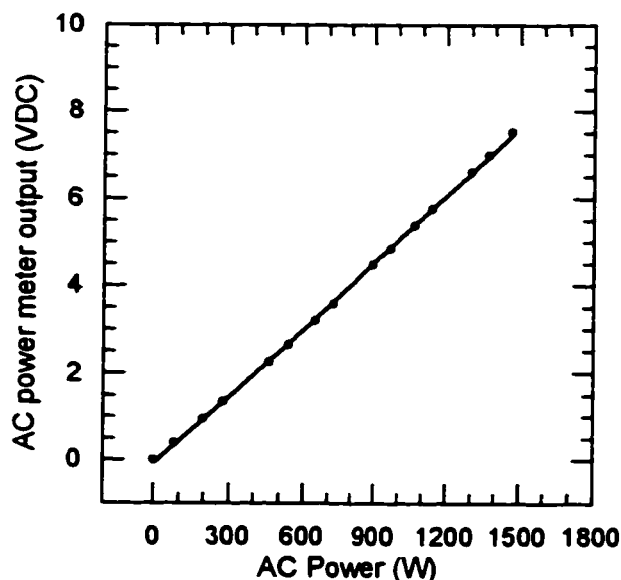


Figure C-6. Calibration curve for output from AC power meter

Appendix D. Uncertainty in linear curve fits and means

More details on the method outlined in this appendix can be found in Practical Statistics for Engineers and Scientists, by Nicholas P. Cheremisinoff, (Lancaster, PA: Technomic Publishing, 1987), p. 129-134 or other statistics books, such as Probability and Statistics for Engineers, 4th ed., by Irwin R. Miller, et al., (Englewood Cliffs, NJ: Prentice-Hall, 1990), p. 327-333.

Uncertainty in least squares linear curve fit

If a linear relationship between an independent parameters, x , and a dependent parameter, y , is hypothesized for a given data set, the slope and zero offset of the best fitting line can be calculated using the following series of equations:

$$S_{xx} = \sum_{i=1}^n x_i^2 - \frac{\left(\sum_{i=1}^n x_i\right)^2}{n} \quad (D.1)$$

where S_{xx} is the sum of squares of the parameter x
 x_i is i^{th} the value of the parameter x in the data set
 n is the total number of data points in the data set

$$S_{yy} = \sum_{i=1}^n y_i^2 - \frac{\left(\sum_{i=1}^n y_i\right)^2}{n} \quad (D.2)$$

where S_{yy} is the sum of squares of the parameter y
 y_i is i^{th} the value of the parameter y in the data set

$$S_{xy} = \sum_{i=1}^n (x_i \cdot y_i) - \frac{\sum_{i=1}^n x_i \cdot \sum_{i=1}^n y_i}{n} \quad (D.3)$$

where S_{xy} is the sum of squares of the parameters x and y

$$\bar{x} = \frac{\sum_{i=1}^n x_i}{n} \quad (\text{D.4})$$

where \bar{x} is the mean value of the parameter x

$$\bar{y} = \frac{\sum_{i=1}^n y_i}{n} \quad (\text{D.5})$$

where \bar{y} is the mean value of the parameter y

$$b_1 = \frac{S_{xy}}{S_{xx}} \quad (\text{D.6})$$

where b_1 is the slope of the linear curve fit

$$b_2 = \bar{y} - b_1 \bar{x} \quad (\text{D.7})$$

where b_2 is the zero offset of the linear curve fit

The correlation coefficient indicates how well the parameters are correlated; the value of the coefficient is equal to 0 if there is no correlation, and equal to 1 if there is an exact correlation.

$$r = \frac{S_{xy}}{\sqrt{S_{xx} \cdot S_{yy}}} \quad (\text{D.8})$$

where r is the correlation coefficient

Often, it is desired to predict the value of the independent parameter given a value of the dependent parameter. For example, predict the actual electrical current flowing in a wire given the output voltage of a Hall Effect current sensor. In such a situation, the above calculations can be repeated with the calibration data after exchanging the parameters, x and y.

The uncertainty in the predicted value of y can be determined using the Student's t statistic for n - 2 degrees of freedom and a chosen confidence level.

$$\delta y = t \cdot S \sqrt{1 + \frac{1}{n} + \frac{(x_0 - \bar{x})^2}{S_x^2}} \quad (\text{D.9})$$

where δy is the uncertainty in the predicted value of y
 t is Student's t statistic for n-2 degrees of freedom and the confidence level
 x_0 is the value of the parameter x at which the value of y is predicted

Uncertainty in mean value

The uncertainty in the calculated mean value of a parameter, x, can be determined using the Student's t statistic for n - 1 degrees of freedom and a chosen confidence level, after calculating the sample standard deviation.

$$S = \sqrt{\frac{\sum_{i=1}^n x_i^2 - \frac{\left(\sum_{i=1}^n x_i\right)^2}{n}}{n-1}} \quad (\text{D.10})$$

where S is the sample standard deviation of x
 x_i is i^{th} the value of the parameter x in the data set
 n is the total number of data points in the data set

$$\delta \bar{x} = \frac{t \cdot S}{\sqrt{n}} \quad (\text{D.11})$$

where $\delta \bar{x}$ is the uncertainty in the predicted value of y
 t is Student's t statistic for n - 1 degrees of freedom and the confidence level

Appendix E. Emissions from the production of gasoline

Estimates of pollution associated with the production of reformulated gasoline (RFG) were reported by K. Shaine Tyson, et al., Fuel Cycle Evaluations of Biomass-Ethanol and Reformulated Gasoline, (Golden, CO: National Renewable Energy Laboratory, 1993). The reported results, given in Table E-1, were presented in g/mi for a vehicle with a fuel consumption of 7.64 L/100 km (30.8 mpg).

Table E-1. Fuel cycle emission estimates for reformulated gasoline

	CO ₂ (g/mi)	CO (g/mi)	NO _x (g/mi)	HC† (g/mi)	SO ₂ (g/mi)	Particulates (g/mi)
Feedstock production	12.9730	0.0073	0.0454	0.0136	0.0027	0.0005
Feedstock transportation	4.2638	0.0136	0.0308	0.0145	0.0009	0.0015
Fuel production	25.7645	0.0081	0.0617	0.0081	0.0399	0.0021
Fuel distribution	1.179	0.0045	0.0081	0.043	0.0003	0.0003

† HC and VOC are assumed to be equivalent

The RFG contained 11% methyl tertiary butyl ether (MTBE); however, emissions from producing MTBE were not included in the results. Therefore, the production and distribution emissions presented in Table E-1 are only associated with the regular unleaded gasoline which constitutes 89% of the RFG (or 6.80 L of gasoline contained in 7.64 L of RFG). A 1994 Escort requires 8.69 L of gasoline to travel 100 km. The emission values in Table E-1 are multiplied by a factor of 1.278 (=8.69 L/6.80 L) to estimate the pollution associated with producing fuel for the Escort. The resulting fuel production and distribution emission for the Escort are presented in Table E-2.

Table E-2. Fuel cycle emission estimates for regular unleaded gasoline

	CO ₂ (g/mi)	CO (g/mi)	NO _x (g/mi)	HC† (g/mi)	SO ₂ (g/mi)	Particulates (g/mi)
Feedstock production	16.6	0.0093	0.0580	0.0174	0.0035	0.0006
Feedstock transportation	5.45	0.0174	0.0394	0.0185	0.0012	0.0019
Fuel production	32.9	0.0104	0.0789	0.0104	0.0510	0.0027
Fuel distribution	1.51	0.0058	0.0104	0.055	0.0004	0.0004

† HC and VOC are assumed to be equivalent